Nº d´ordre : 3410

THESE

Présentée à

L´UNIVERSITE BORDEAUX I

Ecole Doctorale des Sciences Chimiques

Par **Pedro EGIZABAL LUZURIAGA**

Pour obtenir le grade de

DOCTEUR

Spécialité: Physico-Chimie de la Matière Condensée

Influence des particules de TiB_2 sur la microstructure et les propriétés des alliages Al-Si7Mg0,7 et Al-Cu5MgTi renforcés, pour des applications de fonderie à la cire perdue avec des moules en plâtre.

Soutenue le 19 Juillet 2007

Après avis de Messieurs:	Pr. Jordi **TARTERA BARRABEIG**	Rapporteur
	Dr. Jöel **DOUIN**	Rapporteur

Devant la commission d´examen formée de Messieurs:

Dr. Claude **DELMAS**	ICMCB - CNRS	Président
Pr. Yann **LEPETITCORPS**	LCTS	Examinateur
Dr. Jean François **SILVAIN**	ICMCB - CNRS	Examinateur
Dr. Javier **GOÑI**	INASMET	Examinateur
Membre invitée :		
Dr. Ana **GARCIA ROMERO**	UPV/EHU	Examinateur

- 2007 -

PhD Thesis document. Université Bordeaux I. " Influence of Titanium Diboride (TiB_2) on the microstructure and properties of reinforced Al-Si7Mg0.3 and Al-Cu5MgTi alloys for plaster casting applications".

July 2007

Influence of Titanium Diboride (TiB_2) particles on the microstructure and properties of reinforced Al-Si7Mg0.3 and Al-Cu5MgTi alloys for plaster casting applications.

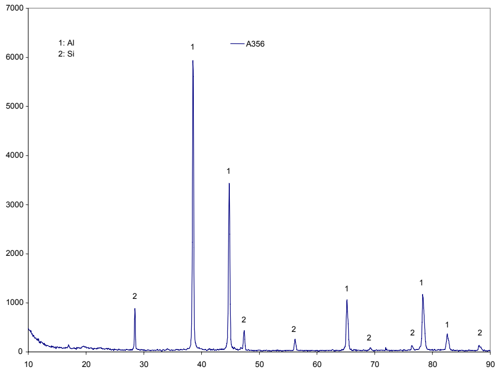

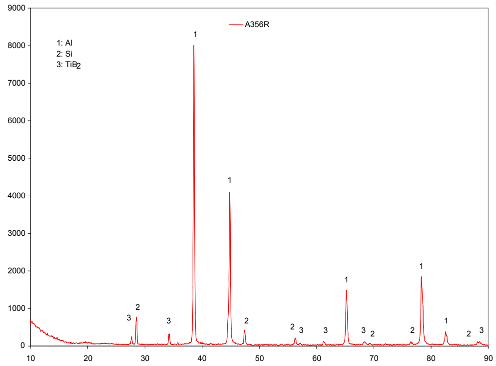

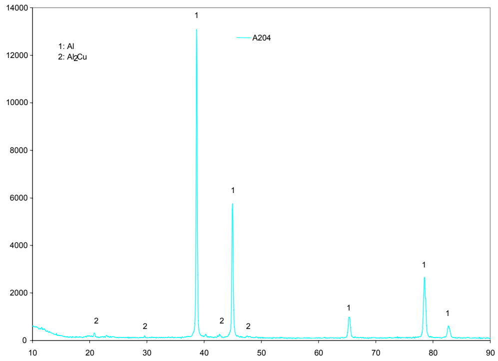

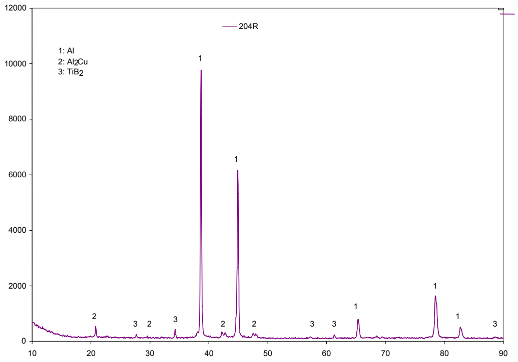

<u>MAY 2007</u>

ACKNOWLEDGEMENTS

This work has been carried out at Inasmet in Donostia-San Sebastián with the collaboration of the Institut de Chimie et de la Matière Condensée de Bordeaux (ICMCB). Part of the work has been carried out in the frame of the research project IMINCAST (Contract number G1ST-CT-2002-50268) partially funded by the European Commission.

I want to thank all the components of the jury and especially the rapporteurs Mr. Jordi Tartera from the Universidad Politécnica de Catalunya and Mr. Jöel Douin from CEMES-CNRS in Toulouse for having accepted to be members of it.

Mr.Jean Francois Silvain from the ICMCB has also honoured me by being the thesis director. In addition to his solid scientific and technical help and counsels, I have greatly appreciated his patience and disposition to solve problems and to accommodate to my needs and pace.

I cannot forget Mrs. Angela Hardman from London Scandinavian who helped me to acquire the material and provided valuable technical comments and Mr. Guilleaume Lacombe from ICMCB who carried out the thermal analysis tests.

There are many people at Inasmet whom I would like to thank. First of all to Mr. Javier Goñi whose help and friendship have been determinant for the realisation of the thesis. Also to all those who have helped and encouraged me along the work, Jon Maudes, Maider Garcia de Cortazar, Iñigo Sarriés, Jorge Bárcena, José Carlos García, Xabi Peña, Ana García, Angel Mari Irisarri, Pierre Marie Geffroy, Miguel Segura and Iñigo Crespo. This work has been easier thanks to them and many others whose encouragement and help has made it easier to complete this work.

I do not really know how to thank my family properly. The support of my parents, brothers, sister and rest of my family has been essencial along all these years. Many thanks to all of them for their encouragement and specially to Amaia for her support during all this time.

LIST OF ACRONYMS

AES: Auger Electron Spectroscopy.
Al_2O_3: Alumina.
AMC: Aluminium Matrix Composite.
ASTM: American Society for Testing Materials (standards).
B: Boron.
B_4C: Boron Carbide.
B_2O_3: Boron oxide.
C: Carbon.
CTE: Coefficient of Thermal Expansion.
EDS: Energy Dispersive X-Ray Spectroscopy (mapping)
EPMA: Electron Probe Micro-Analysis.
FAS: Flux Assisted Synthesis.
FIB: Focused Ion Beam.
HIP: Hot Isostatic Pressing
KBF_4: Potassium Tetrafluoroborate.
K_2TiF_6: Potassium Hexafluorotitanate.
MMC: Metal Matrix Composites.
NLLSF: Non Linear Least Squares Fitting.
OM: Optical Microscopy.
SDAS: Secondary Dendrite Arm Spacing.
SEI: Secondary Electron Image.
TiB_2: Titanium Diboride.
TiC: Titanium Carbide.
TiO_2: Titanium Oxide.
UTS: Ultimate Tensile Strength.
YS: Yield Strength.
XRD: X-Ray Diffraction.

INDEX **PAGE**

CHAPTER 1: INTRODUCTION. OBJECTIVES OF THE THESIS.

1.1 INTRODUCTION

The low density of aluminium alloys and the excellent combination of properties they present have led to their extensive application in a large number of applications in the automotive, aeronautical, aerospace, construction, food and beverage, sports and energy sectors.

Pure aluminium is a soft material with low mechanical properties and a very limited range of applications. Yet, it was discovered that the addition of alloying elements such as Si, Cu, Mg, Ti, Zn, Mn and Ni increased its properties and range of use and it is a long established practice in the industry. At the beginning of the 1950s it was discovered that the incorporation of certain ceramic elements led to the further improvement of their mechanical and thermal properties. The presence of the second phase strengthens the alloy through different mechanisms that restrict the movement of dislocations (load transfer, grain size decrease, Orowan strengthening and increase of dislocation density due to Coefficient of Thermal Expansion (CTE) mismatch). These materials are called Metal Matrix Composites (MMCs) and they were first studied in the 1950s-1960s. The first commercial applications were those of boron reinforced aluminium alloys used for the space shuttle struts. Afterwards the automotive maker Toyota applied them for a diesel piston insert in the 80s and henceforward a continuous funding on the research of these materials has entailed the apparition of more MMC developments and applications.

The present work is based on the study of MMCs reinforced with TiB_2 particles. Samples of two different reinforced aluminium alloys have been cast by a lost wax process known as plaster casting in which the metal is cast into a refractory plaster mould. The main objective of the work is to study the effect of around 6 wt. % of titanium diboride (TiB_2) particles on the microstructure, solidification pattern and mechanical and thermal properties of the Al-Si7Mg0.3 and Al-Cu5MgTi casting alloys. Lost wax processes are ideally suited to produce complex shaped high quality components for the aeronautical industry. The Al-Si7Mg0.3 alloy is the most used by lost wax foundries due to its good balance of properties and castability. Al-Cu5MgTi is usually chosen when higher properties are required even though the alloy is more difficult to cast. The aeronautical industry demands light materials with even improved properties and MMCs are seen as good candidates that may increase the range of applications of aluminium based alloys. The combination of the plaster casting process and MMC materials could therefore be a feasible alternative for the production of high added value light components with excellent mechanical properties. Nevertheless the technical aspects surrounding the lost wax of MMCs have not been much researched so far and there is a lack of understanding of the influence of the reinforcements on the microstructure and properties of the castings.

Even though MMCs offer an excellent combination of properties (high wear resistance, high Young´s Modulus, improvement of mechanical properties at high temperatures, lower CTEs than equivalent unreinforced alloys, high thermal conductivity, damping properties, good fatigue behaviour etc.) the number of industrial applications presently available is much lower than that foreseen in the 1970s and 1980s. In spite of some interesting features, there are some drawbacks that continue to hinder their use in large volume applications. (Cost of raw material, low ductility and toughness when compared to the unreinforced material, difficult to be machined and recycled, higher cost of secondary processes, etc.). The reinforced alloys selected in this work have been designed to overcome these drawbacks. The amount of particles is low (around 6 wt. %), their size is small (average diameter lower than 5 µm) and the production route used (in situ production through the Flux Assisted Synthesis (FAS)) is cost effective. In fact the incorporation of the TiB_2 particles was made in two consecutive steps through a process patented by the company London Scandinavian Ltd. in the United Kingdom. Around 1% of the particles were created “in situ” through the FAS process in which two salts, Potassium Boron Tetrafluoride (KBF_4) and Potassium Titanium Hexafluoride (K_2TiF_6), are mixed in the correct ratio and then reacted with the molten aluminium alloy. Commercially available TiB_2 particles (average diameter 5 µm) were subsequently added as a powder to obtain the desired particle content and to make the alloy much cleaner than that obtained with the all-salt process.

1.2 OBJECTIVES

The main objective of the work is to study the influence of the TiB_2 particles (6 wt. %) on the properties and physical features of aluminium casting alloys processed through a lost wax process known as plaster casting. The work has been carried out in the frame of a project partially funded by the European Commission (Reference IMINCAST G1ST-CT-2002-50268) devoted to the use of advanced aluminium based materials in investment casting applications.

Two different alloys were selected as the base materials. First of all the Al-Si7Mg0.3 alloy, an Al-Si alloy containing around 7 wt. % of silicium and that is extensively used in casting applications due to its excellent castability and good balance of properties. Secondly, the Al-Cu5MgTi alloy, an Al-Cu alloy with around 4.5 wt. % of Cu that provides higher mechanical properties but presents a lower castability and is less used in industrial applications than the previous one.

The main tasks of the work have been the selection of two reinforced different alloys, the production of castings via plaster casting for characterization purposes, the physical, thermal and mechanical characterization, the comparison of their properties with those of the corresponding unreinforced alloys and the analysis of the differences between the reinforced and unreinforced alloys.

1.2.1 Analysis of the influence of the TiB_2 particles on the solidification and microstructure of the reinforced Al-Si7Mg0.3 and Al-Cu5MgTi alloys

TiB_2 particles have traditionally been added to aluminium melts incorporated into Al-Ti-B master alloys for grain refining purposes. The addition of only 0.15 wt. % is enough to refine the grains. Even though the main effect of the addition of TiB_2 particles into aluminium alloys is the refinement of the aluminium grains, there are other additional microstructural changes that can also be explained by the presence of these particles. TiB_2 particles that have not participated in nucleation events tend to be pushed by the solidification front and lie at grain boundaries. Moreover the porosity of the samples decreases through the addition of grain refiners. The average size of the pores is lower and furthermore the remaining porosity is more evenly distributed.

Furthermore the effect of the particles incorporated into the alloys has been observed in other solidification related phenomena. TiB_2 particles are substantially insoluble in aluminium and they change the solidification characteristics of the alloy. Solidification events start earlier due to the lower undercooling required and solidification time is reduced.

The two reinforced alloys studied in this work have been charged with around 6 wt. % of particles. This amount exceeds the level necessary for grain refining. The aim was that the particles improved the properties of the alloys following the patterns shown by other particle reinforced aluminium matrix composites (AMC). At the same time the increase of the amount of particles has an influence on other features of the alloys such as the solidification pattern, microstructure and thermal properties. All these aspects have been studied in the present work.

The solidification curves of the reinforced and unreinforced materials have been studied and the effect of the presence of TiB_2 particles on the main solidification parameters such as the maximum temperature of primary α-Aluminium growth, temperature and time difference between the maximum and minimum of the liquidus recalescence, as well as the precipitation of the different phases have been analysed and their influence on the microstructure of the alloys explained.

The microstructure and composition of the reinforced alloys has been thoroughly studied through all Optical Microscopy, Scanning Electronic Microscopy (SEM), Transmission Electronic Microscopy (TEM) and Auger Electron Spectroscopy (AES). Image analysis and the identification of the elements of the different phases have also been carried out in order to study the influence of the presence of the TiB_2 particles on the microstructure of the alloy. The main objective of the microstructural analysis was to check the interaction of TiB_2 particles with the matrices. (see Chapter 4 on Solidification and Microstructure).

1.2.2 Analysis of the influence of the TiB_2 particles on the mechanical and thermal properties of the reinforced Al-Si7Mg0.3 and Al-Cu5MgTi alloys

The thermal and mechanical characterization has been carried out with samples obtained with the plaster casting process. The production route chosen was previously optimised in order to obtain sound samples with a correct and homogeneous distribution of TiB_2 particles.

The mechanical characterization has consisted on tensile tests at room temperature and 200ºC. As cast and thermally treated (T6) samples have been tested and results have been compared to those obtained with the corresponding unreinforced materials.

Thermal characterization has consisted on the measurement of the thermal conductivity and CTE. Results have been compared to those of the corresponding unreinforced alloys.

Furthermore, the experimental results have been compared with values obtained through different models that have been extensively applied for the calculation of mechanical and thermal properties of other particulate reinforced materials. Eventually the reasons that account for the differences between the experimental values obtained with the reinforced materials when compared to the results obtained with the unreinforced alloys have also been analysed.

CHAPTER 2: LITERATURE REVIEW.

2.1 Introduction

Aluminium is one of the most abundant metals on earth and it has been long used for multiple applications since the XIX century when it was firstly discovered. Nowadays it is mainly obtained from bauxite through an industrial process that isolates the metal through the application of different transformation processes. The first studies of the material showed that it had several interesting properties that could be useful for a large range of applications. It was light, could conduct both heat and electricity, and was easily formed and recycled. A very thin transparent oxide layer formed on its surface, transparent and that hindered any further oxidation of the material, rendering it very useful for aesthetic applications. Nevertheless, pure aluminium is soft and the mechanical properties of the material are low so the applications of pure aluminium are constrained to only a few fields such as the electrical and chemical industries.
The situation changed when it was discovered that the addition of small amounts of alloying elements had an enormous influence into the properties of the new material. In this way deep studies were carried out in which different alloying elements were added that obtained new materials with new enhanced properties. Ultimate Tensile Strength (U.T.S) increased from values of 70 MPa to up to 400-500 MPa by alloying pure aluminium.

Nowadays aluminium alloys are extensively used in industrial applications. Transport industry makes a large use of these materials to take advantage of their low density and good mechanical properties. It is also extensively used in other sectors like electricity and electronic devices that account for its good electrical conductivity and large heat dissipation properties.

The main alloying elements presently used for Aluminium are Silicon, Magnesium, Copper, Zinc, Manganese and Tin. Each of these elements has a direct influence on the final features of the alloy. In this way Silicon enhances tensile properties and improves castability, the presence of Magnesium improve the hardenability after solution treatments and quenching as it helps the precipitation of small Mg_2Si precipitates that strengthen the alloy by hindering the movement of dislcations. Copper provides strengthening to the alloy, the maximum values obtained with 4-6 wt. % as they permit the precipitation of hard intermetallics. Manganese is usually applied to prevent the negative influence of impurities like Iron or Silicon as it combines with them avoiding the precipitation of other more brittle phases that tend to decrease the mechanical properties of the alloys. Tin is used to make it easier to machine the final components as it forms low melting phases that promote chip breaking [1].

Aluminium alloys can be classified according to different criteria. On the one hand they can be divided in forging or casting alloys. The former usually present a lower amount of alloying elements and present better mechanical properties than casting alloys. The latter can be easily melted and present a large fluidity making them an ideal material for different casting processes in which very complex shapes can be easily obtained.

Another typical classification of the aluminium alloys is based on the nature of the alloying elements and phases that are formed during the solidification of the materials. Depending on the main alloying elements used, wrought aluminium alloys can be classified in any of the following eight families or series.

1xxx series This series accounts for non alloyed aluminium. Aluminium with a pureness greater than 99% percent may be applied in the electrical and chemical fields due to its corrosion resistance and high thermal and electrical conductivity. Its mechanical properties are low though.

2xxx series These alloys present the copper as the main alloying element. Other elements such as magnesium or titanium are also often added. They are used when high mechanical properties are required and they must be thermally treated to obtain the highest mechanical properties possible.

3xxx series Manganese is used as the main alloying element and it may also contain magnesium. Their main feature is the high corrosion resistance. Manganese may be present in solid solution, as submicroscopic precipitates or within the larger Al6(Mn,Fe) or Al12(Mn,Fe)3Si phases.

4xxx series This series comprises some alloys where silicon is the main alloying element (up to 10-12 wt.%). These aluminium-silicon alloys are used as welding wire and as brazing alloys where their lower melting point is required.

5xxx series The alloys belonging to this series have magnesium as the main alloying element. These non heat treatable alloys show high strength and present an outstanding corrosion resistance and good welding characteristics.

6xxx series The main alloying elements in this series are Magnesium and Silicon that can form magnesium silicide (Mg_2Si) and strengthen the alloy through thermal treatments. These alloys present a good formability, weldability and are easy to machine. Furthermore they have a good corrosion resistance and mechanical strength.

7xxx series The main alloying element of this group is Zinc (1 to 8 wt. %). Both magnesium and copper are usually added as well in order to obtain high mechanical properties after the corresponding heat treatments.

8xxx series It is composed of the rest of aluminium alloys that cannot be integrated in the previous main families or series (such as those with Lithium as the main alloying element).

In the case of casting alloys there is not any classification system that has international acceptance. The most commonly used is that of the Aluminium Association of the United States (AAUS) and it is based on the main alloying elements. The following nomenclature is used. 1xx.x, 2xx.x etc. The first number 1-9 indicates the main alloying elements (1 for pure aluminium, 2 for copper, 3 corresponds to silicon, copper and/or magnesium, 4 to only silicon as the main alloying element, 5 magnesium, 6 is unused, 7 zinc, 8 tin and 9 to other alloying elements. The digit to the right of the decimal point indicates the product form: 0 means "castings" and 1 means "ingot” and the second two digits are simply serial numbers.

The 1XX.X series is related to aluminium with a pureness higher than 99% where the second two digits indicate the minimum percentage of aluminium.

The 2XX.X series encompasses aluminium-copper alloys with copper contents of 4-5%. They are heat-treatable and are used for high strength applications. They show a high ductility. Mn is usually added in order to restrict the negative effect of impurities like Si and Fe that tend to form brittle phases. The solidification interval of these alloys is large and they present hot tearing related defects.

The 3XX.X series is comprised by aluminium alloys containing both copper and silicon as the main alloying elements. They are the most extensively used casting aluminium alloys due to the excellent combination of castability and mechanical properties. They can be used either in the as cast or thermally treated conditions depending on the level of properties desired. Anyway heat treatment is used only with those alloys that also contain magnesium.

The 4XX.X series comprises aluminium-silicon alloys that do not contain any copper additions. They present good castability and good corrosion resistance. The addition of magnesium renders them heat treatable, i.e. after solid solutioning and ageing steps the precipitation of small intermetallic phases containing magnesium takes place that strengthen the material.

The 5XX.X series is formed by aluminium-magnesium alloys. They present a high corrosion resistance. The lower the impurity content, the higher the corrosion resistance so these alloys must be handled with care in order to avoid their contamination during foundry activities. These alloys present poor castability and their cost is high.

The 6XX.X series is formed by aluminium-zinc-magnesium alloys. The main feature of these alloys is that they age naturally at room temperature. Nevertheless they can usually present microsegregation of Mg-Zn phases and their castability is poor. General corrosion resistance is good despite some susceptibility to stress corrosion.

The 7XX.X series has tin as the main alloying element. They may contain up to 6% Sn. These alloys are not extensively used and are applied in specific applications such as bearings because of the lubricity imparted by tin.

Another milestone in the aluminium processing industry was the discovery of the great influence that the addition of very small amounts of additives like Na, Sr, P or TiB_2ad also in the final properties of the materials. These elements may alter the solidification pattern of the material and/or prevent the formation of defects. Na and Sr are currently added in very small amounts (less than 0.5 wt. %) to Al-Si alloys to modify the structure of the silicon platelets so that their final shape is more rounded and homogeneous

along the casting. The improvement of mechanical properties that can be so obtained is in the range of 20-40%.
In the 1950´s it was discovered that the addition of some products decreased the size of the aluminium grains formed during solidification and subsequently their mechanical properties improved dramatically. These products acted like nucleation sites of the aluminium grains during solidification. The grains of aluminium solidified over the surface of these materials and the final average grain size of the alloy decreased. Furthermore the grains tended to be more equiaxed and uniformly distributed along the entire component. The use of Al-Ti-B combinations as grain refiners of aluminium alloys has been applied extensively since then due to the large improvement of properties that its use entails. The mechanisms and nature of the grain refinement phenomena have long been researched since this discovery and will be further approached in another section of this chapter (see section 2.2.2).

The research activities dealing with aluminium have increased in the last century due to the increasing interest of different end user sectors, mainly transport, on the application of light metals with high mechanical properties. One consequence of this research effort was the discovery of the so called MMCs in the beginning of the 1950s. In those years it was discovered that the addition of small amounts of a second ceramic phase into a matrix of aluminium provided an excellent combination of properties that could not be reached through any combination of alloying elements or improvement in secondary processes. Subsequently different reinforcements were tried and nowadays there exists a large combination of shapes (long fibres, whiskers, particulates, monofilaments, short fibres) and materials (silicon carbide SiC, alumina Al_2O_3, boron carbide B_4C, boron B, titanium diboride TiB_2, titanium carbide TiC, carbon C) available. The main interest of the new advanced materials is that properties can be tailored in a large extent due to the possibility of combining different amounts of reinforcements (usually from 1 to 70 vol. %). An adequate selection of the nature and shape of the reinforcements does also affect the final properties. In that way they may fit specific requirements of components used in the transport industry, electronic devices, aeronautical or space.

TiB_2 has also been proposed as reinforcement for MMC applications. It presents no reaction with aluminium or its alloys and can be incorporated into the material through both in situ and ex situ processes. TiB_2 particles are always added in small concentrations to avoid problems in the filling of the moulds due to the large viscosity of the resultant MMC.

The following sections within this chapter present a review of the main features of TiB_2 as well as a description of its use in the aluminium industry both as grain refiner and as reinforcement for MMCs.

2.2 TITANIUM DIBORIDE (TIB_2)

2.2.1 TiB_2. Generalities

Titanium diboride, TiB_2, is a ceramic material with a high melting point (3225Cº ± 20) and hexagonal crystal structure. It does not occur in nature and it is usually synthesized by carbothermal reduction of TiO_2 and B_2O_3. It is one of the refractory borides and its main features are its high hardness, chemical stability (it is even stable in the presence of highly corrosive acids such as HCl or HF even though it reacts with H_2SO_4 and HNO_3 and is easily attacked by alkalis), inertness and high melting point. For these reasons it is used in a large variety of applications such as aluminium smelting (crucibles and cathodes), corrosion resistant applications, metal and ceramic matrix composites [2].

Another specific property of this ceramic is that it is thermally and electrically conductive and furthermore it is a stable compound. Very high purity TiB_2 powders can be rather easily produced and the final product has outstanding densification properties as well as high compressive and tensile strengths. Its properties are maintained at very high temperatures and in addition it presents an excellent wettability and stability in liquid metals such as aluminium [3].

It is produced by vacuum arc-casting followed by either hot-pressing or pressureless sintering (with sintering temperatures in excess of 2000ºC) [2]. The most common production process implies the reaction of titanium oxide (TiO_2) with carbon (C) and boron carbide (B_4C) or boron oxide (B_2O_3) through the following chemical reaction:

$$2TiO_2 + C + B_4C \rightarrow 2\mathbf{TiB_2} + 2CO_2$$

or

$$2TiO_2 + 5C + 2B_2O_3 \rightarrow 2\mathbf{TiB_2} + 5CO_2$$

Vacuum arc-melting is used to produce a 100% dense TiB_2 material. The molten material presents a good fluidity even though high temperatures are needed to cast it. TiB_2 powders can also be processed through different sintering techniques such as hot pressing or pressureless sintering. Microwave sintering and dynamic compaction have also been applied in its production [4]. These processes are rather expensive and very high temperatures are required due to the high melting point of the TiB_2. Nevertheless cost effective processes have also been recently set up that have rendered the production of TiB_2 components cost effective (e.g. the self propagating high temperature synthesis (SHS), in which powders of the elemental components are reacted through the application of an external initial energy source that initiates an exothermal reaction that is self propagating). These processes require only an initial energy input and can produce both TiB_2 powder as well as components [2].

Structure

The crystal structure of TiB_2 is AlB_2 type which is designated as C32. It is a simple hexagonal lattice in which HCP Ti layers in alternation with graphite like B layers are found [4-5]. The space group is P6/mmm, $a = b = 3.026$, $c = 3.213$, $\alpha = \beta = 90°$, $\gamma = 120°$.

The nature of bonding at TiB_2 is a mixed bonding consisting of ionic, metallic and covalent natures. The existence of a covalent bonding has a direct influence on the properties of this material and may be used to explain its low ductility and high hardness and melting point [5].

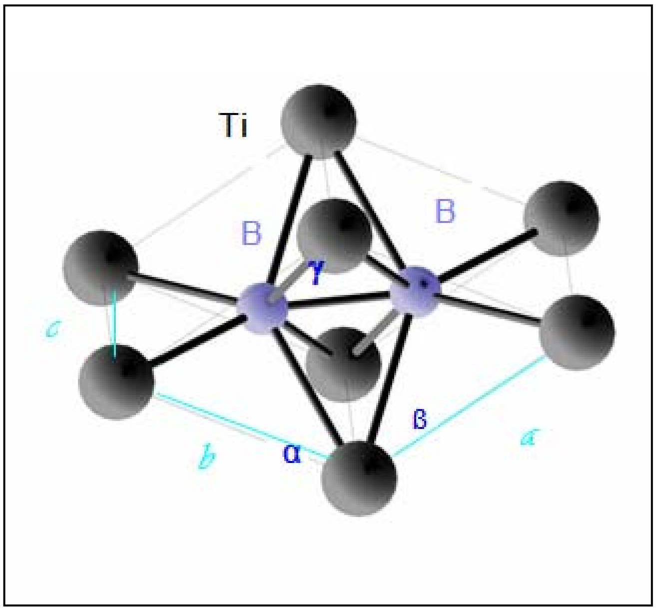

Fig.2.1: Scheme of the crystal structure of TiB_2.

Properties

TiB_2 is an excellent conductor of both electricity and heat, a property very rare among ceramic materials. Some typical thermal data for this material found in the literature are as follows: Thermal expansion $8.1 \times 10^{-6} K^{-1}$ and thermal conductivity 60-120 W/mºK [6].

Apart from its thermal properties, the material presents an outstanding array of mechanical and physical properties that explain the interest and use of TiB_2 in both bulk and powder state for different engineering applications. The following table presents a summary of the main properties of TiB_2. The values therein presented correspond to specimens with a purity of more than 98% and a density of 4.5 ± 0.1 g/cm^3 [7].

Property	20ºC	500ºC	1000ºC	1200ºC	1500ºC	2000ºC
Compressive strength (MPa)	1.8	-	-	-	-	-
Single crystal Density (g/cm^3)	4.500	4.449	4.389	4.363	4.322	4.248
Elastic Modulus (GPa)	565	550	534	-	-	-
Flexural strength (MPa)	400	429	459	471	489	-
Fracture Toughness (MPa m$^{1/2}$)	6.2	-	-	-	-	-
Friction coefficient[a]	0.9	0.9	0.6	-	-	-
Hardness[b] (GPa)	25	11	4.6	-	-	-
Lattice parameter[c] Å	3.029	3.039	3.052	3.057	3.066	3.082
Poisson´s ratio	0.108	0.108	0.108	-	-	-
Shear Modulus (GPa)	255	248	241	-	-	-
Specific Heat (J/Kg.K)	617	1073	1186	1228	1291	1396
Thermal conductivity (W/m.K)	96	81	78.1	77.8	-	-
Thermal Diffusivity (cm^2/s)	0.30	0.17	0.149	0.147	-	-
Thermal expansion ($10^{-6}K^{-1}$)	6.4	7.0	7.7	7.9	8.3	8.9
Weibull Modulus	11					

Table 2.1: properties of TiB_2 [7].

[a] Density 4.32 g/cm^3, grain size 2 µm, V_{slide} /P_{load} = 0.2 ms^{-1} MPa^{-1}

[b] Vickers indentation, load = 5 N

[c] Single crystal, hexagonal unit cell.

Applications

Titanium diboride was originally developed for military applications due to its hardness and temperature resistance. Hence, it was first used in lightweight armours for the US tanks. Nevertheless its excellent combination of properties led soon to its use for other applications such as nozzles, seals, cutting tools, dies, wear and corrosion resistant components etc. [3].

Nowadays TiB_2 is much used in crucibles due to its high melting temperature and chemical inertness. These properties combined with its electrical conductivity have open new applications for TiB_2 in the field of primary aluminium smelting sector as cathodes or melt metals handling tools [2].

2.2.2 TiB_2 as grain refiners for aluminium alloys

2.2.2.1 Introduction

The addition of solid particles into a metallic melt prior to the casting step to nucleate the formation of finely equiaxed grains is known as inoculation. These particles act as nucleation points for the α-Al grains at small undercoolings. The final purpose of adding these inoculants in aluminium alloys is to restrict the formation of columnar grains in favour of equiaxed ones, obtain a uniform size distribution and decrease the average size of the grains. All these features have a positive effect in different properties of the final components (surface quality, reduced hot tearing tendency, improved machining, strength, response to thermal treatments, reduced porosity and microshrinkage levels). These additives are also known as grain refiners and have been used in the aluminium industry for more than 50 years. Grain refinement is technologically attractive because it generally does not adversely affect ductility and toughness, contrary to most other strengthening methods [8].

There are many factors that influence the solidification of aluminium alloys and there are four main methods for achieving grain refining in aluminium alloys; Rapid cooling, mechanical agitation, ultrasonic vibration and addition of a grain refiner. The latter is the most extensively used in the industrial environment due to its low cost and effectiveness. The grain refinement phenomenon produced by the action of the so called grain refiners with aluminium alloys have been historically explained by two main theories: The peritectic nucleation theory and the boride-carbide theory. Presently the latter is less accepted than the former [9].

Grain refiners act as nucleation sites on which a small number of aluminium atoms get joined in stable clusters to form the α-aluminium grains. Nucleation is a thermodynamic process in which a small number of atoms form a stable cluster, called nucleus, within the liquid phase at the solidification temperature. In homogeneous nucleation, the rate of nucleation is dependent on the magnitude of the undercooling i.e. the difference between the equilibrium melting temperature T_m and the freezing (solidification) temperature T_f [8]. The undercooling temperature controls the nucleation process, the lower the undercooling the more probabilities exist for the nucleant agent to work as a nucleation site. Furthermore the activation of the nucleant agents at smaller undecoolings makes equiaxed growth more likely to block columnar growth that is the other solidification process that is derived from the temperature difference within different regions of the cast. Solidification may begin earlier in the environment of cold mould surfaces but this phenomenon leads to a columnar grain growth that is undesirable as the mechanical properties obtained are lower than with equiaxed grains. It is accepted that if there is crystal structure matching between solid particles in the melt and solidifying metal and the difference in the atomic spacing is less than roughly 12%, nucleation of solid can occur on the particle surfaces and grain refinement will be observed [10].

YS and grain size have been found to be related by the Hall-Petch equation for a wide range of metals and alloys. This states that $\sigma_y = \sigma_0 + k_y d^{-1/2}$. Grain refinement provides smaller values for both the secondary dendrite arm spacing and grain size. These parameters directly influence the YS of the final product due to a decrease in the mobility of the dislocations and furthermore they lead to an increase of the UTS due to the decrease of the size of the defects, mainly porosity and microshrinkages [11].

The most widely used grain refiners in the aluminium industry are those belonging to the Al-Ti-B series (Al-5Ti-1B, Al-5Ti-0.2B, Al-3Ti-1B and Al-3Ti-0.2B) even though special refiners such as Si-1B, Al-B, Al-10Ti or Al-3Ti-0.15C have also been used for aluminium alloys. The major problems with the Al-Ti-B family of refiners is the tendency to particle agglomeration and susceptibility to poisoning elements such as Zr or Si that may react with the nucleant element surfaces to form non active compounds [12].

2.2.2.2 Solidification of aluminium alloys

The solidification mechanisms of aluminium alloys have long been studied as the control of its parameters has a direct influence on some of the final properties of the alloys or components produced. A good control of the solidification that permits to obtain a fine equiaxed α-aluminium grain structure may avoid microstructural and surface defects on the final products, decrease the cost of the final component and increase the mechanical properties. One of the methods to obtain this kind of structure is the addition of inoculants or so called grain refiners, i.e. master alloys containing powerful nucleating particles such as TiB_2 or $TiAl_3$ (e.g. Al-Ti-B master alloys). The mechanisms involved in the control of the shape and size of the grains are not yet totally understood. Some questions as the growth of the grains in the presence of different solutes, the role of each constituent or observations recorded for the Al-Si alloys remain open to discussion.

Solidification of a melt may take place from the edge of the castings that is in contact with the internal surface of the mould inwards. The heat dissipation forms a thermal gradient in the melt and the heat in the central region of the casting can be extracted through it. This mechanism produces grains with a columnar morphology in which the grains are oriented and grow anti-parallel to the mentioned thermal flow. This phenomenon is also called homogeneous nucleation. Columnar grains are reported to reduce YS and UTS [13]. Hence, equiaxed morphologies are preferred because the final properties of the material are usually considerably better. Equiaxed grains are formed in the melt ahead of the solidification front either on inoculant particles that have been deliberately added to act as nucleants or on impurities in the melt. Equiaxed grains grow initially as spheroids but finally the grain becomes globular-dendritic due to the instability of the interface. Eventually highly branched dendrites are formed that are typical of equiaxed grain morphologies. This is also known as heterogeneous nucleation. The solidification rate and presence of solutes directly affects the final shape and size of the dendrites and the phenomena involved are quite complex due to the interaction of different factors.

***Heterogeneous nucleation models of α-Al grains* [14]**

The formation of stable α-Al crystallites has been explained through the classical heterogeneous nucleation theory whereby a transfer of atoms from the melt to the α-Al phase is facilitated by inoculant particles. The α-Al phase is considered to have a contact or wetting angle θ with the substrate. The work required to create a stable crystallite decreases in function of the wetting angle.

Other theories are based on the undercooling concept. When the melt metal is in the undercooled state, its temperature is lower than the temperature in equilibrium. The solidification begins at a T that is lower than that of the solidification temperature. Thus, the smaller the undercooling required for a grain of α-Al to form on a particle, the higher the potency of the particle. Particles found in Al-Ti-B and Al-Ti-C refiners (TiB_2, TiC and $TiAl_3$) are very potent nucleants, the nucleation undercooling is less than 1 K implying that wetting angles are small. Kim and Cantor developed an adsorption model for the initial formation of solid, in which a monolayer of liquid at a substrate/melt interface was considered in a binary system [15]. Greer and co-workers used the findings of the adsorption model to develop an alternative criterion for the initiation of grains [16]. Schumacher et al. showed that α-Al forms only on {0001} faces of TiB_2 particles [17]. If α-Al forms and extends over the whole {0001} face with reasonable ease, then subsequent growth must occur outwards which initially increases the curvature of the α-Al/melt interface. If the undercooling is sufficient for the crystallite to reach a hemispherical shape, subsequent growth will decrease the curvature of the interface; therefore, no further increase in undercooling is required for growth to continue. The undercooling ΔT_{fg} required to achieve this state of free growth is given by:

$$\Delta T_{fg} = \frac{4\,\sigma_{lc}}{\Delta S_v\, d_{part}}$$

Where d_{part} is the diameter of the {0001} face of the inoculant particle and ΔS_v is the volumetric entropy of fusion. The free-growth undercooling is inversely related to particle size; hence, as the undercooling increases, the larger particles become active first. If the free-growth undercooling is larger than that required for nucleation, the barrier to free growth determines the activation of inoculant particles. Hence, the term grain initiation was coined to describe the complete process of formation of a freely growing α-Al grain.

2.2.2.3 AL-TI-B systems as grain refiners

The Al-Ti-B grain refiners have been the preferred choice for controlling the as cast structure of aluminium alloys since the 1950´s. The addition of these materials improves homogeneity, reduces porosity, eliminates hot tearing, improves responsiveness to subsequent heat treatment, enhances mechanical properties and machining. They are used in the aluminium industry mainly to prevent ingot cracking during casting, to enhance surface finish and as a means of improving mechanical properties. Al-Ti-B grain refiners are three phase alloys that contain TiB_2 and $TiAl_3$ particles mixed with very small amounts of Ti and B in solid solution in an aluminium matrix [13, 18-19]. When added to the melt, the grain refiner melts and the dilution of the titanium content leads to rapid dissolution of the $TiAl_3$ at Ti concentrations lower than 0,15 atm. %, i.e. the hipoperitectic compositions, while the TiB_2 remains stable [12]. According to the binary Al-Ti phase diagram, liquid Al can dissolve around 0.15 at. % Ti at 720ºC. The standard terminology in the grain refinement literature is that 0.15 atm. %. Ti is referred to as the peritectic concentration [20]. The amount of Ti added to liquid Al in the form of master alloy (Al-5Ti-B) for 0.2 vol. % addition rate is only 0.01 vol. %. This amount of Ti is much lower than the solubility limit at the operating temperature. Hence, at this composition, $TiAl_3$ particles are not stable in liquid Al and tend to dissolve. TiB_2 is a more thermodynamically stable phase compared with $TiAl_3$ but a longer time is required to produce this phase. In the presence of excess boron, in the form of AlB_{12}, $TiAl_3$ will decompose fast by reacting with AlB_{12} to form TiB_2 (AlB_{12}) [21-22]. The peritectic reaction occurs at approximately 665ºC. Boron encourages the peritectic reaction to take place even at Ti concentration levels that are well below the 0.15 atm. % threshold limit by significantly reducing the solubility of Ti in aluminium [23].

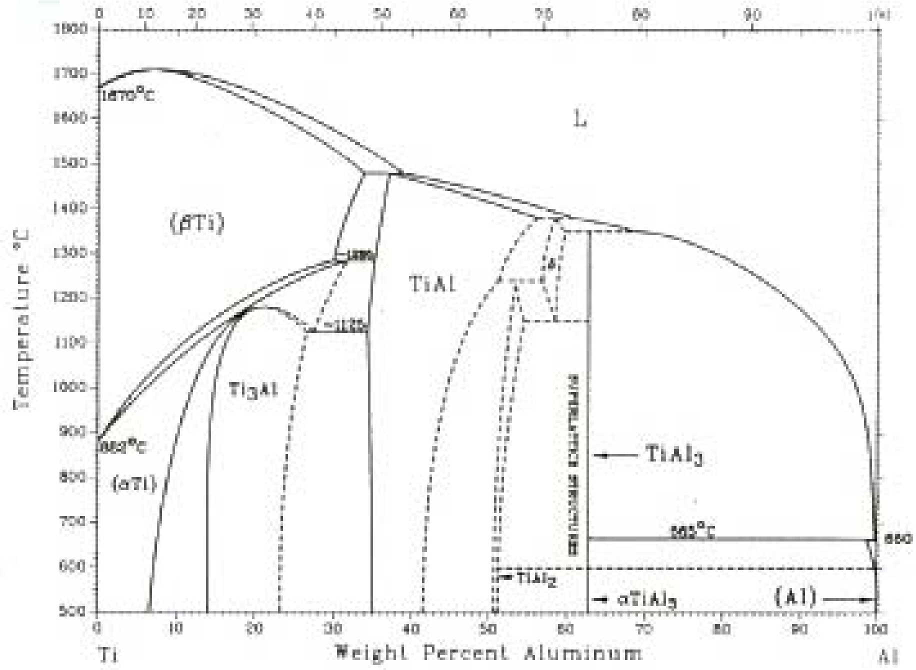

Fig. 2.2: Al-Ti phase diagram.

Peritectic reaction: $\boxed{\textbf{Liquid} + \textbf{TiAl}_3 \longrightarrow \alpha\textbf{-Al } (665^{o}\textbf{C})}$

Two main theories have been developed to account for the grain refining effect of Al-Ti-B compounds. The Carbide Theory due to Cibula (1949-1952) coexisted with the Crossley and Mandolfo´s Peritectic Theory (1951) for many years but now the latter is much more accepted. The peritectic nucleation theory proposes that some transition elements present in the melt (Ti, Zr, Cr, Mo, W) undergo a peritectic reaction with aluminium. α-aluminium is nucleated on the surface of the $TiAl_3$ particle after the concentration of Ti around it has attained a critical level for initiating the peritectic reaction. According to this theory, once the particle is enclosed by the α-aluminium the new grain grows by means of the diffusion of Ti through the initial solid α-aluminium layer. Eventually the nucleus attains a critical size to allow the dendritic growth of the grain. The boride-carbide theory proposed that nucleation of aluminium initiated on the surface of TiC and/or TiB_2 particles after the addition of the corresponding master alloy but this theory is not able to explain all the related phenomena discovered in the last years such as the confirmation that these particles cannot nucleate α-aluminium grains by themselves without the presence of Ti [9].

Discrepancies exist on which is the actual nucleation mechanism and main nucleant agent in the system but nowadays it is generally accepted that, even though $TiAl_3$ is a better nucleant than TiB_2, the latter is the nucleant agent in the hipoperitectic compositions.

Nevertheless the need of all Ti, TiB_2 and $TiAl_3$ in the solidification process has been stressed in all the main recent publications that have approached this subject. The {110} planes of $TiAl_3$ match well with the {112} planes of α-aluminium. The lattice disregistry between the two planes is lower than 2% and therefore α-aluminium grains can nucleate very easily there. It is accepted that atomic spacing mismatches or disregistries lower than 12% allow nucleation phenomena [10, 20]The lattice disregistry between TiB_2 and α-aluminium is 4.3% for $(111)_{AL}//110)_{TiB2}$ and even though it is larger than with $TiAl_3$ it is still very low and therefore TiB_2 should also be a good nucleant. The $TiAl_3$ forms large (usually 30-40 μm size), coarse and brittle particles that have an undesirable effect on the properties of the aluminium alloy components and therefore industry standards tend to keep the Ti content below the peritectic percentage where $TiAl_3$ is not a stable phase and therefore apparently TiB_2 particles are the only nucleation sites available in the melt during solidification [8]. Even so, two mechanisms have been proposed to explain the nucleation event. Nucleation takes place either through a layer of $TiAl_3$ that is surrounding the TiB_2 particles or a mixed boride $(Al,Ti)B_2$ is found which is the active nucleant agent. Different theories have been proposed that would explain how $TiAl_3$ phases could be preserved locally by the presence of TiB_2 particles even in hypoperitectic alloys. One suggests that a shell is formed around the former by the latter [24] and the duplex nucleation theory explains that TiB_2 particles are surrounded by $TiAl_3$ layer that is further surrounded by the α-aluminium [8].

On the other hand the major problems when using Al-Ti-B systems are susceptibility to particle agglomeration and to poisoning. It must be always taken into account that they are known to be adversely affected by zirconium, silicon and chromium. The presence of these solutes may have a direct fading and poisoning effect on the grain refiner. The poisoning effect of Zr is essentially due to the formation of complex aluminides containing Ti and Fe, Ti aluminides containing Zr and Fe aluminides containing Zr and Ti [22, 14].

2.2.3 TiB_2 as reinforcements for aluminium alloys

2.2.3.1 Introduction

The origin of MMCs dates back to the 1950s and early 1960s. Boron fibre reinforced aluminium alloys and tungsten reinforced copper attracted the attention of researchers in those first years and the use of boron/aluminium composites in the Space shuttle struts was one of their first significant applications. Afterwards the application of a MMC diesel piston insert by the Japanese firm Toyota in the 70s represented a milestone for the industry. Nevertheless nowadays the use of MMCs in industrial applications is much lower than foreseen in the 70s. In 1990 the worldwide market of MMCs was estimated to be between 3-37 million US $ and in 1999 it was estimated to be around 103 million US $ [24]. 62% of this volume was within the ground transportation applications and 26.5 % in thermal management applications. Aerospace comprised around 5.4% of the total market [24-25].

In this kind of materials a continuous metallic or intermetallic matrix embeds a continuous or discontinuous reinforcing phase that can be presented in several different shapes (continuous fibres, particles, whiskers, short fibers) and composition (C, SiC, B_4C, Al_2O_3, TiB_2). The resulting materials have attracted the interest of the industry and research organisations due to the excellent combination of properties they exhibit; high specific mechanical properties, high and tailorable thermal and electrical conductivity, low to moderate CTE, good wear resistance, good behaviour at high temperatures etc. MMCs present several drawbacks though. Even though the too high final cost of the materials remains the most important barrier that prevents their use in many technically suitable applications already identified, there are other aspects that must be improved to increase the use of these materials such as difficulties in secondary processes, too low ductility and toughness, anisotropy, lack of data regarding the behaviour at long term, lack of data for modelling and simulation as well as lack of standardisation.

MMC materials are usually produced by casting or by powder metallurgy, although common processes also include diffusion bonding, liquid phase sintering, squeeze infiltration and stir-casting. They offer a wide range of advantages compared to ordinary metals. They have greater strength, improved stiffness, reduced density, improved high temperature properties and tailorable CTE. However, there are several disadvantages that have not yet been solved. These include: higher cost than conventional materials, lack of technology maturity and limited service experience.

Types of MMC materials

There is a wide range of metals that have been used as matrices but the most important ones are: aluminium, magnesium, titanium, copper, iron, steel and superalloys. Nevertheless MMCs are more usually classified according to the reinforcement shape:

* *Continuously reinforced MMCs:*

They comprise a metal or intermetallic matrix, usually an alloy of Al, Ti, or Cu, reinforced with a continuous reinforcement (typically fibre tows of either C or Al_2O_3, or monofilaments of B or SiC, with diameters below 20 µm). Continuous reinforcements are very sensitive to chemical attack by the matrix, since even a small amount of interaction can significantly decrease the reinforcement strength. A protective fibre coating along the axis of the reinforcement should be used (transverse properties of these materials are much poorer).

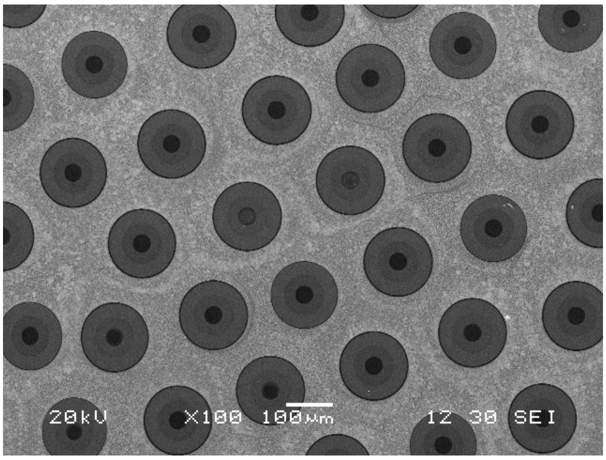

Fig. 2.3: Titanium matrix composite reinforced with continuous SiC monofilaments. (Source: Fundación Inasmet).

* ***Discontinuously reinforced MMCs:***

They comprise a continuous metal or intermetallic matrix, typically alloys of Al, Mg, Ti, Cu, steel, Co and Ni and a discontinuous reinforcing phase. Reinforcements are usually SiC, Al_2O_3, C, B_4C, TiB and TiB_2. They are far less sensitive to chemical interactions between the reinforcement and the matrix than continuous MMCs. Discontinuous MMCs are now commercially available in a wide range of product forms: castings, forgings, sheet and extruded forms. Their physical and mechanical properties are largely isotropic. Furthermore the properties are tailorable as a result of the flexibility in the size, volume fraction, composition and morphology of the reinforcement as well as the possibility to vary the matrix alloy composition and apply thermal treatments.

There are three different types of discontinuous MMCs:

- Particulate-reinforced metal matrix composites (PMMC)
- Whisker or short fibre-reinforced MMC (SFMMC)
- Discontinuous fibre-reinforced MMC (DFMMC)

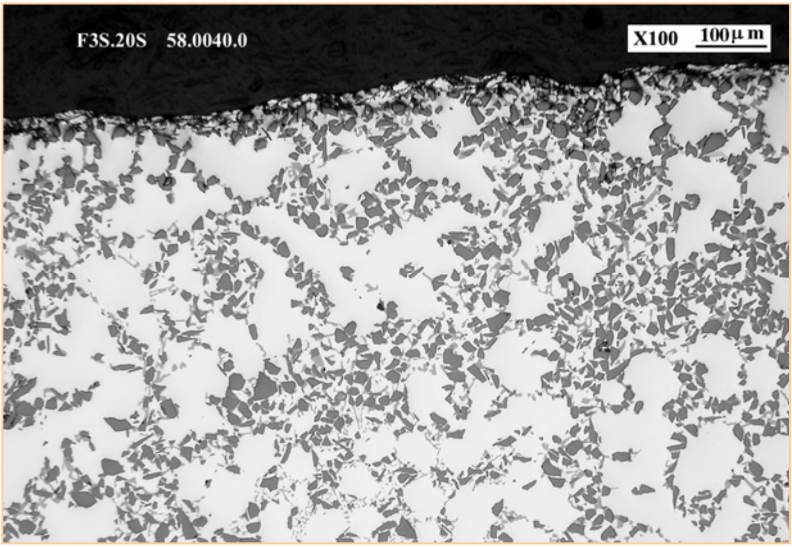

Fig. 2.4 Optical microscopy image of a sample of aluminium matrix composite reinforced with 20% of SiC particles. (Source: Fundación Inasmet).

2.2.3.2 Particulate reinforced aluminium alloys

Particulate reinforced MMCs are combinations of a metal or alloy and particles of a second phase, deliberately introduced to improve its properties, that have an aspect ratio lower than 5 [26]. Even though particulate reinforced MMCs present lower mechanical properties than short fiber and continuously reinforced metals, they have been the most used ones in industrial applications. The main reasons that explain this fact are:

- Lower cost of the reinforcement and composite.
- Ease of secondary processes (melting, machining, casting).
- Isotropic properties.
- Commercial availability.

Excellent combination of properties achievable like high wear resistance, good specific mechanical properties, low CTE, good mechanical properties at high temperatures.

They commonly contain below 25 vol. % reinforcement when used for structural applications, but can have as much as 80 vol. % reinforcement when used for electronic packaging applications. They can be produced using both solid state (powder metallurgy) and liquid metal techniques (stir-casting, infiltration).

The most notable commercial use so far is in braking systems of trains and cars, but they have also been successfully used in other components in automotive and aerospace industries as well as the electronic industry that applies high reinforcement content materials with very low CTEs and high mechanical properties. They are also currently being used in applications such as components for helicopters, golf club shafts and heads, horseshoes, bicycle frames, car pistons, tyre studs etc.

TiB_2 particles have been used as reinforcements for MMCs for more than 15 years. When compared to other traditionally used ceramic reinforcements (SiC, Al_2O_3 and C) they present several distinct advantages that have attracted the interest of the researchers and industrial sectors in the last decades. TiB_2 as a reinforcing phase in aluminium matrix is easy to handle and does not produce any brittle phase like in the case of SiC or Al_2O_3 reinforcements that may lead to the formation of Al_4C_3 or $MgAl_2O_4$ with Al alloys containing less than 5% Si and some Mg respectively [21].

Following a short list of the main commercial applications of particulate reinforced MMCs is presented showing the nature of the materials selected and the main reasons that led to their selection.

- **Brake rotors for the German high speed train ICE-2**

Brake rotors for the German high speed train Inter City Express 2 have been developed by Knorr Bremse AG and made of particulate reinforced aluminium alloy AlSi7Mg0.3 + 20 wt. % SiC particulates. The brakes are produced by sand casting and similar concepts have been used in Copenhagen for S-bahn trains. Compared to conventional parts made out of cast iron with 120 Kg/part, the 76 Kg of the MMC rotor offers an attractive weight saving potential. It is calculated that a saving of up to 500 kg. in each boogie can be achieved with this approach. Furthermore heat dissipation is improved and the resulting component presents a large wear resistance.

- **Brake rotors and drums for automotive applications**

A number of different applications have appeared in the last years related to components of the braking system. Volkswagen uses an Al-Si alloy reinforced with 20-30% of SiC particles in the rear brake drums of their Lupo-3L TDI model (weight of the drum 1.55 Kg.). The material is cast by the German company Kolbenschmidt and Volkswagen carries out the final machining. Similar concepts can also be found in the Toyota RAV-4EV vehicle, the Plymouth Prowler, Ford Prodigy or Lotus Elise.

- **Ti-MMC exhaust valves**

These valves were manufactured via a cost-effective powder metallurgy process. The exhaust valve was made of a titanium metal-matrix composite, specially designed for mechanical properties at elevated temperatures of up to 876ºC [27].

The new material had to compete with other alternative materials such as the X53 CrMnNiN 21 9. It offers an excellent balance of characteristics including static strength, fatigue resistance, creep resistance, and oxidation resistance at room temperature and elevated temperature. The studies carried out to select the adequate material led to the selection of the TiB reinforced Ti alloy [27].

- **Eurocopter blade sleeves**

The rotor blade sleeve is in service on Eurocopter France N4 and EC120 helicopters. The large centrifugal loads of each rotor blade (the N4 has five blades) are supported by a blade sleeve, which holds the rotor blade to the drive shaft. This is the first discontinuously reinforced application for Class 1 rotating parts in aeronautical components and was forged by Forges de Bologne in France [28]. These blades were formerly produced with titanium alloys but the forged 2009/SiC/15_p composite material was later selected due to the lower component weight and higher specific properties they present. The 2009/SiC/15p-T4 material has fatigue strength of 270 MPa at 10^7 cycles, compared to 155 and 180 MPa for 2024-T4 and 7075-T6, respectively [29].

- **Electronic packages**

One of the most extended applications for MMC materials is the electronic packaging field. There are different levels of packaging that present different thermal and mechanical requirements and MMCs have already shown its validity and cost competitiveness in many areas [26, 29-30]. A high thermal conductivity is required and the value of the CTE is also important. Electronic packaging materials must match the CTE of the surrounding materials in order to avoid the building up of residual stresses.

2.2.3.3 TiB_2 particles as reinforcements for aluminium alloys

The first works in the production of Al/TiB_2 composites by the Lanxide technique in which aluminium preforms were oxidised by borides to produce the desired TiB_2 particles were published in 1986 [31]. Afterwards in 1998 elemental powders were mixed through powder metallurgical methods and compacted in an exothermic reaction in aluminium powders. Kuruvilla et al. created similar composites through powder metallurgy processes in 1991 [32] and finally the idea of creating in situ MMCs containing TiB_2 particles as the main reinforcing phase was first patented in 1992 by Davies et al. [31]. It was a logical extension of the work done in the production of grain refining master alloys for the aluminium industry based on the Al-Ti-B system. The process is known as flux assisted synthesis (FAS) and was significantly more cost effective than the previously approached methods. Similar materials have been subsequently produced through different technologies like SHS (self propagating high temperature synthesis), reactive infiltration or stir casting technologies [33]. The positive effect of adding these master alloys containing TiB_2 and $TiAl_3$ particles to the aluminium melt was first discovered in the 1950s. The addition of a small percentage of TiB_2 particles (less than 0.2 vol. % is required for refining purposes) had a direct influence in the grain size and associated features of the aluminium alloys. With the advent of the MMCs concept and the discovery of the outstanding properties obtained when different ceramic and metallic reinforcements were added to the aluminium alloys, the first experiments were carried out to increase the TiB_2 content in the melt and produce MMCs based on this system. The production mechanisms first tried were similar to those used to produce the master alloys for grain refining purposes. Salts containing B and Ti were added to the aluminium melt so that they could react and create the particles in situ. In this way MMCs containing up to 8 wt. % of in situ created TiB_2 particles were produced that could be used in secondary forming processes.

TiB_2 based AMCs can be created both through in situ and ex situ processes, i.e. by the in situ reaction of chemical substances that react in the metallic melt to produce the TiB_2 particles or by exogenously adding TiB_2 powders to the melt and dispersing them through mixing techniques.

The main advantages of the in situ materials over ex situ formed composites are: a) the size of the particles is usually lower due to the little time needed to create particles with higher strength and better load transfer possibilities and lower propensity for particle fracture, b) the interfaces between the particles and the matrix are cleaner and they are thermodynamically stable particles [34], c) the material can be easily machined and it can keep its mechanical properties at higher temperatures due to the stability of the particle-matrix bonding.

The presence of TiB_2 particles into aluminium alloys in amounts of more than 5 wt. % increases the E, YS and UTS. At the same time thermal properties such as CTE and thermal conductivity are also directly influenced. Several different research groups have studied the effect of the presence of these particles in different properties of the final products. Tee et al. [33] report that the in situ TiB_2 particles (with sizes of 1-3 μm) formed in the aluminium yielded an improvement of 57% increase in UTS, 66% in YS and 22% in E in an Al/TiB_2 15 vol. % composite. Sprenger et al. found that the addition of only 8 wt. % of TiB_2 to Al-Si7Mg0.3 produced an increase of 15% in the E, an increase of 20% of the UTS, an increase of 30% in the YS but a great reduction, 5 times, in the elongation to fracture when compared to the unreinforced alloy [29]. Nevertheless there is a large dispersion on the data provided in the literature and there are even some studies in which the positive effect of the presence of TiB_2 particles is denied [35].

On the other hand, the main drawback of in situ composites is that the particles that do not act as nucleating sites tend to be pushed by the solidification front and have a tendency to agglomerate in the grain boundaries to reduce the interfacial energy. Furthermore the cost of the final material continues to be too high and even though the secondary processes needed to produce industrial components are not difficult, due to the small size of the particles, there has not yet been any commercial application for TiB_2 reinforced aluminium composites. Up to now the composite materials that can be processed through traditional forging or casting processes (high pressure diecasting, gravity casting, investment casting, etc.) present a maximum TiB_2 particle content of 6-8 wt. % and no applications have yet been found in an industrial scale where the improvement of properties that is achieved compensates the increase in the cost of the final component.

In situ produced Al/TiB_2 composites

There are different in situ processes that have been used to produce TiB_2 MMCs. The most extensively used is known as the FAS. It is based on the production of Al-Ti-B master alloys applied for grain refining purposes. The reinforcement is obtained through the metallothermic reduction of K_2TiF_6, KBF_4 and liquid aluminium [21]:

$$K_2TiF_6 + 2KBF_4 + 10/3Al \rightarrow \mathbf{TiB_2} + 4/3(3KF.AlF_3) + 2AlF_3$$

Other reaction sequences have also been proposed to produce similar compounds by other authors [36-37]:

$$1)\ 3K_2TiF_6 + 13Al \rightarrow 3TiAl_3 + 3KAlF_4 + K_3AlF_6$$

$$2)\ 2KBF_4 + 3Al \rightarrow AlB_2 + 2KAlF_4$$

$$3)\ AlB_2 + TiAl_3 \rightarrow \mathbf{TiB_2 + 4Al}$$

K_2TiF_6 and KBF_4 react with the molten Al to produce some intermediate compounds, $TiAl_3$ and AlB_2. Afterwards the reaction between them takes place and Ti and B ions are released and diffuse into liquid Al. When they reach saturation, they will be separated out as the intermetallic compounds TiB_2, $TiAl_3$ and AlB_2. Furthermore a cryolite (K_3AlF_6) and KF mixture is formed due to excessive KF that must be further separated. The process ends when the remaining rests of the salts are eliminated together with any possible byproduct material or contamination [37].

The flux assisted in situ formation synthesis of London & Scandinavian Co. is based on its aluminium grain refining master alloy production technique and was developed in the 90s. Salts of potassium hexafluorotitanate (K_2TiF_6) and potassium tetrafluoborate (KBF_4) are introduced into a stirred aluminium melt with an atomic ratio in accordance with Ti/2B. The following reaction has been proposed to account for the observed results [21]:

$$K_2TiF_6 + 2KBF_4 + 10/3Al \rightarrow TiB_2 + 4/3(3KF.AlF_3) + 2AlF_3.$$

Ex situ produced Al/TiB_2 composites

The production of ex situ Al/TiB_2 composites has also been studied in the last years. The main purpose of this technology is to avoid the presence of the rests of salts and other byproducts of the chemical reactions involved in the production of in situ TiB_2 that cannot be totally eliminated. Furthermore the addition of TiB_2 powders has been used to improve the segregation of the reinforcements and provide a more homogeneous distribution of the reinforcements within the melt in in situ based synthesis.

A combination of both in situ and ex situ processes is also possible. Once the in situ reaction is finished the slag is removed to eliminate the rests of the salts in it. The incorporation of the powders can be carried out through different methods but the most preferred one is to add the exogenous TiB_2 particles to the fluoride melt, $KMgF_3$ and K_3AlF_6, in contact with molten Al. The process can be therefore considered as a combination of in situ and ex situ processes. The main goal would be to positively affect the final dispersion of boride particles [21]. The U.K. company London & Scandinavian Ltd. has worked in this process by combining both in situ and ex situ TiB_2 particles with the aim of obtaining a cleaner product than that obtained with the in situ process but maintaining the positive features of the process (clean interfaces of the in situ reinforcements with aluminium matrix and particle sizes of less than 1.5 µm) [38-39]. The main objective of combining the two kind of particles is that the final product be much cleaner than that obtained in the 100% in situ process (much less concentration of rests of salts etc.) but that the presence of in situ created particles of low size (typically lower than 1 µm particles with a clean interface with the aluminium matrix) were guaranteed. The thermodynamic stability between the reinforcement and the matrix is higher in the in situ processes and the interface is inherently cleaner. Another important feature is that the thermodynamic stability is a positive factor to keep the mechanical properties of the materials at elevated temperatures and that particles so created tend to be small and they are less prone to particle cracking during processing or when submitted to external stresses.

2.3 PLASTER CASTING OF ALUMINIUM ALLOYS

2.3.1 Introduction. Generalities

Plaster casting is a metal casting process that is part of the lost wax foundry technologies. The fundamentals of these technologies are based on the use of expendable patterns that are invested (lost wax processes are also known as investment casting or precision casting processes) by a refractory slurry (ceramic or plaster materials) that form the mould cavity in which the melt metal will be subsequently cast. Even though it is the most ancient foundry technology, it is presently used to produce some of the most complex and technologically advanced components and lost wax applications can be founded in all aeronautical, electronic and automotive sectors. The main features of lost wax technologies that make them so demanded by these markets are the following ones:

¤ *Possibility of casting extremely intricate parts due to the expendable nature of the pattern. Each casting requires a sacrificial model. Lost wax processes are suitable for both small and large castings.*

¤ *Very high surface quality and dimensional tolerances that cannot be attained with most of the other casting technologies.*

¤ *Adaptable to all kind of ferrous and non ferrous alloys.*

On the other hand, lost wax processes tend to be laborious and slow and require a high degree of specialization of workers and with large direct labour costs. It is most suitable for high added value medium sized volume productions.

The different variants of the process that have been developed along the long history of lost wax can be classified according to different criteria. Plaster casting is the variant in which the mould is composed of refractory plasters.

2.3.2 Plaster casting process

There are two main plaster casting variants. On the one hand, there is the plaster mould casting process (also known as rubber plaster moulding) which employs permanent models composed of silicone and on the other hand the plaster block mould investment casting process which employs expendable patterns.

Both processes present an exceptional surface quality and tight tolerances and the main difference between them is the extra design freedom and tighter tolerances (specially across parting lines and cores) that allows the block mould investment casting route at the expense of an increase on the mould manufacturing process cost.

Plaster mould casting or rubber plaster moulding: The process starts with a pattern, which is a replica of the finished casting except it is slightly larger to allow for aluminium shrinkage during solidification and cooling. The pattern can be rigid (made of sealed wood, metal or sealed and lacquered tooling plaster) or flexible (polysulfide, urethane elastomer, rubber or silicone). A flask is placed around the pattern to contain the liquid plaster mixture. When the plaster has set, the hardened plaster exhibits physical properties that allow it to hold the exact shape of the pattern. Once the patterns are drawn for the moulds, the latter are dried in an air circulating oven at around 260ºC until there is no moisture present. When cores are required, they are placed in the drag prior to assembly of the cope.

Block mould investment casting: The process consists of producing a replica on wax or plastic of the part to be produced. This replica (or pattern) is assembled to a filling and feeding system of similar material. This assembly is coated (or invested) with the plaster based refractory slurry. After allowing the plaster to set, the mould is placed into a furnace at around 150-180ºC to be dewaxed. The mould is then heated or fired to burn off the residual wax and to obtain the refractory properties needed to withstand the casting step. When the firing cycle is completed molten metal is cast into the preheated mould.

It can be said that the key feature of both processes is the material employed for making the moulds: *The plaster bonded investment material*.

These plaster based mixtures are basically special blends composed of:

- Bonding agent. Plaster of Paris or Calcined gypsum (calcium sulfate semi-hydrate).

- Refractory filler. About 40 - 75% of the whole mixture. The most commonly used refractory materials for aluminium investment formulation are crystobalite or quartz (occasionally a mixture of the two) that are usually present in a range of 55 – 75%. Both are allotropic forms of the silica. The main function of the filler material is to avoid mould cracking due to plaster shrinkage when dewaxing and firing.

- Additives and modifying agents. About 5% of various additional compounds or additives. Small amounts of additives are added to many commercial investment powders in order to adjust their properties to the intended application (e.g. accelerators or retarders to control the setting rate, reducing agents to protect the cast metal, expansion modifier agents, antifoaming agents to aid in the elimination of the air from the mixture during de-aeration or vibration operation, wetting agents to enhance the investment mixture fluidity properties, rheology agents, reinforcing fillers for the improvement of the mechanical properties of the mould, etc.).

These plaster blends are formulated to meet specific requirements. The required performances will depend on:

- The intended moulding and casting process.
  - Rubber plaster moulding or block mould investment casting.
  - Gravity, vacuum, centrifugal or pressure assisted casting.

- Alloys to be cast.
  - Aluminium, magnesium, copper, zinc, noble or semi-noble alloys.

- Component features.
  - Component size or weight and geometry or complexity.

In general terms the investment materials used for metal casting processes should meet the following features:

1- Refractory properties. The mould has to keep its physicochemical properties during the process steps, burning out of the model and casting of the metal.

2- Mechanical properties. The mould has to keep its integrity without cracking during the elimination of the pattern, burning out stage and heating to thermal treatment and casting the metal.

3- Surface finish. The mould composition should provide a smooth surface.

4- Permeability. The mould should be permeable to allow air (and if the case, generated gases) evacuation when filling the mould.

5- Easy demoulding. The mould material has to be easy to remove.

Setting Behaviour

When plaster or calcium semi-hydrate is mixed with water an over-saturated semi-hydrate solution is formed. The semi-hydrate reacts with water to give the stable bi-hydrate which is less soluble. The aqueous phase is therefore super-saturated with respect to the bi-hydrate, which crystallizes out at suitable nucleation centres in the suspension. Thus, once more, the water can dissolve more semi-hydrate material, over-saturating, reacting and re-crystallizing to bi-hydrate until all the mass is transformed.

The setting operation starts after 2–3 minutes and ends 15–20 minutes later, releasing heat and producing an increase of the temperature of around 20ºC. The re-crystallization reaction is an exothermic reaction. As a consequence of this re-crystallization a mass expansion of about 1% can be observed. This special dilatation feature is very interesting to reproduce small details and it is one of the reasons that explains the use of the plaster for moulding applications.

2.3.3 Aluminium based plaster casting alloys

The plaster casting process allows the use of any aluminium casting alloy and in fact there is a large amount of possible alloys that can be used in this process. Similarly to other casting processes, alloys belonging to the Al-Si family are used in more than 90% of the applications due to their good castability and balance of cost and properties. The rest of the alloys are mainly used for special applications where the requirements cannot be entirely complied by Al-Si alloys (higher service temperature, corrosion resistance etc.). Following a review of the Al-Si and Al-Cu alloys used for investment casting applications is presented.

2.3.3.1 Aluminium-Silicon alloys

These alloys are used when good castability and good mechanical properties are needed. The silicon increases the fluidity of the melt (up to the eutectic composition, around 11 atm. %), reduces the melting temperature, decreases the contraction associated with solidification and is very cheap as a raw material. Furthermore it has a low density (2.34 g/cm^3), which may be an advantage in reducing the overall weight of the cast component. Silicon has a very low solubility in aluminium. It improves the abrasion resistance and can be combined with other alloying elements such as Mg or Cu to provide excellent mechanical properties.

The aluminium-silicon alloys have exceptional casting characteristics, which enable them to be used to produce intricate castings of both thick and thin sections. Their ductility enables castings to be easily rectified or modified in shape. It is specially suited for castings that need to be welded.

The physical properties of aluminium-silicon alloys are especially advantageous for both small and intricate castings such as motor parts and miscellaneous fittings as well as comparatively large structural shapes. They are generally used with silicon contents of about 3-15% together with a small amount of iron as impurity and containing copper, nickel, zinc or magnesium alloying elements that can be added to obtain enhanced properties.

One of the most popular Al-Si alloys is the Al-Si7Mg0.3 alloy. Following some properties of this alloy in the T6 thermally treated condition are shown:

- Density (g/cm^3): 2.69.
- Coefficient of thermal expansion (10^{-6} ºC^{-1}): 21.4.
- Thermal Conductivity (W/mºK): 152.
- Young´s Modulus (GPa): 72.
- YS 0.2% (MPa): 186.

- UTS (MPa): 262.
- Elongation (%): 5.

2.3.3.2 Aluminium-Copper alloys

Copper is one of the most used alloying elements in the aluminium industry. Copper is added mainly for enhanced strength purposes, achieved by precipitation hardening. It is added in concentrations of up to about 10%, although alloys for structural applications contain smaller concentrations. Aluminium-copper alloys containing 4-5% of copper, with the usual iron and silicon impurities can reach quite high strength values and ductility. However, they have a poor castability and are therefore mainly used for sand casting of not very intricate shapes.

Aluminium copper alloys containing higher copper contents (7-8%), formerly the most commonly used aluminium casting alloys, have been replaced by Al-Cu-Si alloys. Their best attribute is their insensitivity to impurities but they have very low strength and fair castability. Aluminium-copper alloys with a Cu content of 9-11% are in limited use.

The addition of further alloying elements has been tried to overcome the poor castability of Al-Cu alloys. In this sense the most widely used aluminium casting alloys are those containing silicon together with copper. Copper contributes to strength and the silicon improves the castability, increases the soundness of the castings and reduces hot tearings. Wear resistance is increased by the presence of hard phases but there is normally a reduction of ductility and fatigue resistance.

There is an alloy, Al-Cu5MgTi, which has also been used for investment casting applications. It has good machining properties and is used in aircraft parts but it is rather difficult to cast. Magnesium increases the strength and hardness of this alloy through thermal treatment and titanium is used for grain refinement purposes. Its main properties in the T6 condition are listed below [40-41]:

- Density (g/cm^3): 2.80.
- CTE (10^{-6} $^{\circ}C^{-1}$): 25.
- Thermal Conductivity (W/mºK): 140.
- Young´s Modulus (GPa): 72.
- YS 0.2% (MPa): 220.
- UTS (MPa): 340.

- Elongation (%): 4.

The solidification pattern of the Al-Cu5MgTi alloy has been studied by different researchers and the following reactions have been identified [1]:

1) Creation of the α-aluminium dendritic network at 654ºC
2) Liq. = Al + Al_3Fe at 650ºC
3) Liq.+ Al_3Fe = Al + $Al_6(CuFe)$ at 620ºC
4) Liq. + $Al_6(CuFe)$ = Al + Al_7Cu_2Fe at 590ºC
5) Liq. = Al + +Al_2Cu + Al_7Cu_2Fe at 545ºC
6) Liq. = Al + Al_2Cu + Al_2MgCu at 507ºC
7) Liq. = Al + Al_2Cu + Al_2MgCu + Al_7Cu_2Fe at 505ºC

The microstructure of the solidified material presents some relevant features like the presence of the eutectic Al-Al_2Cu and black Al_7Cu_2Fe needles that are part of the ternay eutectic. The main effect of thermal treatments (T6) is to get that part of the eutectic phase Al_2Cu goes into solution and the residual ones get more rounded [42].

The formation of small copper rich phases provides an increase in the mechanical properties of the alloy through the precipitation hardening mechanism. A typical T6 treatment consists of a solution treatment at 530 ± 5ºC during 4-8 hours followed by quenching in water at 15-25ºC and ageing during 5 days (accelerated at 120-130ºC during 2 hours) [43].

2.3.3.3 Reinforced aluminium alloys

There is not much information available on the use of MMC materials for investment casting applications. It seems that there are only three American companies that allegedly can offer these products within their available materials range, Hitchiner, Alphaform and Howmet. They have all worked with particulate reinforced aluminium alloys [49].

Different researchers have worked on the subject of investment casting of MMCs. The possibility of combining such flexible materials and process should have immediate commercial applications in the aeronautical, military and automotive sectors. Most of the studies carried out were based on particle-reinforced MMCs and the most studied materials were Al-Si7Mg0.3 and AlSi7Mg0.6 alloys with 10, 15 and 20% of SiC particles. No references were found on the use or research of TiB_2 reinforced materials for investment casting applications.

The research works carried out in the last years have concluded that the addition of particles to these casting alloys produces several problems that are unusual from the foundry point of view. The following considerations are given by the materials suppliers for casting applications that should also be taken into account in the case of investment casting practices [50].

- Since particles are in suspension rather than solution, the molten mixture must be stirred to prevent settling of the particles on the bottom.
- Melt cleaning methods must be avoided as much as possible. Otherwise, the particles will be removed.
- The melt metal must be kept in an inert gas atmosphere all the time.
- Degassing and fluxing techniques must be avoided.
- Turbulences must be avoided whenever possible.

It has also been observed that dispersions of discontinuous fibres and particles affect fluidity. Particles increase viscosity of the molten metal. The larger the volume percent of particles, the lower is the fluidity. Large sized particles are used to increase the fluidity and to make the alloy castable.

Among the major defects encountered in the castings the most common are: misruns, trapped air and oxides. Therefore, a system of traps should be included in gating systems to remove the bubbles formed when the alloys are exposed to any atmosphere in a turbulent manner.

There is an alternative method for casting MMCs. This method is based on the preforms technologies and comprises the following steps [51].

1) Forming a “preform mixture” of liquid flow medium, binding agent and reinforcement into the desired shape of the reinforced region in the final component.
2) Allowing the so called “preform mixture” to solidify into the desired shape in a mould.
3) Compress the “preform mixture” at a controlled rate to eliminate water and the whole flow medium.
4) Casting the selected molten metal on the preform, with the help of pressure or vacuum if so needed, depending on the geometry of the final component and the features of the preform and metals.
5) Solidifying the molten metal to form a MMC in the shape of the preform.

CHAPTER 3: EXPERIMENTAL PROCEDURE.

CHAPTER 3: EXPERIMENTAL PROCEDURE.

3.1 INTRODUCTION

Plaster casting is a foundry process that belongs to the family of lost wax technologies in which wax or similar easily burnable materials are used to produce intricate patterns (through injection or casting). The feeding and filling elements that are also built in wax or similar materials are subsequently attached to the patterns and the assembly is located inside a metallic cylinder where it is invested with the slurry composed of water and plaster. Plaster hardens and afterwards the plaster moulds containing the patterns are submitted to thermal cycles to eliminate the wax and provide the necessary strength to the plaster.

The plaster casting process has been selected to carry out the study on the influence of TiB_2 particles on reinforced aluminium alloys as it presents several features that make it very attractive for the production of MMC components. On the one hand it is possible to cast near net shape components that do not need much machining operations (an important aspect for the MMC industry due to the high wear that the ceramic particles can produce in the machining tools). On the other hand it is also a very suitable foundry technology for the production of high added value cast components. The final cost may be compensated by its suitability to obtain intricate shapes, for being suitable for prototypes and low and medium series of fabrication and for providing excellent surface quality, dimensional tolerance control and soundness.

On the other hand the industrial plaster casting process is a labour intensive technology with many different production steps that require a large degree of specialisation. Moreover, the nature of the plaster mould entails a very low solidification rate of the cast metal when compared to metallic moulds. As a result, the feeding and filling designs of the moulds are largely different from other foundry processes like sand casting or gravity casting. The burning out of the wax patterns is also a delicate step with a high risk of mould breaking due to the expansion of the wax in the first minutes of the process. All these aspects explain that the number of industrial companies dealing with the plaster casting process is small compared with other processes (high pressure diecasting, gravity casting and sand casting). The number of scientific publications based on this process is similarly small due to the large difficulty to implement such a complicated process in a basic research scheme. In consequence the number of publications dealing with MMCs processed through lost wax technologies is extremely low. The literature is basically reduced to a few articles dealing with the shell casting (the classical lost wax process with ceramic moulds built by immersion of the wax assemblies into different ceramic slurries) of the Duralcan commercial composites [55-57].

3.2 SELECTION AND ACQUISITION OF MATERIALS

3.2.1 Introduction. Selection of materials

The reinforced materials acquired for this work are not commercially available and are produced at lab scale for research related projects or industrial casting trials. They are based on two different aluminium alloys to which around 6 wt. % TiB_2 particles were incorporated to improve their performance. The Al-Si7Mg0.3 is a hypoeutectic aluminium-silicon alloy and the Al-Cu5MgTi alloy belongs to the aluminium-copper family. The castability of the latter is worse than the former´s due to its large solidification range (530-650ºC) that frequently leads to hot tearing related problems. Its mechanical properties are however better than those of the AlSi7Mg03 alloy due to the strengthening produced by precipitation hardening of small phases produced during the age hardening phase in thermal treatments.

Both alloys are commercially available and used in lost wax applications (even though the Al-Si alloy is much more used due to its better castability). On the opposite, the alloys containing 6 wt. % TiB_2 particles are not commercially available and have been produced by the company London & Scandinavian Co. Ltd. through a patented process based on the addition of two salts (K_2TiF_6 and KBF_4) to the melted aluminium alloy. The salts react with each other and TiB_2 particles result that have a size in the range of 0.5-1.5 µm. Even though alloys with up to 10 wt. % particles content can be directly produced by this process, the viscosity of the resultant material is too high and the material cannot be cast. Furthermore the rests of the salts are very difficult to remove and affect negatively the final properties of the castings. Therefore it was decided that the reaction were adjusted so that only 1 wt. % of TiB_2 particles were formed in situ. Subsequently 5 wt. % of commercially available TiB_2 particles of around 5 µm were added to obtain a material that could keep the sufficient castability and provide the best possible combination of mechanical and thermal properties.

3.2.1.1 Al-Si7Mg0.3 and Al-Si7Mg0.3 + TiB_2 6 wt. %

The Al-Si7Mg0.3 alloy is one of the most popular aluminium alloys in the foundries because of the excellent combination of properties that it presents. It is also known as A356 or AS7G03. Its castability is very good thanks mainly to its silicon content and its small solidification interval. It is heat treatable even though it can also be used in the as cast condition depending on the final requirements needed. It is one of the casting aluminium alloys for which more experimental data is known and it is extensively used in the lost wax foundries. The following table shows the composition range for this alloy:

	Si	Fe	Cu	Mn	Mg	Zn	Ti	Al
wt. %	6.5-7.5	0.2-0.6	0.10-0.25	0.1-0.3	0.2-0.4	0.10-0.35	0.15	Balance

Table 3.1: Typical composition ranges of the Al-Si7Mg0.3 alloy.

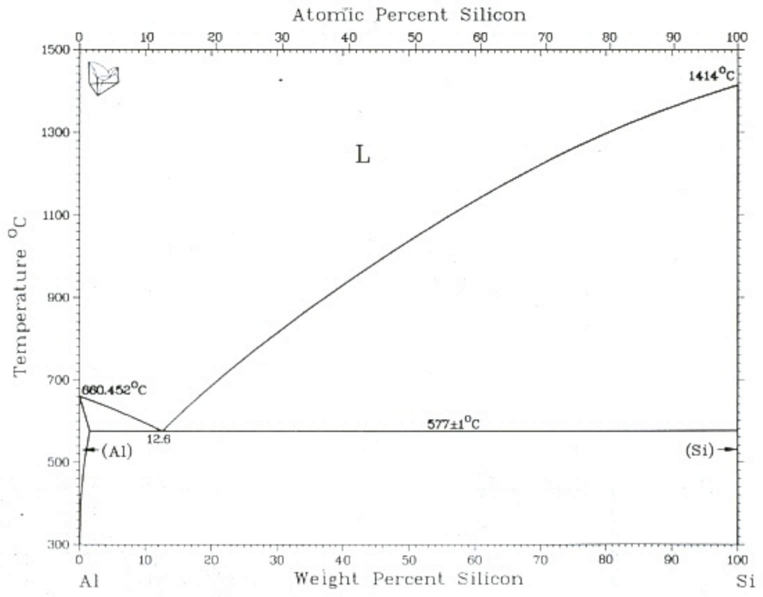

Fig. 3.1: Al-Si phase diagram.

The Al-Si phase diagram presents several specific features. The eutectics formed by Si and α- aluminium are one of the main distinct aspects. The eutectic composition is around 12.6% of Si and its formation takes place at 577ºC.

Furthermore the presence of silicon particles has a great influence on the properties and behaviour of the material as it controls the fluidity of the alloys as well as their mechanical properties.

The solidification and microstructure of the Al-Si7Mg0.3 aluminium alloys have been deeply studied. The microstructure is characterized by α-aluminium solid solution dendrites and the needle shaped eutectic network formed by α-Al-Si. There are also black dispersed Mg_2Si phases as well as α (AlFeMnSi) phases. Other shapes that can also appear are the Al_5FeSi dark needles and AlFeMgSi ($Al_8Mg_3FeSi_6$) very light Chinese type structures (see Fig.3.3) [55].

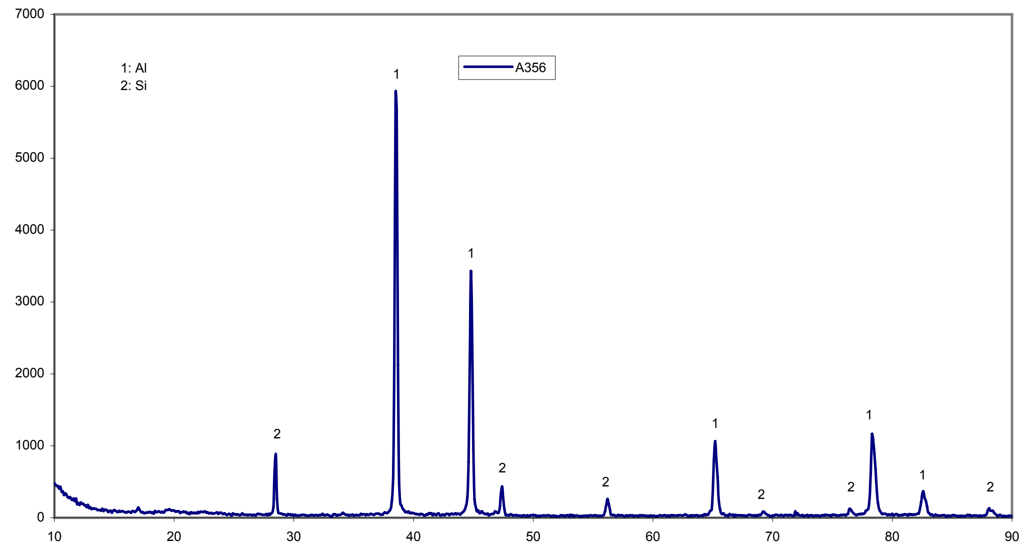

Fig.3.2: X-ray diffraction image of the Al-Si7Mg0.3 alloy. Si and α-Al are the main crystalline phases.

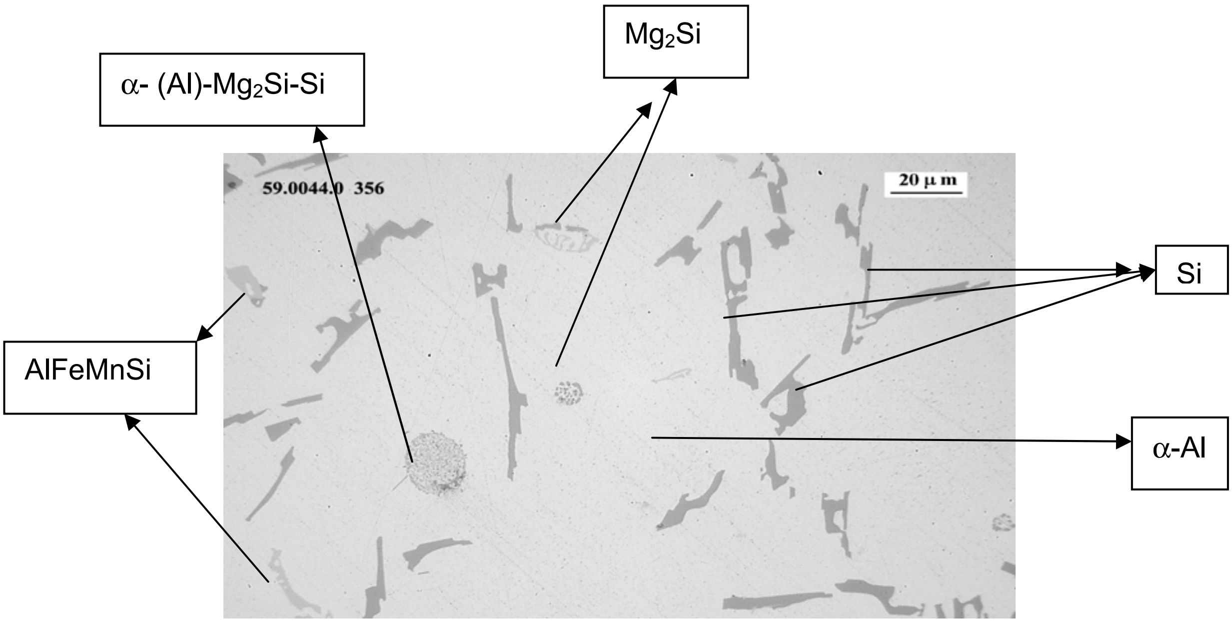

Fig.3.3: Optical microscopy image of the Al-Si7Mg0.3 alloy.

The mechanical properties of the Al-Si7Mg0.3 alloy depend on multiple variables such as foundry process used, composition, use of silicon grain modifiers and α-aluminium dendrite refiners, purity of the alloy, porosity levels and thermal treatment used. There are few bibliographic references of the properties obtained in plaster casting. According to the Tempocast® plaster casting process the properties obtained for a similar alloy, Al-Si7Mg0.5, are as follows [57]:

As cast:	UTS: 146 MPa	Elongation: 1.8%
Thermally treated (T5):	UTS 192 MPa	Elongation: 1.5%

There are different possible thermal treatments that have been applied to this alloy. The T6 treatment is the most commonly used and has been selected in the present work. In this case the hardening effect is attained through the solid solutioning and quenching treatment followed by an artificial ageing. The mechanical properties of the alloy are increased by precipitation of the Mg_2Si phase but also due to the spherodisation of the eutectic silicon particles. Furthermore the morphology of the Al_5FeSi phase may change from an acicular shape to a spheroidal one and the treatment homogeneizes the α-Al dendrites. The thermal treatment consists of two successive stages, holding the alloy at 540ºC during 8 hours followed by a quench in water and ageing at 150-170ºC for 4 to 8 hours [42, 57-59].

In the case of the reinforced material, Al-Si7Mg0.3 + TiB_2 6 wt. %, the number of references that can be found in the literature is much smaller and none of them are related to lost wax applications [29, 58- 60]. This material is not commercially available and there are only a few related articles. R. Taghiabadi et al. [58] provide UTS values of as cast and thermally treated (T6) Al-Si7Mg0.3 and AlSi7Mg0.3 + TiB_2 materials processed through sand casting:

		U.T.S. (MPa)
As cast:	Al-Si7Mg0.3	145-180
	AlSi7Mg0.3 + TiB_2	115-165
Thermally treated (T6):	Al-Si7Mg0.3	250-290
	AlSi7Mg0.3 + TiB_2	195-290

The terms **A356** and **A356R** will be used in this work from now onwards to refer to the **Al-Si7Mg0.3** and **AlSi7Mg0.3 + 6 wt. % TiB_2** particulates materials respectively.

3.2.1.2 Al-Cu5MgTi and Al-Cu5MgTi + TiB_2 6 wt. %

The Al-Cu5MgTi alloy belongs to the Al-Cu family. It is also known as A204 and AU5GT. It presents better mechanical properties than the Al-Si7Mg0.3 alloy but its castability is poor, its solidification range is very large and this makes it prone to hot tearing related problems. It is also heat treatable and has been used in lost wax applications even though much less extensively than the Al-Si7Mg0.3 alloy. The Al-Cu5MgTi alloy is applied when high mechanical properties are needed at high temperatures. The use of grain refiners in these alloys is highly recommended. The hot tearing related problems become alleviated, mechanical properties get improved and surface quality and the answer to thermal treatments is better. Al-Ti-B type grain refiners have been used with this alloy in different foundry processes. Their use is of more importance in the case of low cooling rate processes like sand casting or lost wax processes as the large solidification intervals of the alloy (650-450ºC according to the work of Grandier Vazeille P. and Morice J. [61]) together with the low heat dissipation capacity of the moulds, tend to create problems related to hot tearing and poor mechanical properties.

The following table shows the composition range for this alloy:

	Si	Fe	Cu	Mn	Mg	Zn	Ni	Sn	Ti	Al
wt.%.	0.15	0.1-0.2	4.2-4.9	0.05	0.2-0.35	0.05	0.03	0.05	0.15-0.25	Balance

Table 3.2: Typical composition range of the Al-Cu5MgTi alloy.

The main role of the different elements is as follows: Cu provides strengthening, it has been measured to be maximum between 4-6% [1, 62]. Mg improves hardenability after solution treatment and quenching through the formation of more intermetallic compounds like Al_2CuMg, Al_6CuMg_4, AlCuMg and $Al_5Cu_6Mg_2$. It increases the strength and hardness but decreases the ductility. Mn reduces the detrimental effects of impurities. Fe and Si are impurities even though the latter may control the presence of the Fe as α-FeSi constituent. Ti is added for grain refining purposes through the so called peritectic reaction mechanism. Ni improves hardness and strength at elevated temperatures and reduces the CTE. Sn is usually employed to improve machining features of the alloys as they form low melting phases that promote chip breaking and help lubricate the machining tool. Zn together with Mg controls the ageing process through the formation of $MgZn_2$ [1].

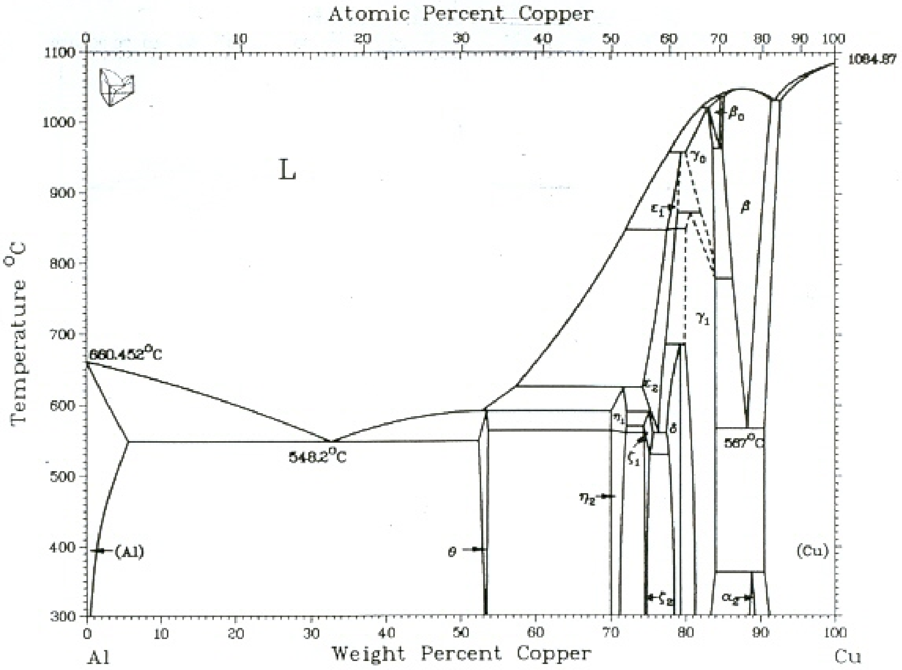

Fig. 3.4: Al-Cu phase diagram.

The phase diagram for the Al-Cu system shows the presence of different intermetallic phases in contrast to the Al-Si diagram. In this case the eutectic composition is 33 wt. % and the eutectic reaction takes place at 548.2ºC. The eutectic presents a lamellar structure α-Aluminium-Al_2Cu and this phase plays an important role in the determination of the final features of these castings. Nevertheless the strengthening mechanisms are completely different from those of Al-Si alloys. Silicon bearing phases do not play an essential role in the mechanical properties and the main phase that controls the final properties of the alloy is Al_2Cu.

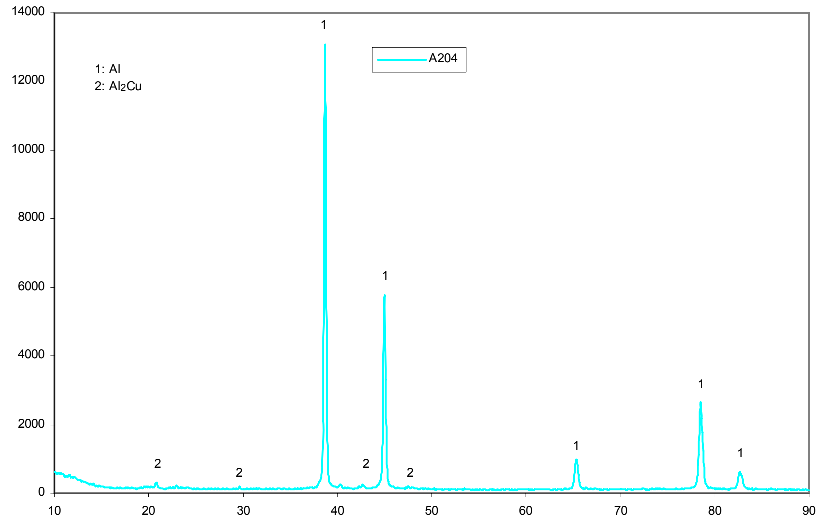

Fig.3.5: X-ray diffraction image of the Al-Cu5MgTi alloy. α-Al and Al_2Cu appear as the main crystalline phases.

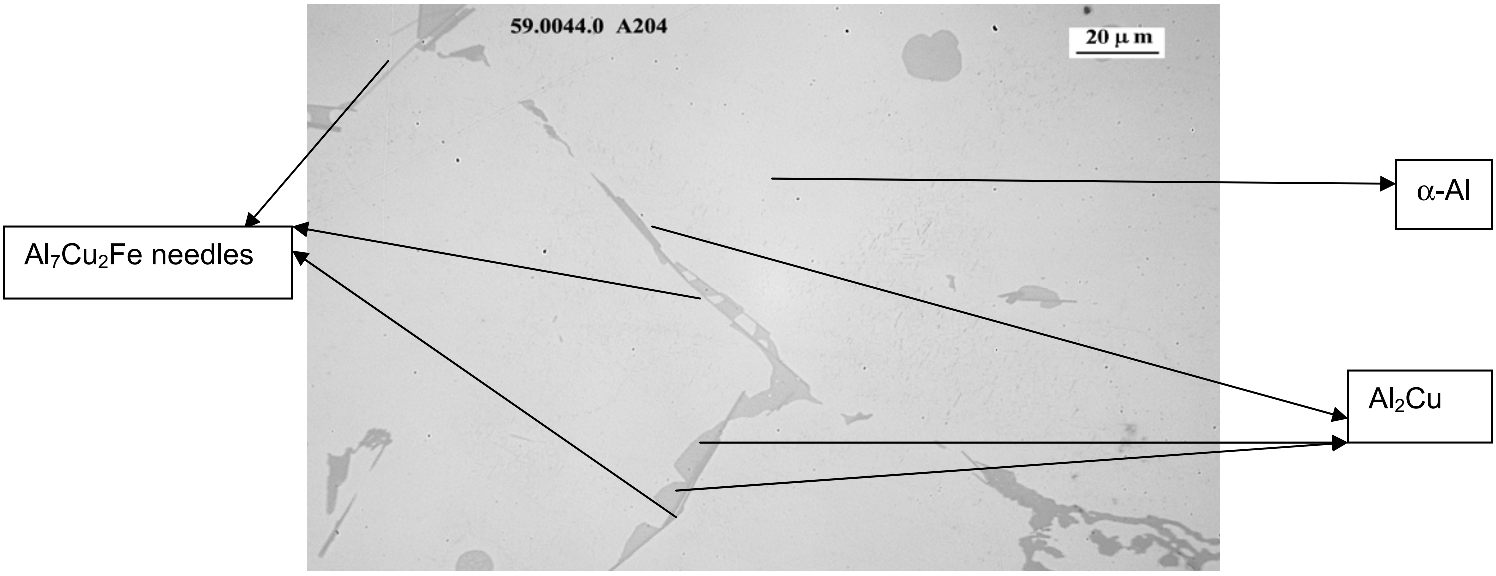

Fig. 3.6: Optical microscopy image of the Al-Cu5MgTi alloy showing some of the most typical features of the alloy.

There are almost no bibliographic references of the Al-Cu5MgTi alloy cast through lost wax and none has been found on plaster casting. Following some properties obtained with lost wax (shell casting) process are detailed [40]:

As cast:

Al-Cu5MgTi	UTS: 280 MPa	YS: 200 MPa	Elongation: 4%

Thermally treated (T6):

Al-Cu5MgTi	UTS: 340 MPa	YS: 220 MPa	Elongation: 4%

Not any references have been found on the Al-Cu5MgTi + TiB_2 (6 wt. %) material either in lost wax applications or in other foundry uses. Nevertheless there have been some studies on different Al-Cu alloys reinforced with TiB_2 particles such as Al-Cu5MgTiAg or Al-Cu-Mg alloys that have focused on the microstructural features of the resulting alloys [2, 63-64]. The present study will be focused on the study of the microstructure of this novel reinforced material (both as cast and in T6 condition) as well as the analysis of its tensile and thermal properties.

The terms **A204** and **A204R** will be used from now onwards to refer to the **Al-Cu5MgTi** and **AlCu5MgTi + TiB_2 6 wt. %** materials used in this work respectively.

3.2.2 Acquisition of the alloys

The two reinforced alloys were produced by the company London & Scandinavian Co. Ltd. in the United Kingdom. Their composition is based on the Al-Si7Mg0.3 and Al-Cu5MgTi alloys but they present a larger % of Ti and B coming from the TiB_2 particles that have been incorporated into them. Some of the particles (around 20% of the total number) have been created into the alloy through an in situ reaction. The FAS method or mixed salts synthesis has been used for it and the rest have been exogenously added as powders of around 5 μm up to complete the desired reinforcement concentration of around 6 wt. % in the alloys [39]. The following tables present the composition of the two reinforced alloys as supplied by London & Scandinavian Co. Ltd.

Al-Si7Mg0.3 + TiB_2 6 wt. % (A356R)

	Al%	Si%	Fe%	Cu%	Mg%	Zn%	Ti%	B%	Others%
wt. %	Balance	7.12	0.14	0.01	0.42	<0.01	3.7	1.8	0.21

Al-Cu5MgTi + TiB_2 6 wt. % (A204R)

	Al%	Si%	Fe%	Cu%	Mg%	Zn%	Ti%	B%	Others%
wt. %	Balance	0.08	0.11	5	<0.01	<0.01	3.4	1.7	0.14

The corresponding unreinforced alloys were prepared with commercial master alloys. Pure aluminium was mixed with different master alloys (Al-Cu 50%, Al-Si 10%, Al-Ti 10%, Al-Zn 10%) and pure magnesium up to attain a composition similar to that of the reinforced materials received from London & Scandinavian but without the TiB_2 particles.

The composition of the alloys used for comparison purposes along the present study are as follows:

Al-Si7Mg0.3 (A356)

	Al%	Si%	Fe%	Cu%	Mg%	Zn%	Ti%	B%
wt. %	Rest	7.50	0.1	0.013	0.29	0.01	0.01	0

Al-Cu5MgTi (A204)

	Al%	Si%	Fe%	Cu%	Mg%	Zn%	Ti%	B%
wt. %	Rest	0.18	0.10	5	0	0.01	0.01	0

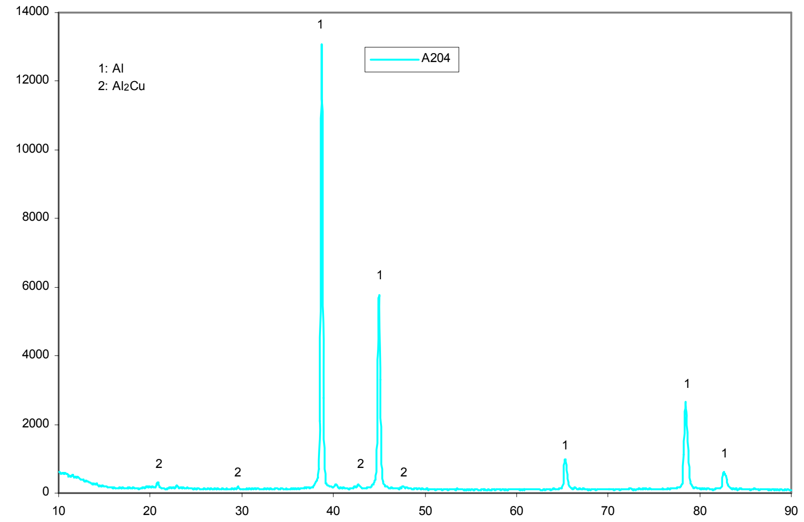

Fig. 3.7: X-ray diffraction image of the A204R reinforced alloy.

α-Al and Si appear as the main crystalline phases together with the TiB_2.

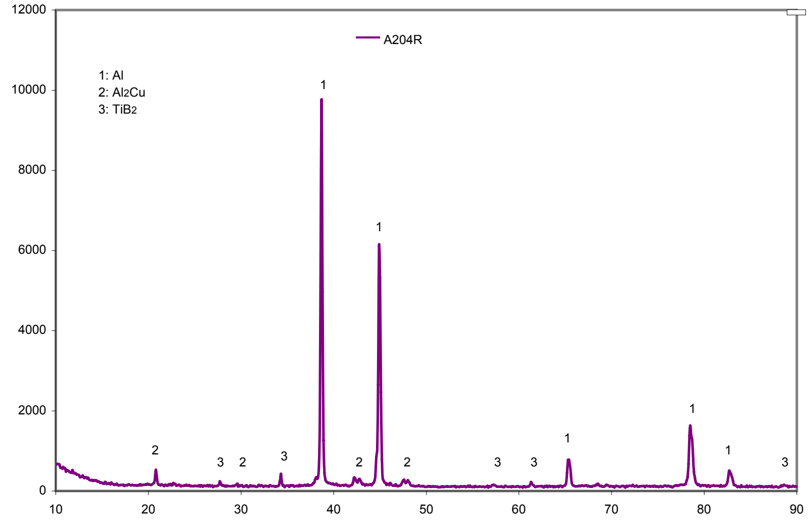

Fig. 3.8:X-ray diffraction image of the A204R reinforced alloy.

The peaks corresponding to Al_2Cu are more visible than in the Fig. 3.7 corresponding to the unreinforced alloy and peaks corresponding to TiB_2 appear.

3.3 SETTING UP OF THE PLASTER CASTING PROCESS AND PRODUCTION OF SAMPLES

3.3.1 Production of the plaster moulds

The plaster casting variant used in this work is known as block casting or plaster block mould investment casting. It is one of the two main variants that are currently used, together with the so called plaster mould casting process (also known as rubber plaster moulding). In the latter variant there are parting lines on the surface of the patterns and the demoulding can be carried out without destroying the model (made of silicone or wood) that will be reused for further castings. The plaster block mould investment casting process employs expendable patterns (normally wax) and the production of the plaster mould is carried out in a unique step.

Both processes present exceptional surface quality and tight tolerances and the main difference between them is the extra design freedom and tighter tolerances (specially across parting lines and cores) that allows the plaster mould casting route at the expense of an increase of the mould manufacturing process cost.

The production of the plaster mould is one essential phase of the process as it directly affects the quality of the final casting. The following section presents an overview of the steps and materials needed to produce the plaster moulds through the block casting process used in this work:

Main materials

Silicone for the production of the moulds into which the wax has been cast to produce the wax patterns and filling and feeding systems (channels, feeders, etc.).
The production of the wax patterns was carried out with silicone moulds. Industry uses metallic injection moulds similar to those used in the injection process for polymers but silicone moulds that are produced by casting castable silicone on a wood or metallic model may be used for laboratory and prototype building purposes.

Wax for the production of the expendable patterns and the assembly of the patterns and the filling and feeding elements.
This wax is commonly used in the lost wax industry for the production of injected patterns. It can be either cast or injected. The wax is melted and heated by an electrical

heating plate up to around 70-80ºC and cast into the silicone mould. In the case of difficult geometries (complex shapes, large moulds or thin walls) the wax can also be injected into the mould with a specially designed injector. The raisers, feeding channels and rest of the elements that will form the filling and feeding system are produced similarly. Eventually, once all the components that will form the final wax assembly have been produced, they are joined together manually with the help of specially designed sticky waxes and heated handtools.

Plaster that will be mixed with water, cast over the wax assembly and set to create the refractory mould. Plaster is mainly a calcium sulfate bi hydrate, $CaSO_4.2H_2O$. At room temperature and before being mixed with water it is a soft white material.

Main steps in the production of the plaster moulds

The following pictures show the different stages in the production of a plaster mould for the production of cylinders (dimensions of 14 mm diameter and 80 mm height) that have been subsequently machined to obtain the tensile specimens according to the standard ASTM A-370. Subsequently four cylindrical tensile specimens can be drawn from each mould. Tensile specimens are drawn from the centre of the cylinders. The material left has been used to obtain specimens for the microstructural analysis (AES, SEM, TEM, OM), chemical analysis, measurement of porosity and density and CTE and thermal conductivity.

1) Production of wax components and assembly of the wax pattern

The wax patterns are produced by casting the hot wax into silicone moulds. Fig. 3.9 a) shows the silicone mould filled with the wax (green material) that has been previously poured into it in liquid state (at 70-80ºC) and showing the clamping system used. The central hole corresponds to the feeding column located symmetrically with regards to the two cylinders to be obtained in each wax casting.

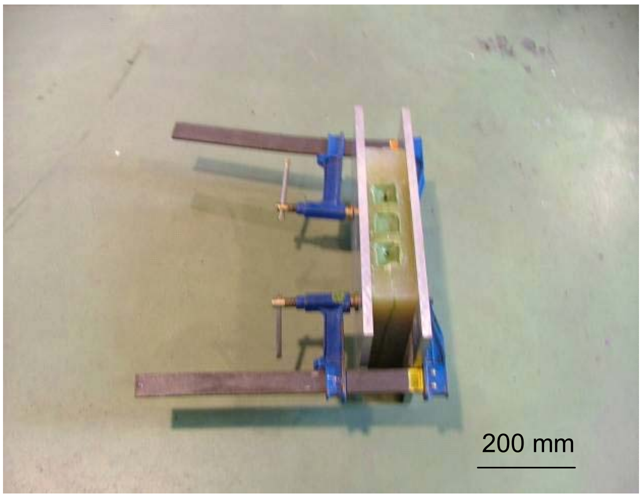

Fig. 3.9: a) Silicone mould for the production of wax patterns filled with the wax (green material).

Once the wax gets solidified in around 90 minutes, the mould can be opened to extract the patterns. Figure 3.10 shows the wax components that will be used to produce the final wax pattern. (see figure 3.11). The different wax components are glued together with some sticky wax specifically designed for that purpose to form the final wax assembly containing the four cylinders and the filling and feeding system for the aluminium casting step.

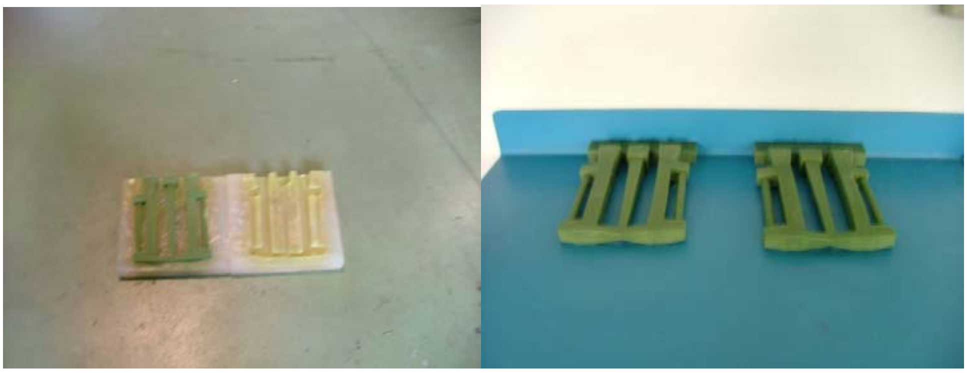

Fig. 3.10: Silicone mould opened to draw the wax pattern (left image) and demoulded wax components (right image).

Fig. 3.11: Final wax pattern assembly for the production of cylindrical samples.

2) Investment of the wax pattern assembly with plaster

Once the wax pattern assembly is eventually finished, the next step is to produce the plaster moulds. The fabrication of the moulds has been carried out in a plaster casting unit composed of a mixing unit where water and plaster are mixed in the correct ratio and the casting unit where the mixture is cast into a steel cylinder that contains the wax pattern assembly. All the mixing and casting steps are made under vacuum to avoid the appearance of defects on the surface of the mould.

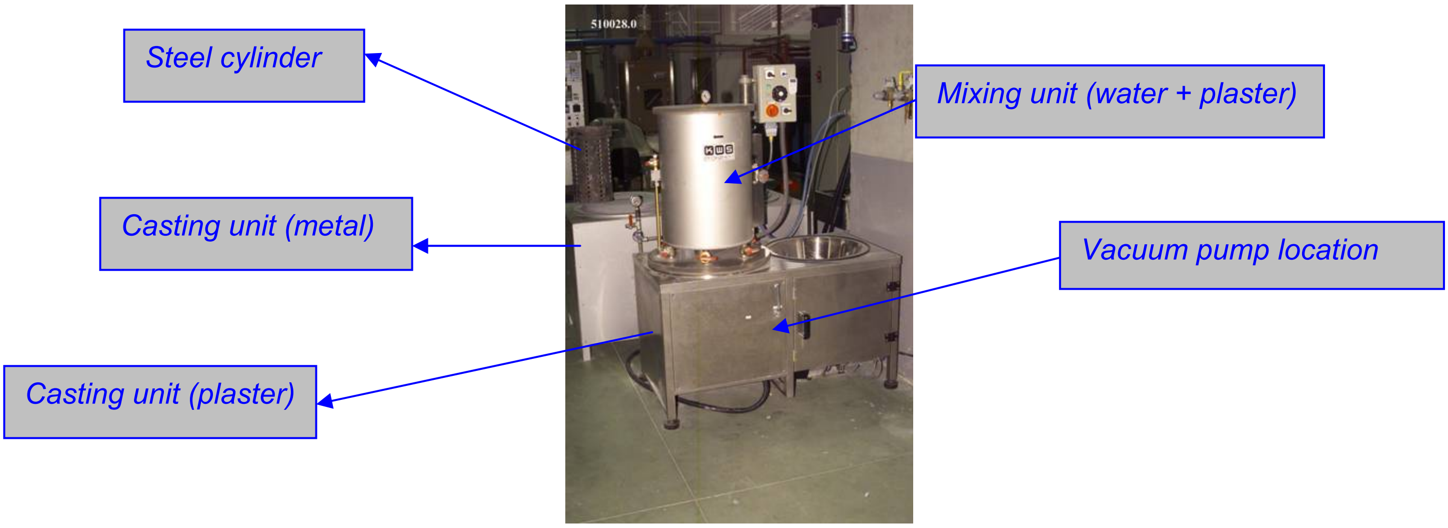

Fig. 3.12: Plaster casting unit.

In the figure 3.13 the wax pattern can be seen within the steel cylinder that is located in the plaster casting unit. The same pattern after the plaster mixing and casting steps are also shown The two figures show the two different sides of the same metallic cylinder.

Fig. 3.13: Cylinder containing the wax assembly within the plaster casting unit. Before the plaster casting step (left image) and after having cast the plaster under vacuum by gravity from the mixing unit (right image).

3) Dewaxing and thermal cycling of the plaster

Afterwards a thermal cycle is applied to the metallic cylinder that contains the plaster mould and the wax assembly to eliminate the wax and provide the required thermal and mechanical properties to the plaster. The thermal cycle comprises several steps and is carried out in an electrical furnace (dimensions 500x 500x 600 mm) that can reach up to 1000ºC.

1) The metallic cylinder containing the wax assembly and the plaster (already set around 2 hours after the casting step) is first heated from 20ºC to 150ºC as rapidly as possible to avoid that the wax can expand itself easily and produce cracks in the plaster mould.

2) The mould is kept at 150ºC during 3 hours for dewaxing purposes. Most of the wax is recovered in liquid form from a hole located at the bottom of the furnace.

3) Afterwards all the assembly is heated again at a 200ºC/h rate up to 250º and kept during 90 minutes at that temperature. Soluble γ anhydrous calcium sulfate formation takes place.

4) The temperature is increased up to 650ºC and the assembly is kept at that temperature for 3 hours. This stage makes it sure that insoluble β anhydrous calcium sulfate formation is attained. In the case of large moulds the time should be increased in order to make it sure that the plaster that is in the internal parts or far from the walls of the metallic cylinder gets heated appropriately.

5) Finally the mould is cooled down to the temperature selected for the casting operation. In the case of aluminium alloys it is normally kept between 25ºC-300ºC depending on the complexity of the geometry of the part and the physical properties of the casting alloy selected. Figure 3.14 shows the furnace with the cylinder containing the plaster mould after having completed the dewaxing and thermal cycles.

Fig.3.14: Furnace used for the dewaxing and thermal treatments.

3.3.2 Production of components and samples

Apart from the plaster moulds for the production of the cylinders for the tensile specimens, other moulds were similarly produced to carry out the analysis of the solidification curves (see chapter 4 section 4.2). Aluminium alloy samples were also obtained from other regions of the cylinders to carry out the study of the microstructure (Chapter 4), thermal analysis (Chapter 6) as well as the density and porosity measurements (Chapter 5).

The aluminium components are eventually produced by gravity casting into the hollow plaster moulds. The casting is carried out in a casting unit connected to a vacuum pump that extracts the air to help fill the mould. The casting parameters were selected following previous experiences in the investment casting process and data obtained from literature. [32, 58-61].

The casting temperature was established at around 100ºC over the liquidus temperature of the unreinforced alloys, i.e. 710ºC in the case of the A356 and A356R and 730ºC for the A204 and A204R materials.

The plaster mould temperature was kept at 200ºC and it was tried that the rest of parameters were also kept unchanged through all the castings. (time needed to fill the moulds, vacuum applied during the castings and amount of plaster used to build the moulds).

Figures 3.15 and 3.16 show the different steps of the production of the metallic components (casting of four cylinders from which the tensile specimens and samples for the microstructural analysis were drawn). Figure 3.17 shows one casting carried out with the A204R in which three of the four cylinders that are obtained in each casting can be appreciated.

Fig. 3.15: Casting of the metal into the plaster mould under vacuum.

Fig. 3.16: Demoulding step. After the solidification of the metal the plaster mould is destroyed.

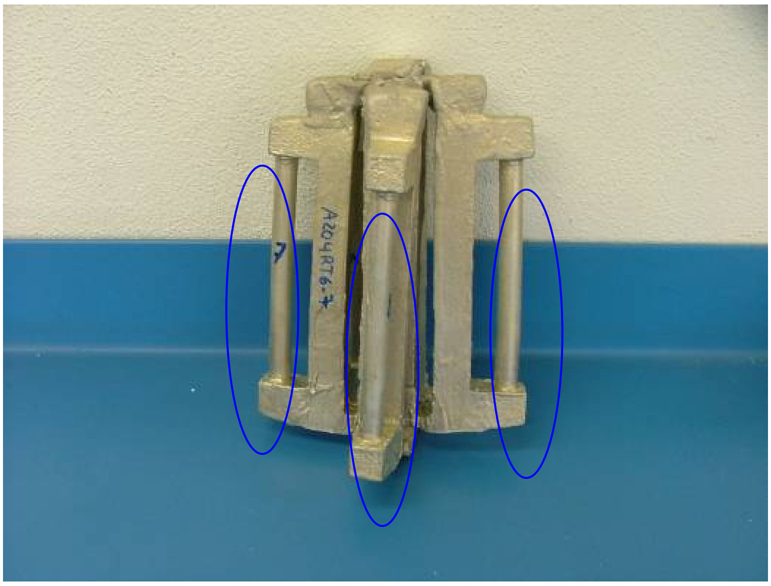

Fig. 3.17: Casting of a four cylinder component with the A204R alloy. (three of the four cylinders are only visible).

3.4 EXPERIMENTAL TECHNIQUES USED FOR THE ANALYSIS OF THE RESULTS

The four different materials (A356, A356R, A204 and A204R) were cast following the procedure explained in the previous section, the only difference being the casting temperature used for the Al-Si based alloys (710ºC) and Al-Cu based alloys (730ºC). Half of the castings were submitted to the T6 thermal treatment and specimens were machined from them for tensile tests at room temperature and 200ºC.

Following a list of the experimental techniques used in the characterization and analysis of specimens obtained from the plaster cast cylinders are listed.

* Tensile tests at room temperature and 200ºC, ASTM-A370.
* AES analysis (together with line profile analysis).
* TEM analysis and EDS mapping (reinforced alloy specimens prepared with the FIB technology).
* SEM analysis.
* OM analysis.
* Measurement of density and porosity. (water displacement and geometrical measurement, i.e. volume and weight relation).
* Chemical analysis.
* XRD.
* CTE measurements.
* Thermal conductivity (samples were previously submitted to HIP in order to eliminate and decrease the effect of porosity).

CHAPTER 4: SOLIDIFICATION & MICROSTRUCTURE.

CHAPTER 4: SOLIDIFICATION AND MICROSTRUCTURE.

4.1 INTRODUCTION

This chapter is devoted to the analysis of the solidification and microstructure of the two reinforced alloys A356R and A204R. The comparison with the corresponding unreinforced alloys A356 and A204 should provide valuable information to explain the influence of the TiB_2 particles. Moreover, the microstructure is directly linked to the properties of metallic materials and therefore this analysis is essential to understand the differences between the mechanical and thermal properties of the reinforced and unreinforced alloys that will be further discussed in chapters 5 and 6 respectively.

The plaster casting process used to produce the different samples is characterised by a low solidification rate due to the low thermal conductivity of the plaster that is used to build the moulds. Moreover ceramic particles such as TiB_2 have a strong influence on both the solidification pattern and final microstructure as they play the role of nucleating agents of both the aluminium matrix and intermetallic phases. Furthermore, they tend to form clusters and agglomerate together to reduce their free energy. In MMCs, particles are usually pushed by the solidification front and they tend to lay in the interdendritic and intergranular spaces. It was to be expected that these features that have already been pointed out in many different particle reinforced metallic composite systems could also take place in the TiB_2 reinforced materials that are the object of this work [58-60, 65].

This chapter deals with two main aspects. On the one hand the solidification of the reinforced alloys has been studied through a thermal analysis technique in which a thermocouple located in the centre of a plaster mould measures the temperature of the material that is poured into it along the entire solidification process. The T-t data are subsequently recorded and processed by a software that provides the corresponding solidification curves (representation of T versus time). The derivative of each point in the curve corresponds to the cooling rate of the material and therefore any increase that is observed in it can be associated with an event that produces a decrease in the solidification rate such as the appearance of a new phase with the associated release of latent heat. Consequently the analysis of the derivative curve provides valuable information on the influence of the TiB_2 particles on solidification events.

The second aspect studied is the analysis of the microstructure and the chemistry of the reinforced alloys and the comparison with the unreinforced materials. Optical Microscopy (OM), Scanning Electron Microscopy (SEM), Auger Electron Spectroscopy (AES) and Transmission Electron Microscopy (TEM) techniques have been used to analyse the microstructure and the chemistry of the composite materials. The analysis of the information collected from the obtained micrographs and the comparison with the microstructure of the corresponding unreinforced alloys provide essential information to explain the behaviour and properties of the reinforced A356R and A204R materials.

4.2 INFLUENCE OF TIB$_2$ PARTICLES ON SOLIDIFICATION

4.2.1 Introduction. Solidification curves

The solidification curves of the materials were obtained through a time-temperature recording system based on the use of commercial sand cups which incorporate a thermocouple protected by a glass tube. (See figure 4.1).

The first step was to produce the same cups made with the plaster used along the work and to adapt the thermocouples to them. The cups were produced by casting the plaster/water mixture into silicone moulds that had been obtained using the commercial sand cups as models. The glass covered thermocouples of the commercial sand cups were extracted and located in the plaster cups to record the T during the solidification stage. A commercial software NOVACAST ATAS allows the data acquisition and produces the corresponding T-t curves.

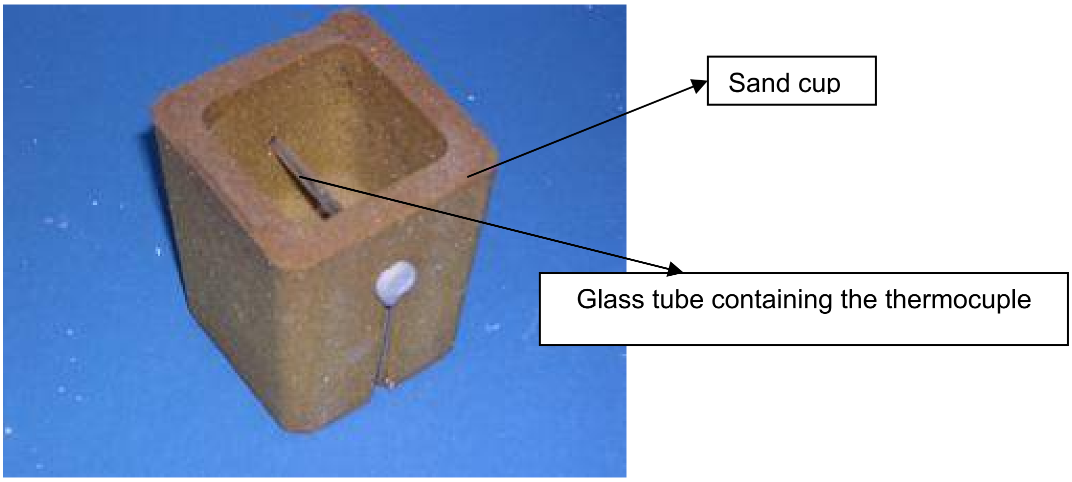

Figure 4.1: Commercial sand cup with detail of thermocouple´s location.

Figure 4.2 shows the plaster cups and the data acquisition system with the plaster cups. Much care has been taken to control experimental parameters so that the possible changes observed in the features of the materials can only be related to the presence of the TiB_2 particles.

Figure 4.2: Plaster cups mounted on the data acquisition device, the aluminium alloy has already been cast into the cup on the left.

Temperature measurements are done each second and the system software provides both the T-t and the corresponding derivative curves dT/dt v t curves. Cooling curves provide interesting information on the nature of the alloys. Solidification rates can be calculated from them. Moreover solidification reactions are exothermic and they cause a change in the slope of the curves [59, 61]. Furthermore it is known that the SDAS of the alloys is directly related to the cooling rate through the relation $D = kt_s^m$, where D is the dendrite size, t_s is the solidification time and k and m are constants for each alloy. The SDAS parameter directly affects the microstructure and mechanical properties of the material like UTS and ductility [11]. Cooling curves provide additional information on parameters like the solidification time and solidification temperature range, temperature of primary α-Al growth as well as temperature and time difference between the maximum and minimum of the liquidus recalescence.

The analysis of the cooling curves has been previously applied to MMCs. The SiC reinforced composites have been the most studied among them but the pure Al/TiB_2 system has also been studied by Youssef et al. [59]. They recorded a reduction of the latent heat and solidification time and afterwards related this effect to microstructural aspects of the materials.

4.2.2 Solidification of the A356R reinforced alloy

The solidification curves obtained with the A356 and A356R materials together with their derivative curves can be seen in the following figures (Fig. 4.3-4.6). Both materials have been cast in the same conditions, mould temperature 200ºC and casting temperature 710ºC. The casting step has been controlled so that there were no differences in the casting parameters and procedure. Two castings of each material have been carried out to check that repetitive data were obtained.

The main values obtained from the curves have been summarized in the table 4.1. The solidification interval is shorter for the reinforced material and the precipitation of the different phases begins earlier with the exception of the aluminium dendrites that begin some ten seconds earlier and 10ºC higher in the A356 alloy. Nevertheless this may be due to small initial temperature differences between the alloys. The main differences are seen in the peaks that correspond to the precipitation of Fe based intermetallics, the eutectic Al-Si and the Mg_2Si that appear signalled like points 2, 3 and 4 respectively in the curves, figures 4.5 and 4.6 [1, 32, 59, 61-62].

Solidification Parameters/Materials	**A356**	**A356R**
Solidification temperature interval (ºC).	610ºC - 455ºC	600ºC - 495ºC
Solidification time (s).	515 s.	410 s.
Development of the α-aluminium dendrites (ºC, s.) Point 1 in the graphics.	610ºC, 65 s.	600ºC, 75 s.
Onset of Fe based intermetallics precipitation (ºC, s). Point 2 in the graphics.	585ºC, 130 s.	595ºC, 85 s.
Onset of the eutectic reaction (ºC, s) Point 3 in the graphics.	540ºC, 225 s.	570ºC, 160 s.
Onset of Mg_2Si precipitation (ºC, s). Point 4 in the graphics.	470ºC, 515 s.	515ºC, 445 s.
End of solidification (ºC, s). Point 5 in the graphics.	455ºC, 580 s.	495ºC, 485 s.

Table 4.1: Main solidification parameters of the two Al-Si based materials obtained from the experimental castings with the plaster cups.

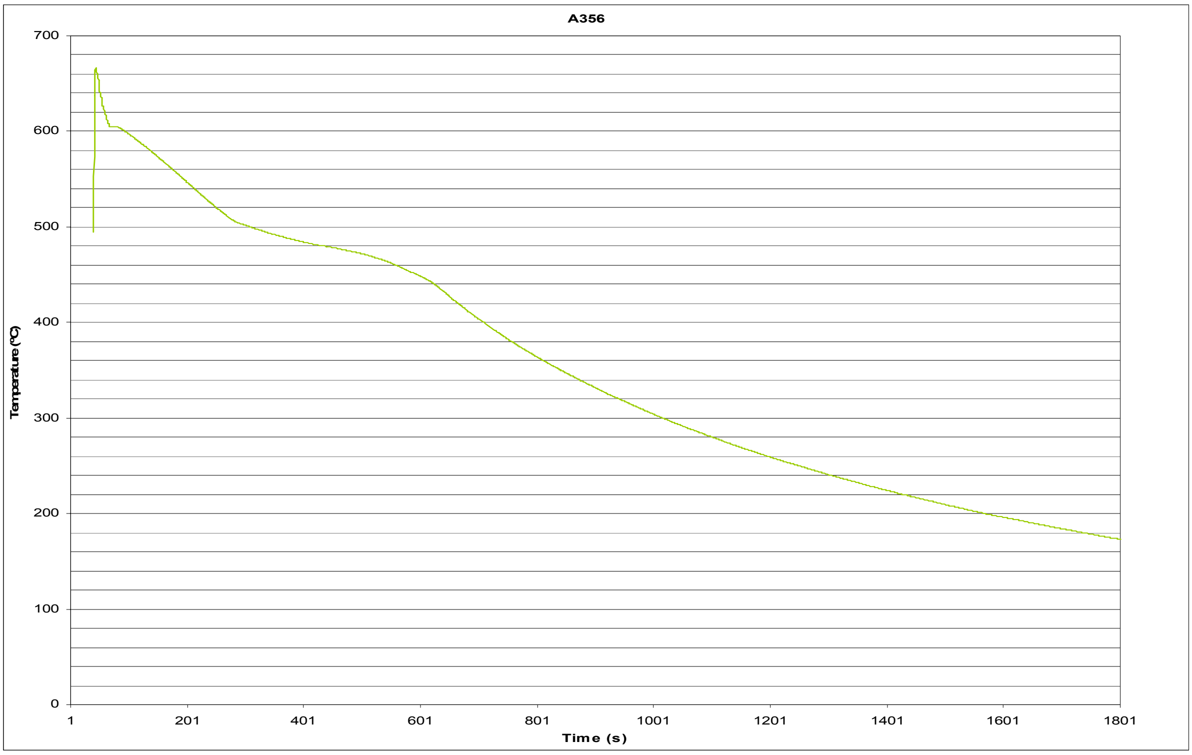

Fig. 4.3: Solidification curve of the unreinforced A356 alloy.

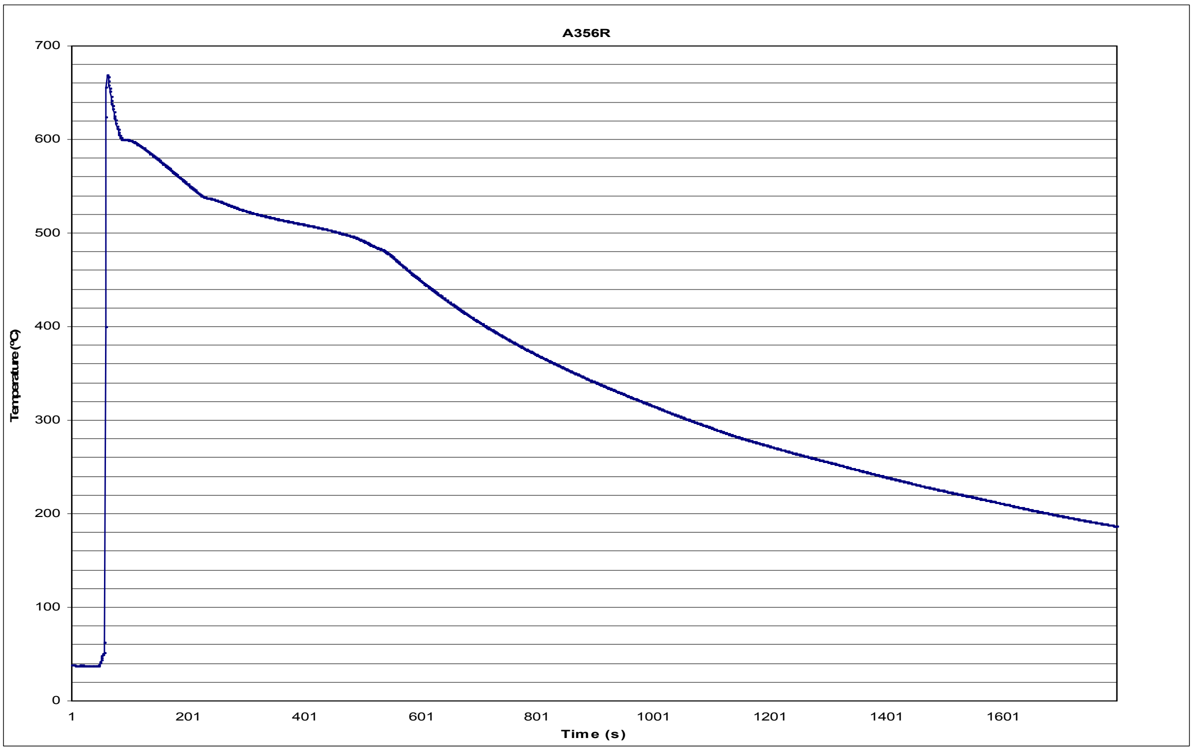

Fig. 4.4: Solidification curve of the reinforced A356R alloy.

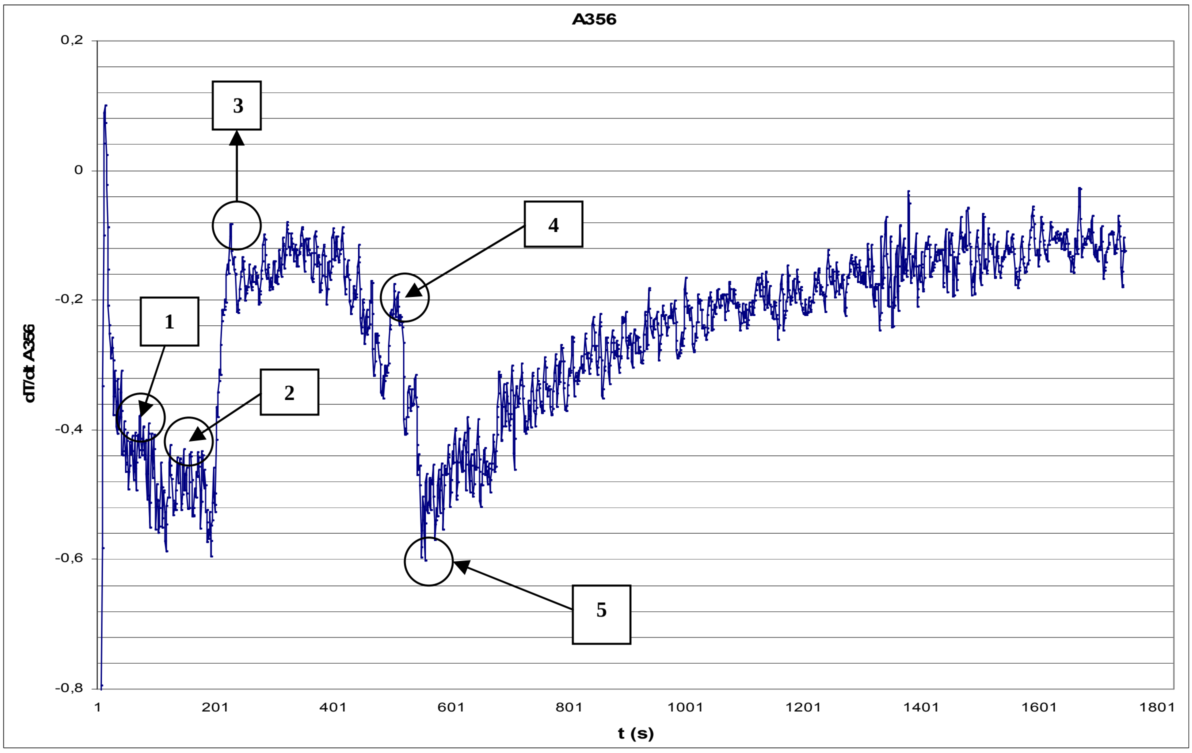

Fig. 4.5: Derivative curve of the unreinforced A356.

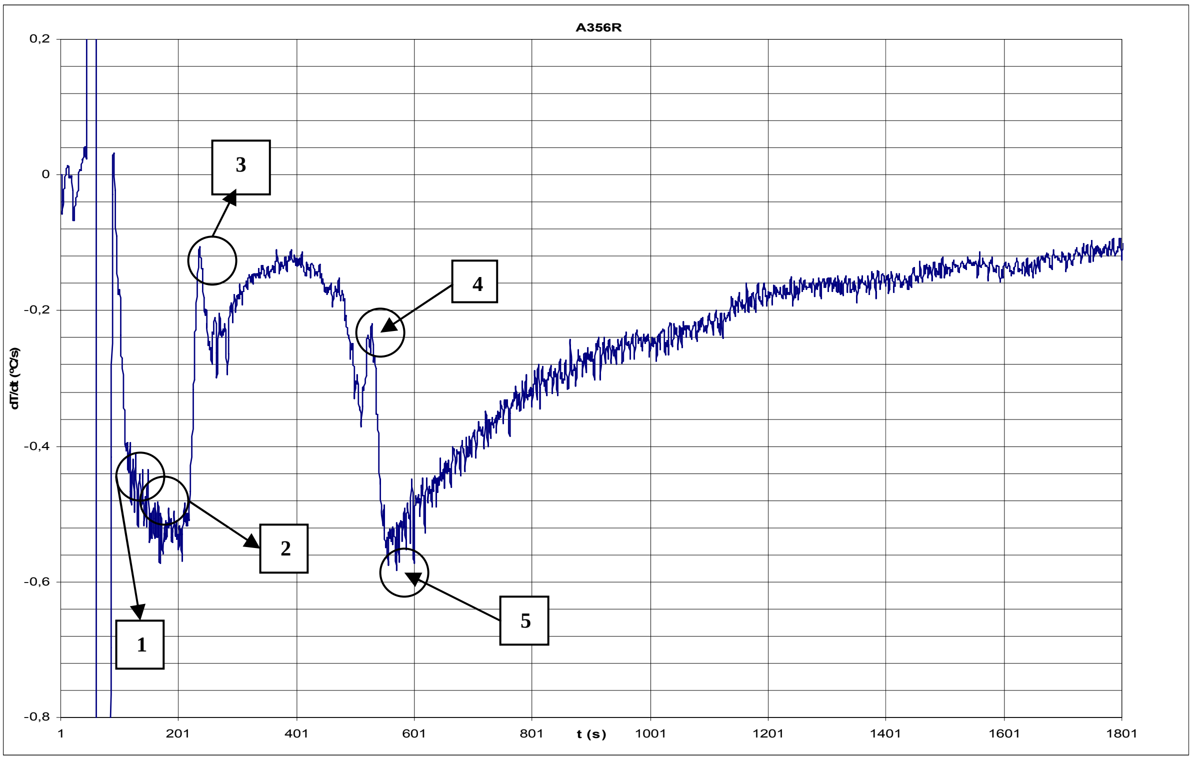

Fig. 4.6: Derivative curve of the reinforced A356R.

4.2.3 Solidification of the A204R reinforced alloy

The A204 alloy has been much less studied than the A356 alloy and is much less used in foundries due to its poor castability. It usually presents a large solidification interval (650ºC-450ºC) that may lead to hot tearing related defects or microshrinkages that are difficult to eliminate in the final castings. The solidification of the A204 alloy is more complex than the solidification of the A356 alloy due to the formation of many different Al-Cu-Fe-Mg intermetallics whose precipitation depends strongly on casting conditions and alloy composition. Table 4.2 summarises the main solidification parameters and the differences between the A204 and A204R alloys. The data have been obtained through the curves (figures 4.7-4.10) following the same scheme used for the Al-Si materials with a casting temperature of 730ºC and a mould temperature of 200ºC.

Solidification Parameters/Materials	**Al-Cu5MgTi**	**Al-Cu5MgTi + 6 wt. % TiB_2**
Solidification temperature interval (ºC).	630-420ºC	635-440ºC
Solidification time (s).	600 s.	420 s.
Development of dendritic network (ºC, s). Point 1 in the graphics.	630ºC, 65 s.	635ºC, 50 s.
Onset of the peritectic reaction (ºC, s). Point 2 in the graphics.	625ºC, 120 s.	630ºC, 85 s.
Onset of the eutectic reaction (ºC, s). Point 3 in the graphics.	465ºC, 470 s.	470ºC, 430 s.
End of solidification (ºC, s). Point 4 in the graphics.	420ºC, 665 s.	440ºC, 470 s.

Table 4.2: Main solidification parameters of the Al-Cu based materials.

The preliminary analysis of the data in the table shows clear similarities to the Al-Si alloys. The reinforced material presents a noticeably shorter solidification process, only 420 seconds and 195ºC in contrast to 600 seconds and 210ºC in the A204 alloy. Additionally there are some changes in the shape of the curves and solidification events take place earlier and at higher temperatures. TiB_2 particles must have a direct participation in the solidification of the A204R alloy and the precipitation of the different phases that appear in the final microstructure.

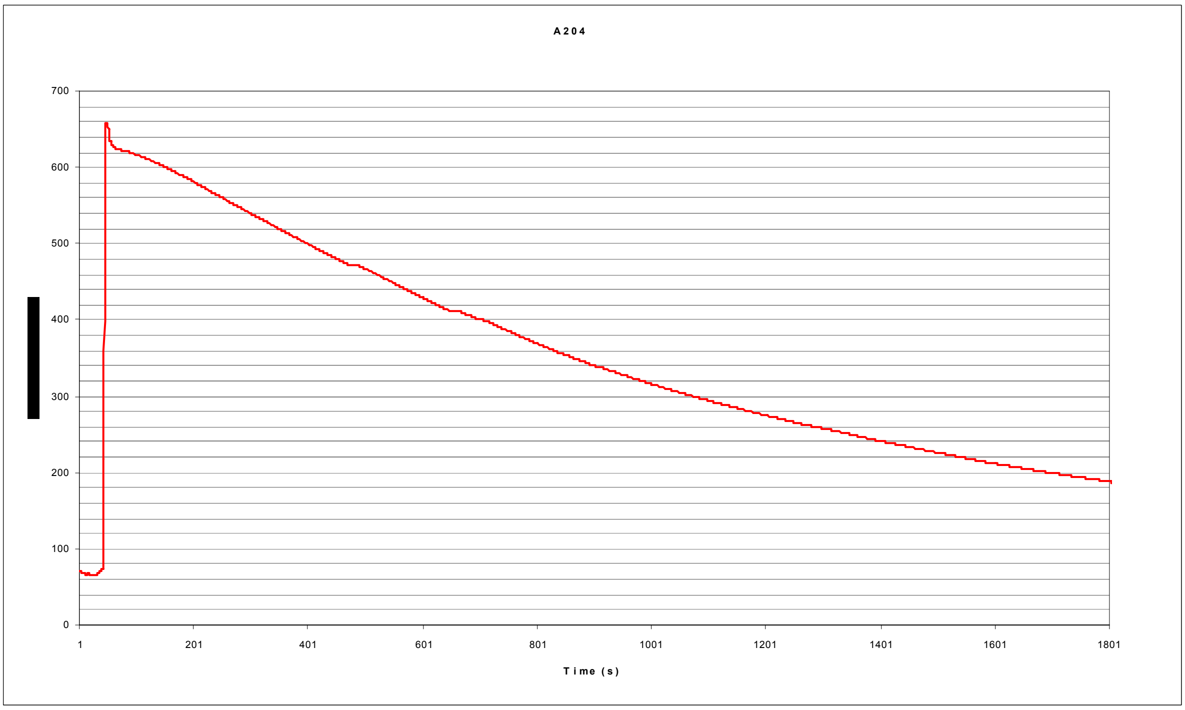

Fig.4.7: Solidification curve of the unreinforced A204 alloy.

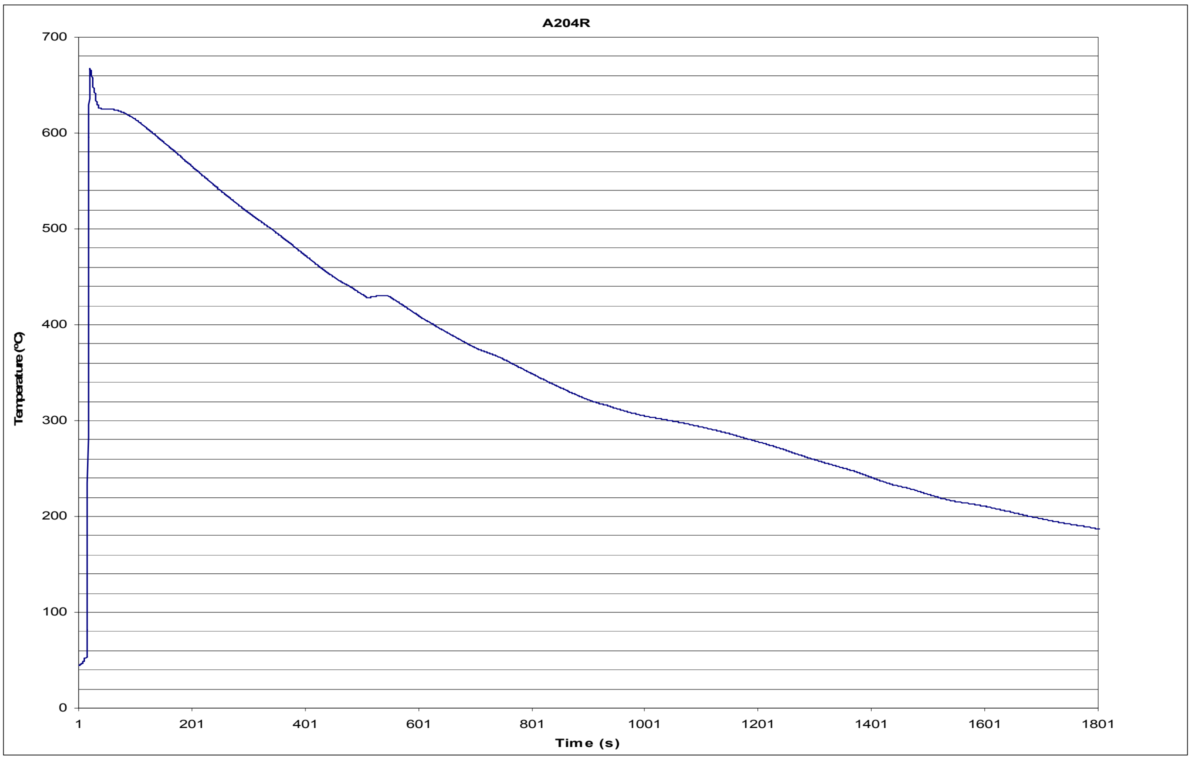

Fig. 4.8: Solidification curve of the reinforced A204R alloy.

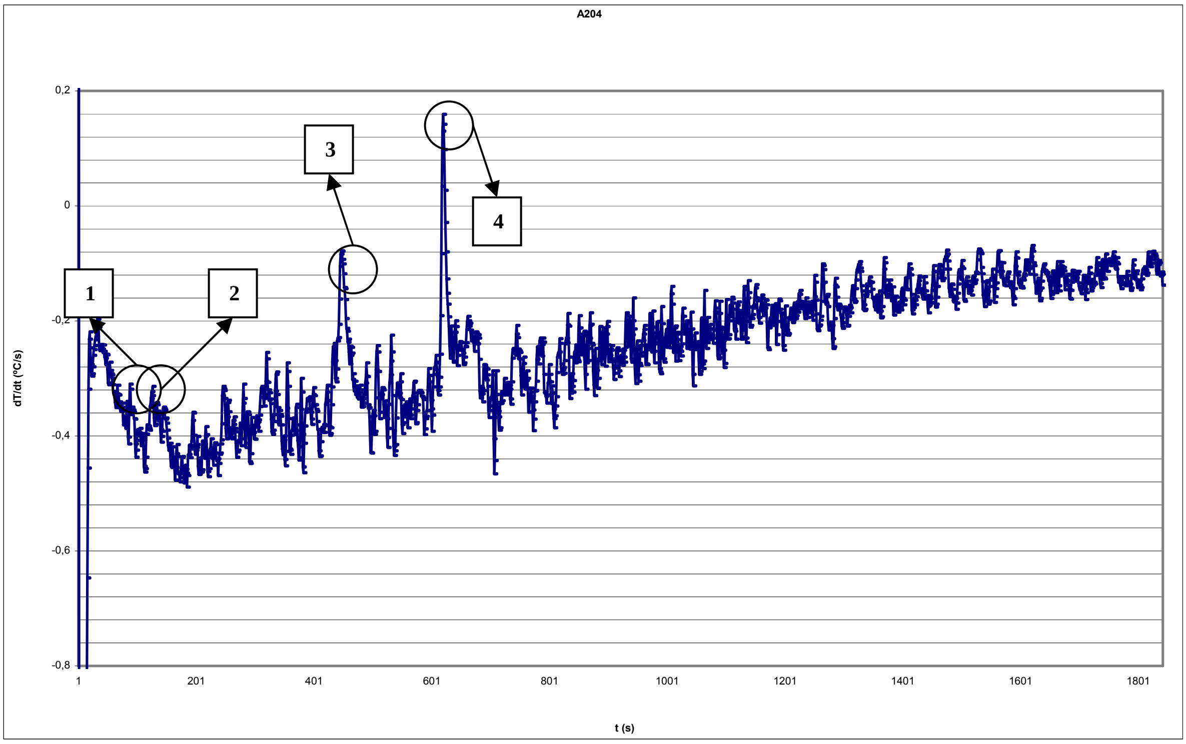

Fig.4.9: Derivative curve of the unreinforced A204 alloy.

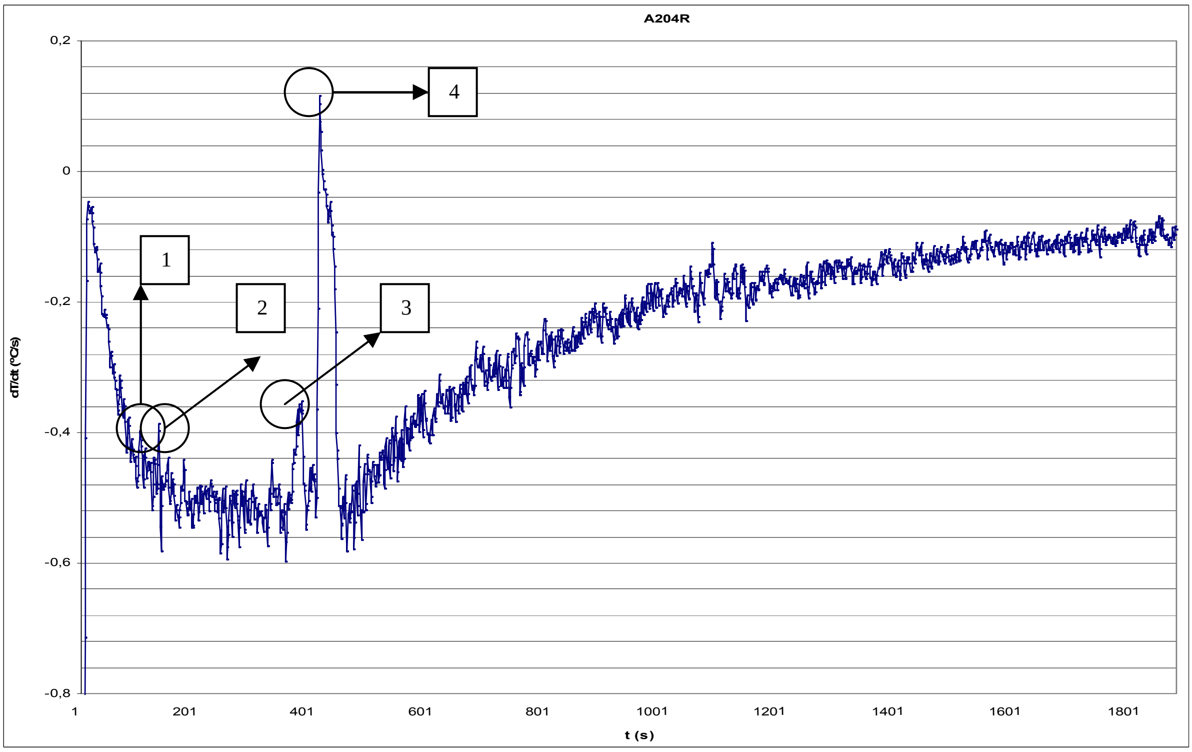

Fig.4.10: Derivative curve of the reinforced A204R alloy.

Discussion of the results

Solidification curves of both the reinforced and unreinforced materials have been obtained by casting the materials into plaster cups containing thermocouples linked to a data acquisition system. The T-t curves and their corresponding dT/dt curves provide valuable information on the solidification and precipitation of intermetallic phases.

A356 and A356R

The main reactions that take place during the solidification of the A356 during the solidification stage have been already previously studied by different researchers even though not any such data has been obtained with plaster moulds. The temperature at which the reactions take place may vary according to the exact alloy composition and process conditions but the main features of the solidification of this alloy have been identified [1, 32, 59, 61-62] as follows:

1) *Development of the α-aluminium dendrites at around 615ºC.*
2) *Precipitation of Fe based intermetallics around 595-600ºC.*

   $\text{Liquid} \longrightarrow Al + Al_{15}(Fe,Mn)_3Si_2$ and $\text{Liquid} \longrightarrow Al + Al_5FeSi$
3) *Main eutectic reaction at around 575ºC.*

   $\text{Liquid} \longrightarrow Al + Si + Al_5FeSi$
4) *Precipitation of the magnesium silicide phase and further iron based intermetallics at around 550-555ºC.*

   $\text{Liquid} \longrightarrow Al + Si + Mg_2Si + Al_8Mg_3FeSi_6$

The values obtained with the plaster cups are in accordance with these studies and the peaks corresponding to these main events have been identified in both the A356 and A356R alloys.

Compared to other processes using metallic moulds (in gravity casting the solidification interval and solidification rates have been measured to be of 614-539ºC and 0.2-5 ºC/s respectively [62]) the solidification times obtained are larger, more than six minutes, and the solidification rates are lower (0.16ºC/s). Plaster cannot actually dissipate the heat so easily but the main four reactions pointed out previously have been similarly identified to take place in both A356 and A356R alloys. Even so, there are some differences between both alloys that are pointed out in the table 4.1. The onset and end of the reactions are different. This fact must be directly related to the presence of the TiB_2 particles that play the role of nucleation agents. The results confirm that the TiB_2 particles interfere in the solidification of the Al alloys. It was known that TiB_2 has a grain refining effect and this phenomenon has been much studied by different researchers but additional interactions seem to exist that could explain the changes observed in the solidification curves. It is possible that the TiB_2 particles have an additional role in the nucleation and growth of other phases during solidification. In order to confirm this possibility microstructural analysis have been carried out (see point 4.10) that confirm that TiB_2 particles act as nucleating agents for primary aluminium dendrites and silicon. These interactions decrease the necessary undercooling for those phase transformations to occur and directly affect the microstructural features of the materials (grain size, precipitation and shape of intermetallics etc.). Consequently they should be taken into account in the selection of process parameters, design of the feeding and filling systems and parameters of the thermal treatment for the A356R alloy.

A204 and A204R

The analysis of the results obtained through the solidification study of the A204 and A204R alloys leads to similar conclusions to those drawn with the Al-Si based alloys.

The presence of TiB_2 particles affects the behaviour of the material during the solidification step and they seem to have an important role in the precipitation of the different phases. The Al-Cu5MgTi system has been much less researched than the Al-Si7Mg0.3 one and there is not any data related to plaster casting studies. Nevertheless the main solidification reactions of this alloy have been identified by some researcher groups working with different casting processes. According to these works [1] the main reactions of the Al-Cu5MgTi system are as follows:

1) *Development of dendritic network at 654ºC and formation of Al_3Fe at 650ºC.*

   $$Liq. \longrightarrow Al + Al_3Fe$$

2) *Peritectic reaction at 620ºC.*

   $$Liq. + Al_3Fe \longrightarrow Al + Al_6(CuFe)$$

3) *Precipitation of Al-Cu-Fe phases at 590ºC.*

   $$Liq. + Al_6(CuFe) \longrightarrow Al + Al_7Cu_2Fe$$

4) *Main eutectic reaction at 545ºC.*

   $$Liq. \longrightarrow Al + Al_2Cu + Al_7Cu_2Fe$$

5) *Precipitation of further intermetallics around 505ºC and end of solidification.*

   $$Liq. \longrightarrow Al + Al_2Cu + Al_2MgCu$$

   and

   $$Liq. \longrightarrow Al + Al_2Cu + Al_2MgCu + Al_7Cu_2Fe$$

The derivative curves obtained (see figures 4.7-4.10) confirm the presence of these main reactions (see peaks 1-5 in the curves). The differences in the temperatures can be accounted for the differences in the alloy composition, nature of the mould and process parameters. On the other hand and similarly to the Al-Si based alloys, the curves become shortened in the reinforced material and the presence of TiB_2 particles affects both the onset of the precipitation of the different intermetallic phases and the solidification rate. This effect has been corroborated by the analysis of the microstructure of the A204R alloy in which the Al_2Cu phase appears associated to the ceramic particles. In addition, the size of the α-Al grains is distinctly lower when compared to the unreinforced A204 alloy (see point 4.3.2 further in this chapter). This effect coupled with the reduction of the solidification interval should positively affect the properties of the A204R alloy by decreasing the hot tearing related problems. Furthermore and similarly to the A356R material, these interactions between TiB_2 particles and the Al-Cu matrix should be taken into account in the design of the castings at industrial scale if the optimum features of the reinforced alloy are to be obtained.

4.3 INFLUENCE OF TIB_2 PARTICLES ON THE MICROSTRUCTURE

The microstructure of the TiB_2 reinforced alloys has been analysed with OM, SEM and TEM. These studies have been completed with image analysis and Electron Probe Microanalysis (EPMA) of the reinforced materials as well as AES analysis. Both as cast and thermally treated (T6) samples have been studied and their microstructures have been compared to the unreinforced alloys cast in the same conditions.

The main objective was to analyse the chemical interactions between the particles and the aluminium alloy matrix components that helped understanding the measured change of thermal and mechanical properties of the reinforced material. It is known that the TiB_2 particles have a grain size decreasing effect following mechanisms already much researched and used by the aluminium grain refining industry. The role and mechanisms of the Al-Ti-B grain refiners, that contain such particles, have been thoroughly studied but the main interest of the microstructural analysis was to check any other possible interactions that may appear with higher TiB_2 contents.

4.3.1 Microstructure of the Al-Si based materials

The Al-Si7Mg0.3 alloy has been one of the most studied and used aluminium casting alloys due to the excellent combination of properties it shows, good castability and mechanical properties. The number of works related to the study of the microstructure of the alloy reinforced with TiB_2 contents higher than 0.5% is very low though and not any reference has been found where the Al-Si7Mg0.3 + TiB_2 alloys have been cast within plaster moulds, i.e. in plaster casting. The analysis of those previous works suggests that the presence of TiB_2 particles has an influence on the grain size and morphology of the α phase of the composite materials [29].

The microstructure of the Al-Si7Mg0.3 alloy is characterized by an eutectic network formed by α-Al-Si, dispersed Mg_2Si and Al-Fe-Mn-Mg-Si based intermetallics such as $Al_8Mg_3FeSi_6$, their presence being dependent on the exact composition of the alloy and casting conditions. Al_5FeSi dark needles or AlFeMgSi ($Al_8Mg_3FeSi_6$) chinese type structures have also been identified [42-43, 55, 62].

4.3.1.1 Optical microscopy analysis

The comparison between the A356 and A356R alloys provides clear indications of the effect of the TiB_2 particles on the microstructure. TiB_2 particles cannot be discerned at low magnifications due to their small size (0.5-2.5 microns) but their influence can be indirectly appreciated. Figures 4.11 and 4.12 present a general overview of both materials and it can be seen that their aspect is much different. The α-aluminium in the unreinforced sample (fig.4.11) presents a larger grain size (around 2000 μm) and a dendritic shape while the reinforced material shows more rounded globular dendrites and a lower average grain size (300-500 μm). Furthermore the shape of the silicon is also clearly different. In the A356 samples it presents an acicular shape that is typical of unmodified Al-Si alloys (see Fig. 4.11, 4.13 and 4.15). The silicon in A356R samples loses this acicular shape in a large degree (signalled with green circles in Fig. 4.12, 4.14 and 4.16) and gets more rounded.

On the other hand, the micrographs of the A356R material show a material that presents a higher density of different intermetallic phases together with TiB_2 particles that are located mainly in the grain boundaries. Otherwise the presence of defects like microshrinkages and porosity is lower in them. An example of microshrinkage formation can be seen in Fig. 4.13 in the A356 sample. Such defects have not been detected in the reinforced material (Fig. 4.12, 4.14 and 4.16) though. The composition of the alloys and the casting conditions having been the same, these differences must be accounted for the presence of the TiB_2 particles. In fig. 4.14 it can be seen that the silicon appears in the grain boundary together with intermetallics and TiB_2 particles. Furthermore no porosity is observed in the reinforced samples.

With regards to the thermally treated samples, figures 4.15 and 4.16 present the microstructure of the two materials after having been submitted to the T6 thermal treatment. The unreinforced material A356 presents the classical microstructure of a non modified Al-Si alloy. The eutectic is in the shape of elongated ellipsoids (Figure 4.15). Figure 4.16 corresponds to A356R. It presents a lower grain size (<500 μm) but does not present any other distinct change with regards to the non treated sample shown in fig. 4.12. The silicon phases are more rounded than the unreinforced counterpart but the general aspect is similar to the as cast material.

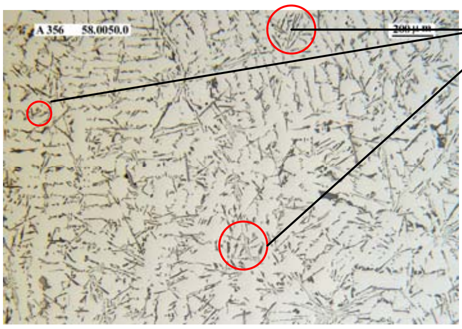

Fig. 4.11: A356. The eutectic silicon appears in acicular shape and grain size is larger than 2000 µm.

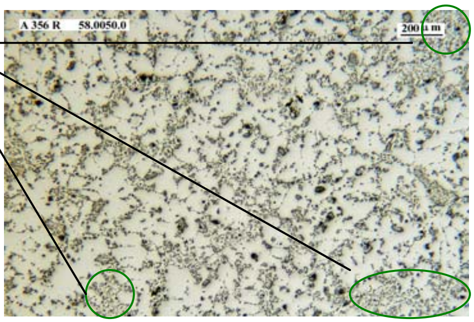

Fig. 4.12: A356R. The Si is more rounded and grain size decreases down to around 315-500 µm.

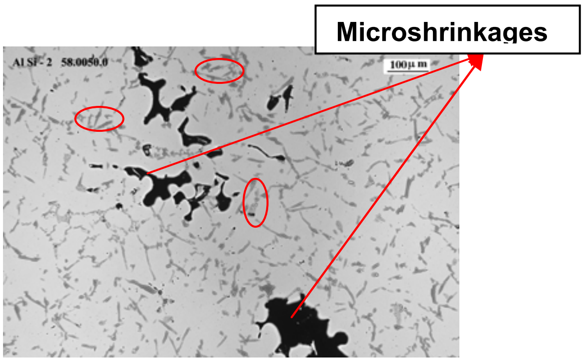

Fig. 4.13: A356. The silicon, signalled with red circles is shown having an acicular shape.

Fig. 4.14: A356R. The amount of porosity is lower than that of the unreinforced sample.

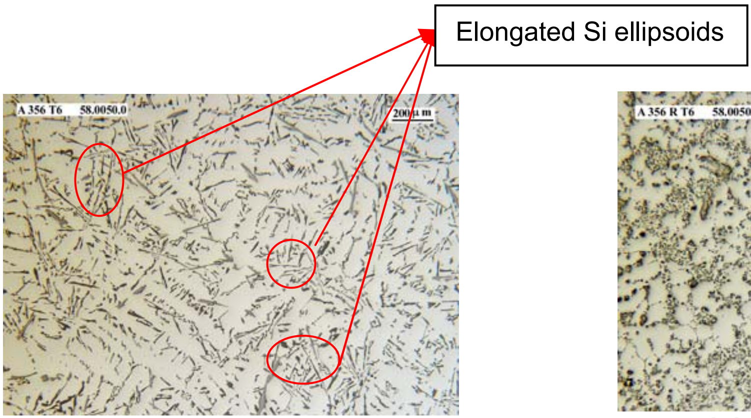

Fig. 4.15: A356-T6. The silicon is not modified and presents a typical elongated ellipsoid shape.

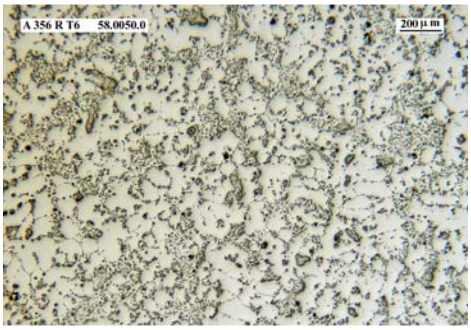

Fig. 4.16: A356R-T6. Not much differences can be appreciated when compared to the as cast sample excepting the more rounded appearance of Si.

4.3.1.1 SEM analysis

The reinforced alloy A356R was also analysed with the SEM technique. The main objective was to identify the different phases and to observe the possible interaction and influence of the TiB_2 particles. Fig. 4.17 presents a general overview of the as cast material. It can be seen that the TiB_2 particles are located in the grain boundaries together with other intermetallic phases while the α-Al grains do not contain any TiB_2. Figure 4.18 presents a detail of the microstructure with AlFeMnSi needles and Mg_2Si black phases surrounding TiB_2 particles. Figure 4.19 shows a detailed micrograph of a region where there are agglomerations of TiB_2 particles. The presence of the $TiAl_3$ phase is scarce and most of the particles are TiB_2 platelets with sizes ranging from 1 to 5 microns. Silicon platelets can be seen associated with the TiB_2 particles. This can be more clearly seen in the figures 4.20 and 4.21 that are the same micrograph treated with the image analysis software. In Fig. 4.20 the agglomeration particles can be seen.

Figure 4.22 shows the centre of an aluminium grain with a detail of the grain boundary at right side where the accumulation of TiB_2 particles can be clearly seen. No such particles have been detected in the centre of the grains. Finally figures 4.23 and 4.24 show the microstructure of the T6 thermally treated samples. Mg_2Si particles have not entirely disappeared (black area in figure 4.24 lower right corner) and the microstructure is similar to the as cast samples with precipitation of intermetallics composed of Fe-Al-Si-Ti (Fig. 4.23) and AlFeMnSi needles.

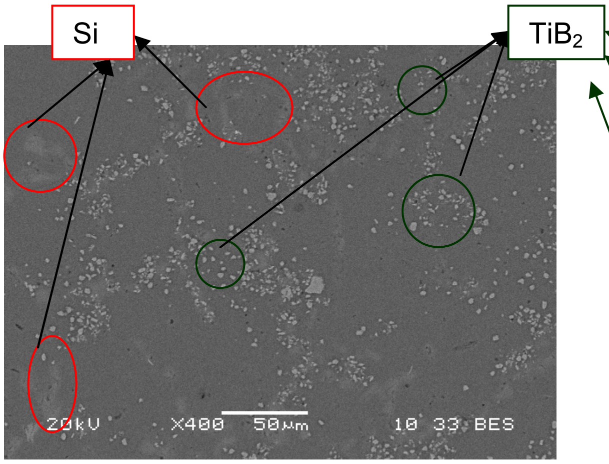

Fig. 4.17: General overview of the A356R material. White clouds are Si and TiB_2 particles appear in the grain boundaries, green circles.

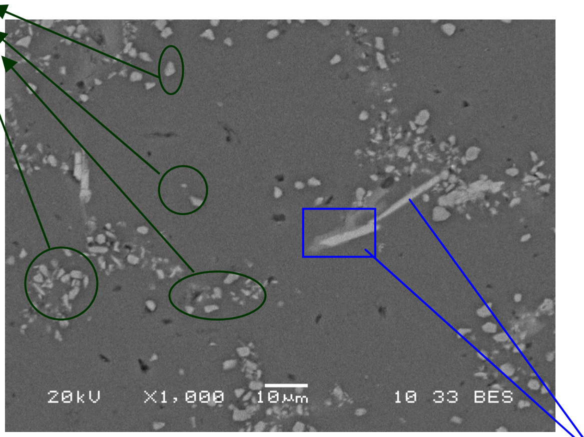

Fig. 4.18: A356R. AlFeMnSi needles signalled in blue. Individual TiB_2 particles can be clearly identified within green circles.

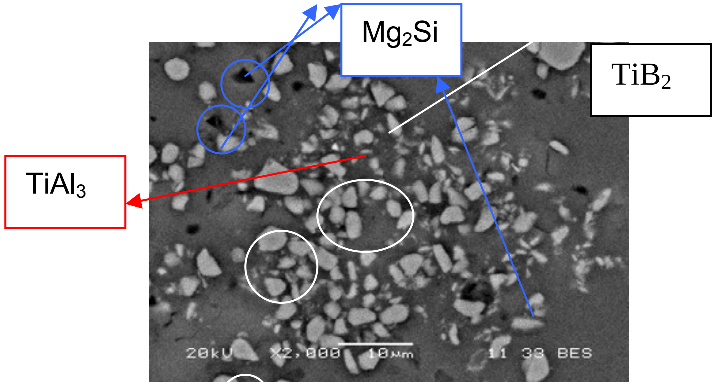

Fig. 4.19: A356R, (The small bright white particle in red is $TiAl_3$, Mg_2Si appears like black particles).

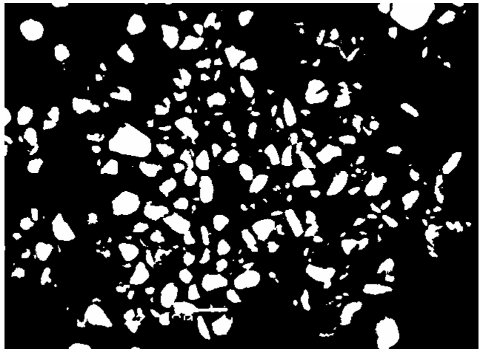

Fig. 4.20: Image analysis showing TiB_2 particles agglomerated in the grain boundary.

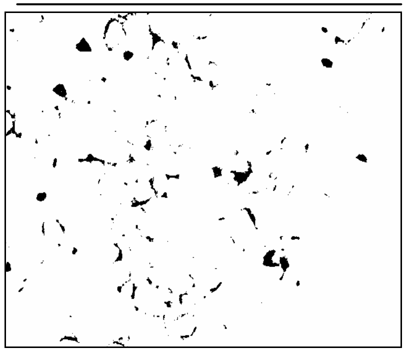

Fig. 4.21: Image analysis showing the Mg_2Si phase in the grain boundary regions.

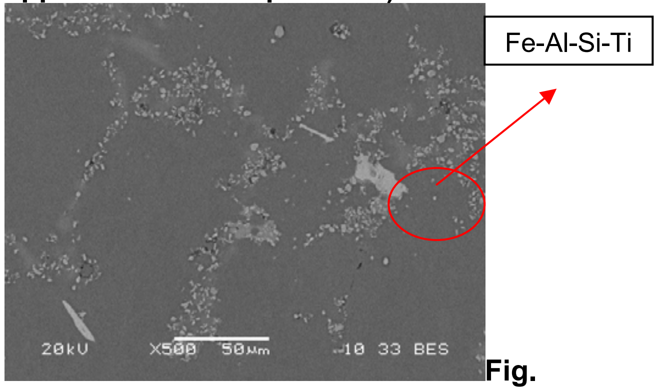

Fig. 4.22: A356RT6, thermally treated sample. Intermetallic composed of Al-Si-Ti signalled in red.

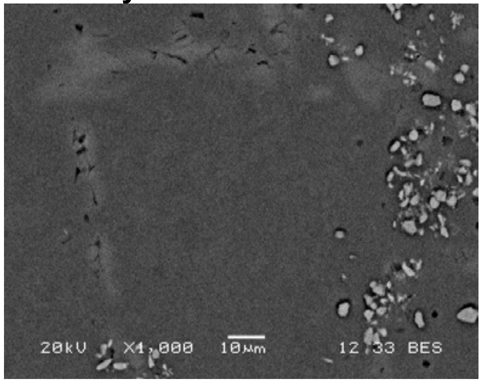

Fig. 4.23: The centre of α- Al is free of TiB_2 that appears forming agglomerations in grain boundaries.

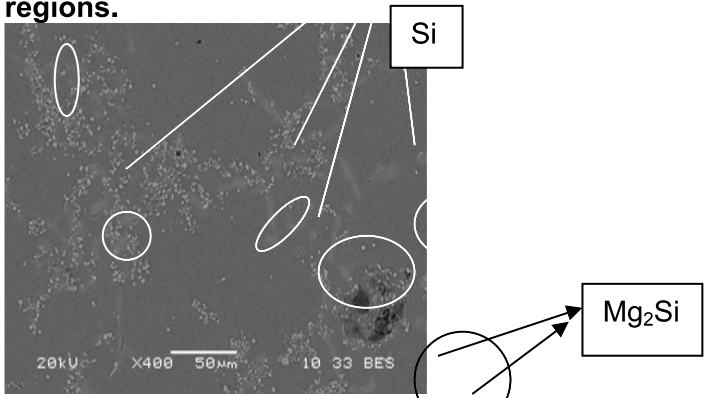

Fig. 4.24: A356RT6, general overview of a thermally treated sample.

4.3.1.3 TEM and AES analysis of the reinforced material

The A356R samples were analysed through TEM in order to study the effect of the TiB_2 particles in the generation of dislocations as well as possible reaction layers between the particles and the matrix and the role of TiB_2 in the precipitation of intermetallic phases. The specimens were obtained with the FIB technology. Isolated TiB_2 particles were identified and the orientation of the different facets was determined. An elemental EDS mapping was carried out that provides further evidence of interactions between the particles, matrix and intermetallic phases. To complete this analysis, the AES analysis technique was used to produce line profiles of areas with TiB_2 particles.

Figures 4.25 and 4.26 correspond to an isolated hexagonal TiB_2 particle surrounded by the A356R matrix and its diffraction pattern respectively. The orientations of the main facets of the TiB_2 particle have been identified. The analysis of the TEM image provides some interesting information on the nature of the interaction between the particle and the surrounding matrix:

1) *The TiB_2 particulate presents very sharp edges.*
2) *The density of dislocations around the particulate is small even though there is a large CTE mismatch between the TiB_2 particle and the matrix ($8.1\ 10^{-6}\ C^{-1}$ and $22.9\ 10^{-6}\ C^{-1}$respectively).*
3) *Small grains can be seen growing on the facets of the TiB_2 particle. Moreover the sizes of all the precipitates that appear all over the TEM image are small even though there is only one TiB_2 particle.*
4) *No clear reactions can be appreciated on the interface of the TiB_2 particulate.*

The sharpness of the edges of the particulate can be explained by the fact that most of the TiB_2 particles within the reinforced alloys have been exogenously created and subsequently incorporated to the aluminium matrix. Only around 10% of the TiB_2 particles have been created in situ according to the material supplier. The ex situ particles can grow without any constraint and that would explain the sharp edges and final appearance of the particulate in Fig. 24 that would be therefore an ex situ particulate.

Another feature shown by the TEM image is that the density of dislocations around the TiB_2 particles is small taking into account the large difference of the CTEs of the TiB_2

particles and the A356R matrix. A larger density was to be expected due to the large mismatch in the CTE values that could lead to the generation of dislocations to accommodate the stresses generated during the solidification of the material containing the particles. Furthermore it can be observed that there are small grains in the whole region even though there is only one TiB_2 particle. Small aluminium grains grow on the facets of the particulates that serve as nucleation sites for further grains. The final structure is that of a TiB_2 particulate surrounded by very small precipitates. These precipitates can easily rotate during solidification to accommodate the generated stresses. This phenomenon would explain that the relaxation of the stresses created by the CTE mismatch does not take place through the appearance of large amounts of dislocations that has been described in other MMC materials.

Finally no any reaction layers could be appreciated on the TiB_2 particles that mainly present clean and sharp edges. Therefore the TEM analysis cannot confirm the interactions between the silicon and the TiB_2 particles that have been appreciated through SEM and AES. Nevertheless it must be taken into account that only some few TiB_2 particles have been analysed by TEM and therefore the presence of reactions between TiB_2 particulates and the aluminium matrix cannot discarded.

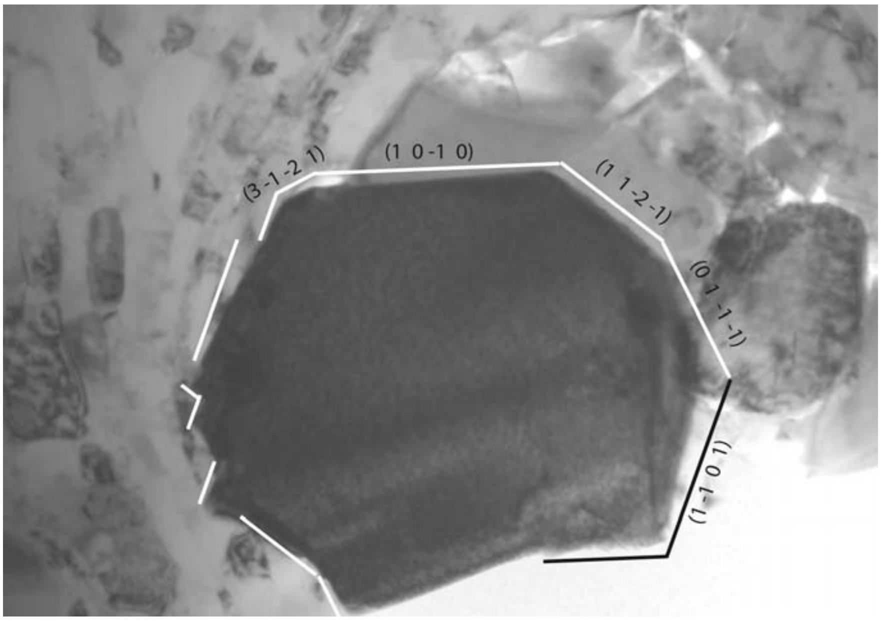

Fig. 4.25: Isolated TiB_2 grain. The hexagonal shape of the particle is clearly visible. The edges of the precipitate are very sharp.

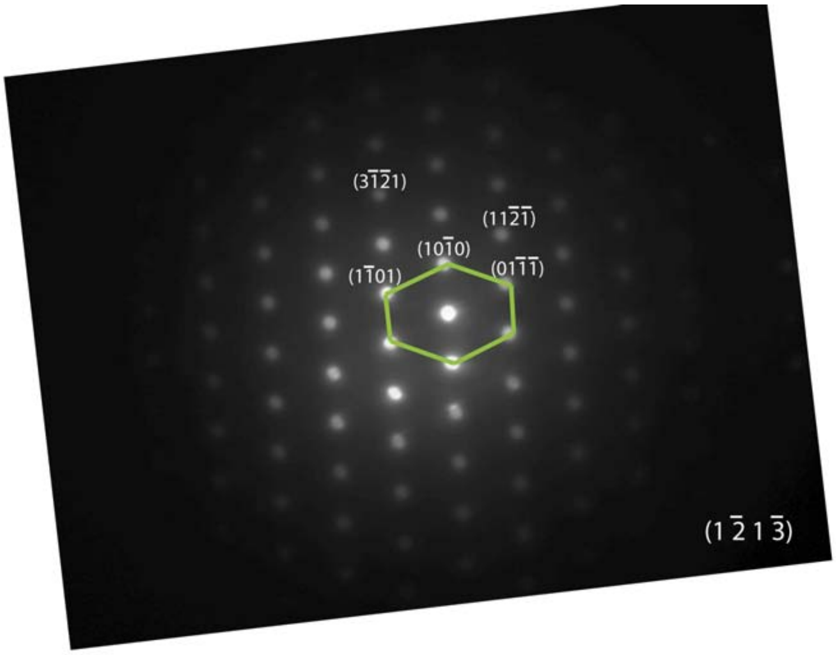

Fig. 4.26: Diffraction pattern of the hexagonal precipitate (TiB_2) in the A356R specimen.

The mapping performed with the EDS provides additional interesting information. Figures 4.27-4.30 are the mapping of the main elements (Al, Si, Ti, B respectively) from a region where an agglomeration of TiB_2 particles exists. It can be clearly seen that the silicon appears frequently associated with the TiB_2 particles. There is a segregation of the former on the surface of the latter clearly visible on several different TiB_2 particles. (See fig. 4.28).

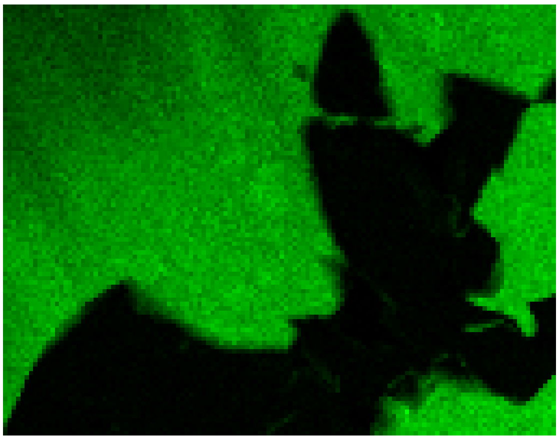

Fig. 4.27: EDS mapping of Al.

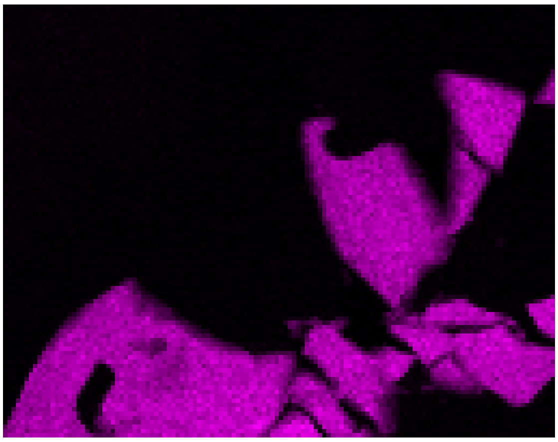

Fig. 4.28: EDS mapping of Si. It often appears linked to TiB_2 particles.

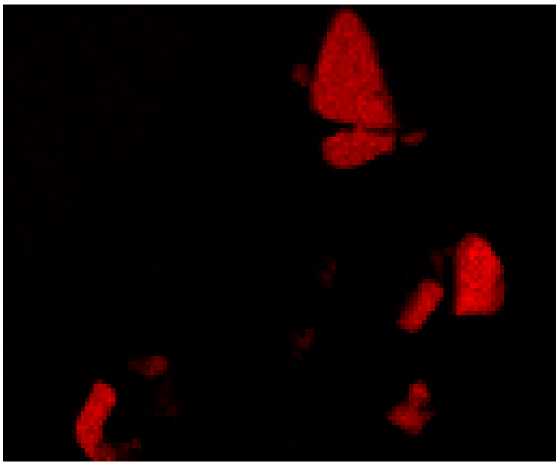

Fig. 4.29: EDS mapping of Ti.

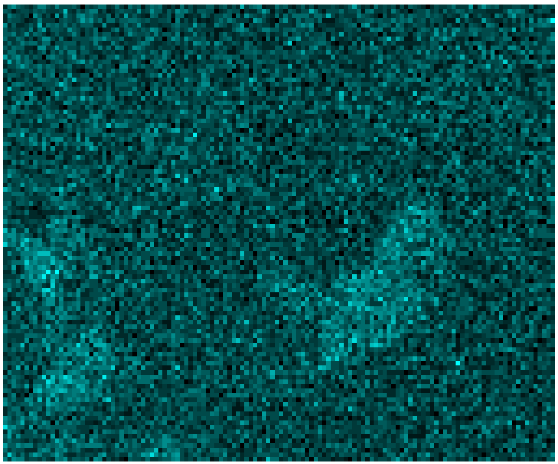

Fig. 4.30: EDS mapping of B.

Finally the analysis of the A356R material was completed with the AES. The figure 4.31 shows the secondary electron SE image obtained in a region of TiB_2 agglomeration. The white region corresponds to the aluminium matrix and the dark area corresponds to the region where TiB_2 particulates coexist with silicon and aluminium. The corresponding AES line profile is shown in Figure 4.32. The main feature observed is the segregation of Si in both sides of the TiB_2 particles. This feature confirms other observations made with the SEM and confirms that an interaction exists between silicon and TiB_2. The nature of this interaction is difficult to be discerned but it is clear that silicon grows on the facets of the TiB_2 particulates. Furthermore these observations are in agreement with other studies of different researchers that affirm that Si poisons the Al-Ti-B grain refiners by covering the facets of TiB_2 particles.[14, 65]. Different theories have appeared to explain this interaction. One of them, postulated by Quested et al. [14], says that the {0001} faces of TiB_2 particles become covered by $TiSi_2$ created from the elements in the melt and this silicide would thus be responsible of the poisoning effect observed in Al-Si alloys refined with Al-Ti5-B1 grain refiners. The results obtained in the present work seem to confirm this theory as Si is clearly segregated on TiB_2 particles with Ti taking part of the interaction.

Another feature of the AES line profile is that some Ti and B appear in all the line including the regions where there are not any TiB_2 particles. This can be explained by a reaction of the particulate with the matrix or a diffusion of atoms but the TEM image presents a very sharp image of the TiB_2 particle and the EDS mapping images do not clearly show it and therefore the diffusion of Ti and B atoms must be low.

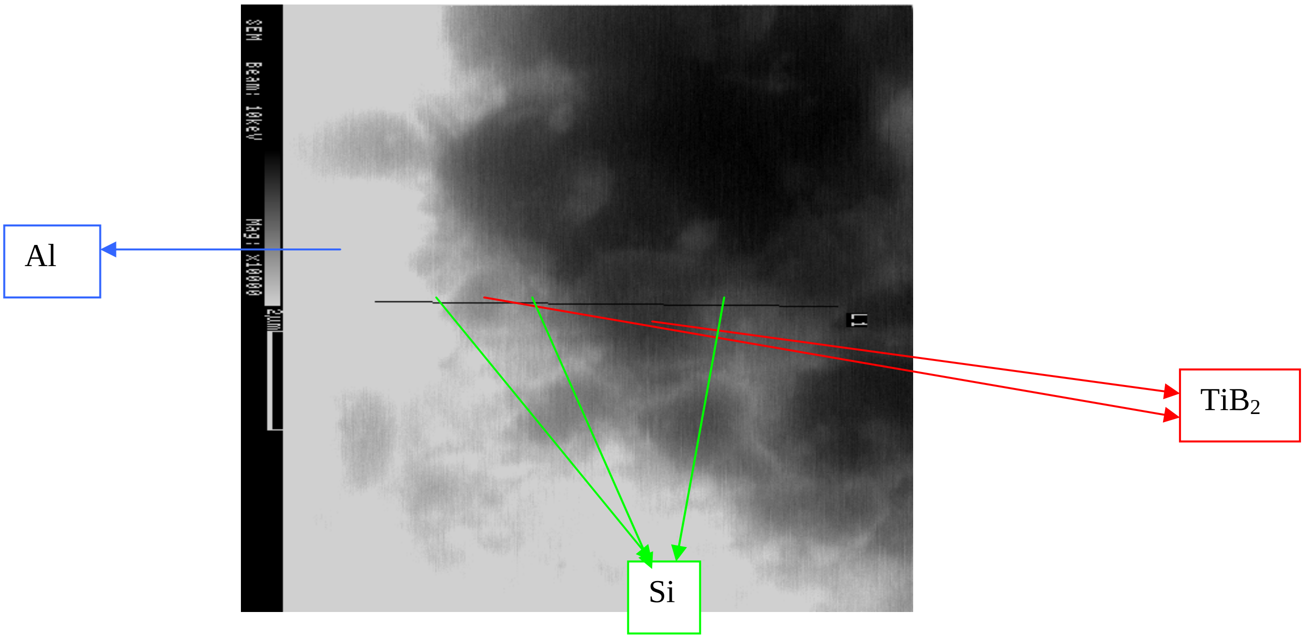

Fig. 4.31: SE image showing the interface between TiB_2 particles and the aluminium matrix.

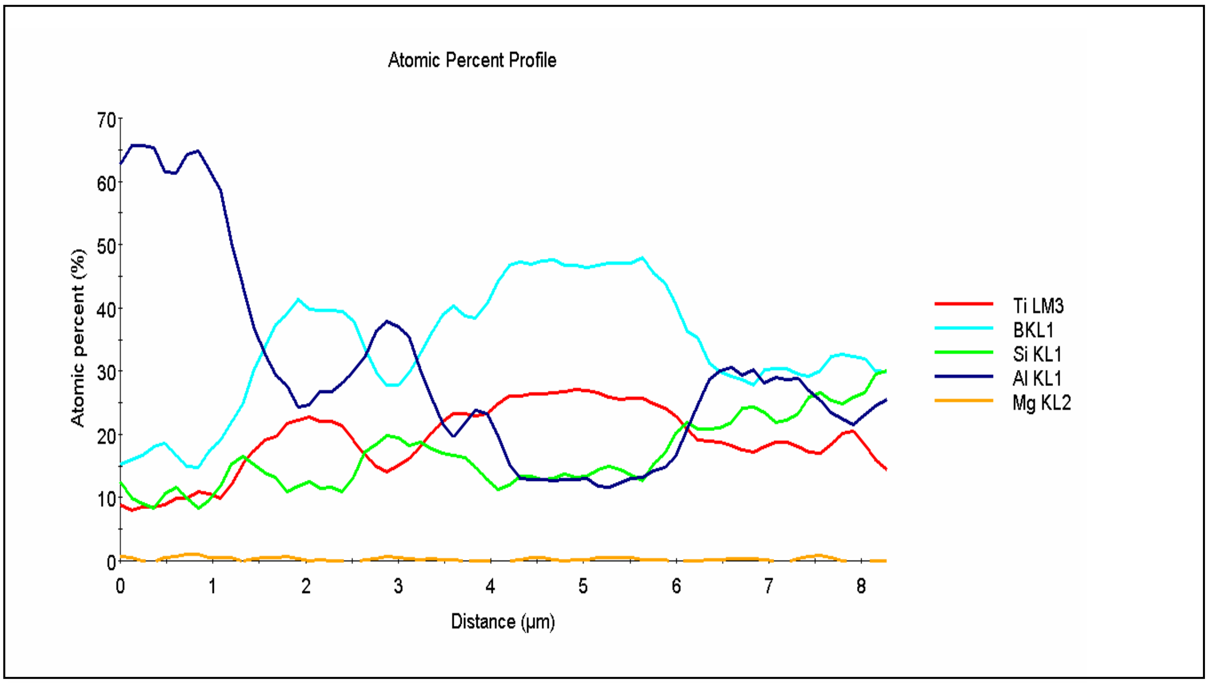

Fig. 4.32: AES line profile. B is linked to Ti (TiB_2). Silicon appears either with Al or segregated on the TiB_2 surface.

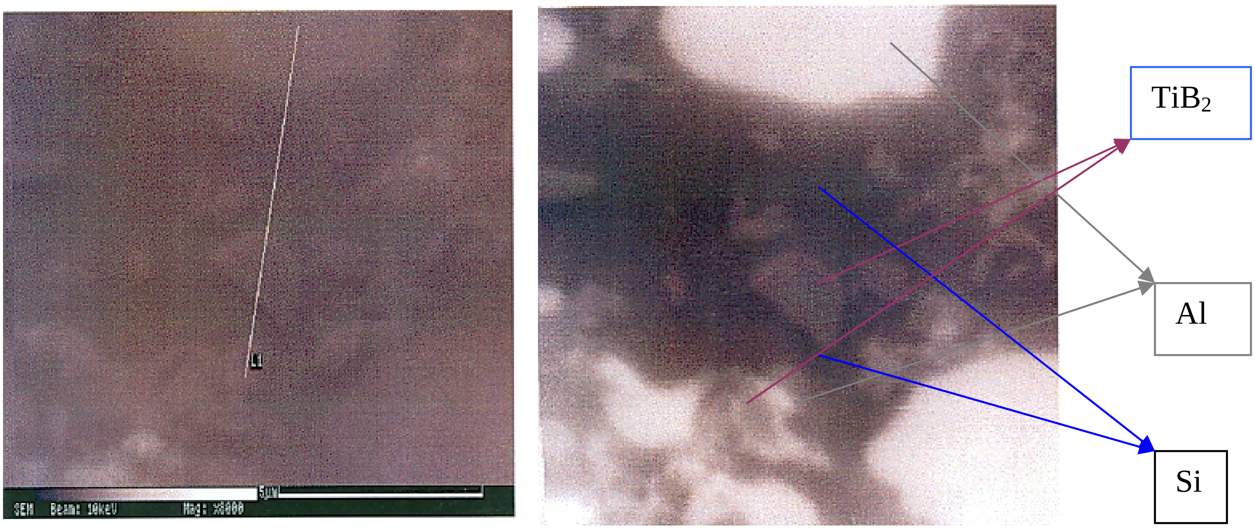

Fig. 4.33: SE image of a different region. The same phenomena observed in Fig. 4.31 can be appreciated. The segregation of Si is clear on the TiB_2 interface.

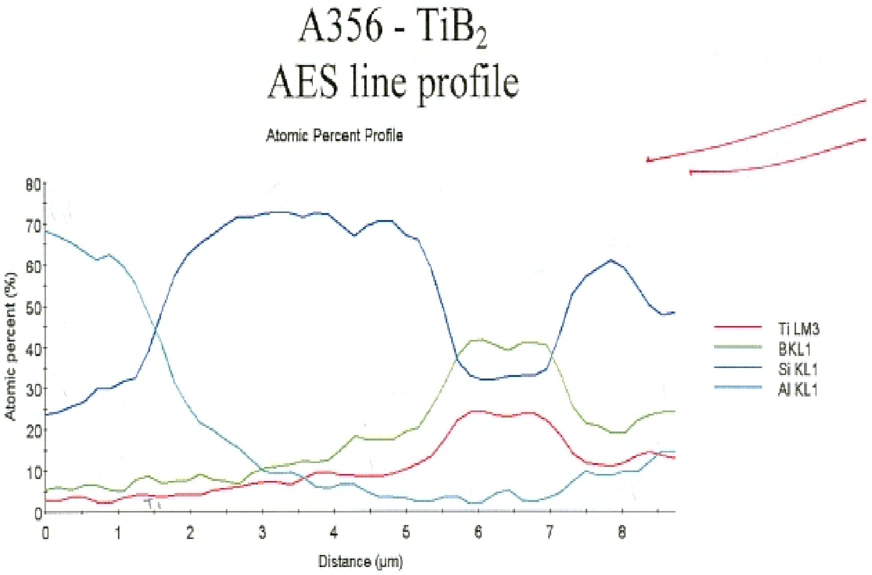

Fig. 4.34: AES line profile corresponding to the region analysed in Fig. 4.33. segregation of Si clearly visible at the TiB_2 interface. Neither Mg nor Fe was found.

4.3.2 Microstructure of the Al-Cu based materials.

The microstructure of the Al-Cu5MgTi alloy has not been so extensively studied as the Al-Si7Mg0.3 but there are some works that provide information on its main microstructural features. The main feature is an eutectic network of α-Al-Al_2Cu and different intermetallics where Fe found combines with Cu and Mg in Al_7Cu_2Fe needles or Al_2CuMg phases [1, 42].

The influence of the T6 thermal treatment has been analysed by different researchers [63-64] that observed that during thermal treatment the light grayish phase Al_2Cu dissolves and only the Al_7Cu_2Fe needles remain, together with the aluminium grains and some $TiAl_3$ polyedric grayish phase. Subsequently and during the ageing treatment small Al_2Cu particulates precipitate that confere the strength to the alloy.

4.3.2.1 Optical microscopy analysis.

The figures 4.35 and 4.38 show a general aspect of the microstructure of the A204 and A204R. The first effect that can be observed is that the TiB_2 has a grain refining effect (the grain size decreases from 315-200 μm in the A204 alloy down to 125-200μm in the A204R). Furthermore, the grain boundaries in the A204R present a high content of additional phases such as Al_2Cu and TiB_2 particles.

Figure 4.36 shows a region of the A204 alloy where microshrinkages exist. This alloy is known to have a tendency for hot tearing and shrinkage related problems due to its long solidification interval. No such microshrinkages have been appreciated in the reinforced material though (Fig. 4.38, 4.39). The grain size decrease and the precipitation of intermetallic phases in the grain boundaries of the A204R (Fig. 4.38 and 4.39) are the most remarkable features when compared to the unreinforced materials.
Regarding the thermally treated samples (Figures 4.37 and 4.40), not any additional relevant features are remarkable.

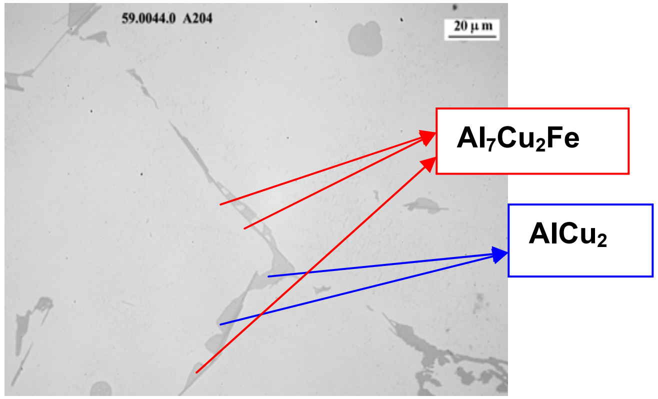

Fig. 4.35: General overview of the A204 material. $AlCu_2$ phases and Al_7Cu_2Fe needles can be observed.

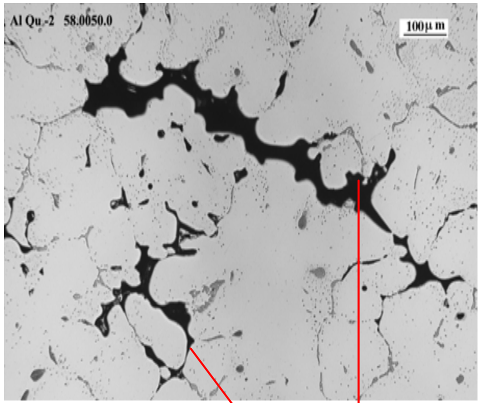

Fig. 4.36: A204. The unreinforced alloy is prone to microshrinkages.

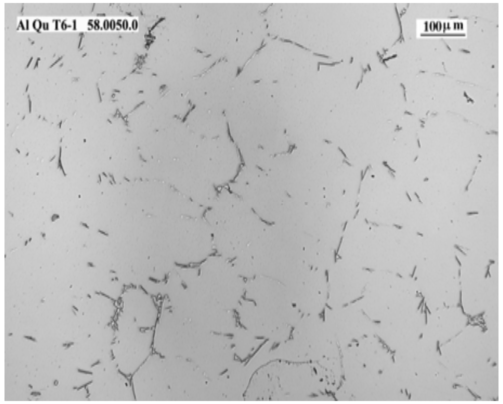

Fig. 4.37: A204-T6. The thermal treatment induces the precipitation of Al_2Cu not observable due to its size.

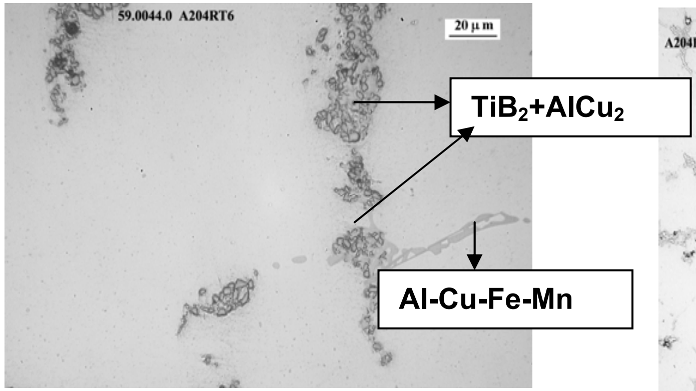

Fig. 4.38: General overview of the A204R material. TiB_2 appears agglomerated with $AlCu_2$ and Al-Cu-Fe-Mn phases.

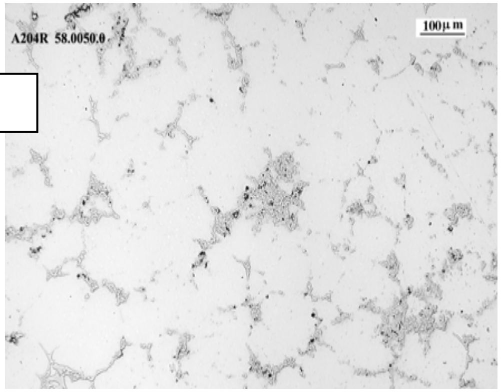

Fig. 4.39: A204R. The presence of TiB_2 particles prevents the formation of defects and refines the grains.

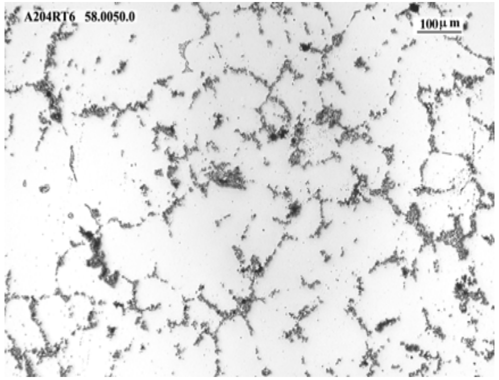

Fig. 4.40: A204R-T6. The sample presents a microstructure similar to the as cast material.

4.3.2.2 SEM analysis

A204R samples were analysed with SEM in order to further study the influence of the TiB_2 particles in the microstructure of the alloy. An image analysis of the regions where agglomerations of particles existed was also carried out to complete the work and discern the presence of TiB_2 particles, Al_2Cu and Al-Fe-Cu intermetallics. One important feature that can be seen and that is different from the previous A356R alloy studied is that TiB_2 particles do appear in the interior of the grains (see Fig. 4.41), isolated grain of aluminium surrounded by a large density of particles and intermetallics) where there are also Al_2Cu intermetallic phases that appear connected to the TiB_2 particles. This phenomenon can be more clearly seen in the detailed micrographs of regions where there is an agglomeration of TiB_2 particles (Fig. 4.42 and Fig. 4.43). In the same way, the image analysis of the fig. 4.43 shows that many Al_2Cu particles are associated to TiB_2 particles (Fig. 4.44 and Fig. 4.45).

The analysis of the region where there exists a concentration of intermetallics and TiB_2 shows additional features of the A204R alloy. In Fig. 4.46 rests of a salt used to form the in situ TiB_2 particles can be appreciated (presence of K and F identified with SEM analyser). The germination of the in situ formed TiB_2 particles can be seen around the rests of the KBF_4 and K_2TiF_6 salts used in the production of the in situ particles. Finally figures 4.47 shows TiB_2 particles found in the interior of the α-Al grains. This feature could not be found in the reinforced A356R alloy. Figure 4.48 is the image of the thermally treated A204RT6 sample where Al_7Cu_2Fe needles can be seen.

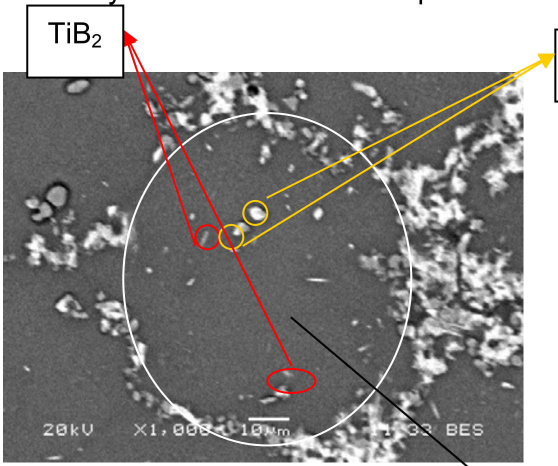

Fig. 4.41: Image of A204R showing an isolated α-Al grain encompassed by the large white circle and TiB_2 and Al_2Cu particles.

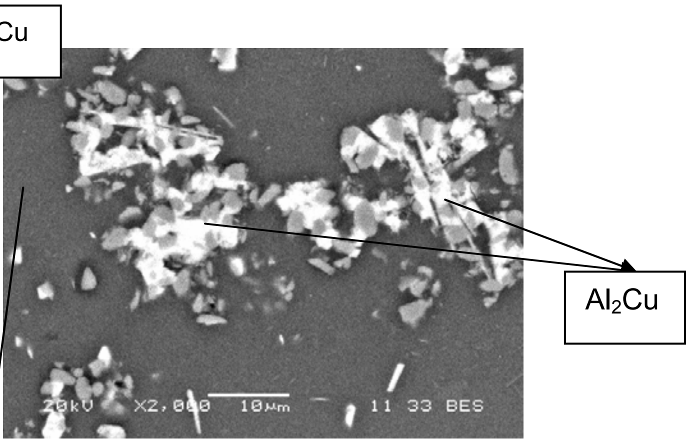

Fig. 4.42: A204R Grey particles are TiB_2. White phases are mainly Al_2 Cu.

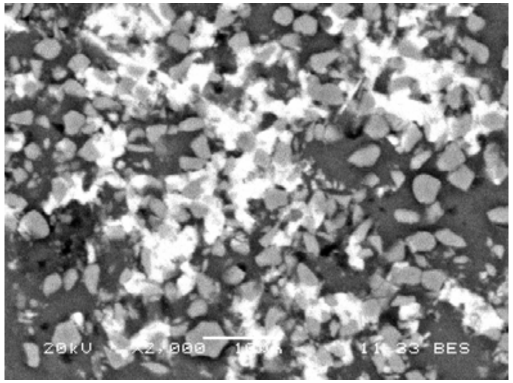

Fig. 4.43: A204R. Agglomeration of TiB_2 (grey) together with Al_2Cu (White).

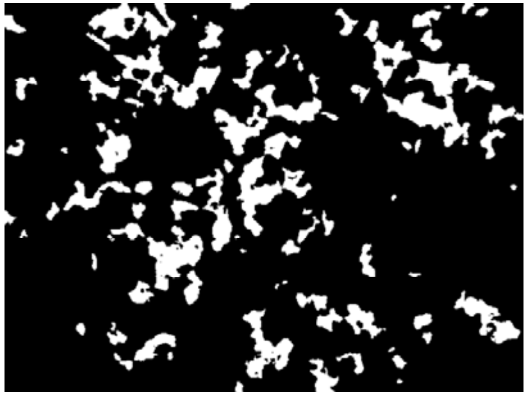

Fig. 4.44: Image analysis of Fig.4.43 showing the Al_2Cu.

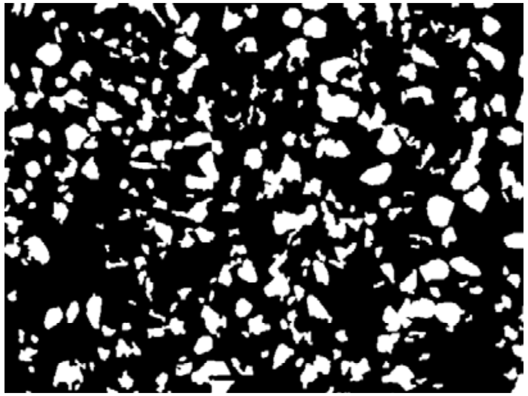

Fig. 4.45: Image analysis of Fig.4.43 showing the TiB_2 distribution.

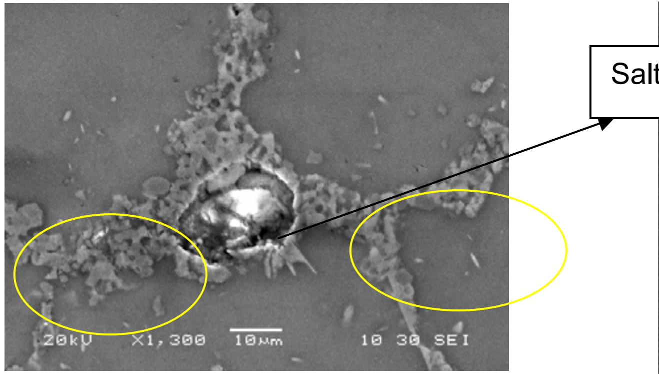

Fig. 4.46: A204R. Rests of the salts and germination of TiB_2 particles, within the yellow circles.

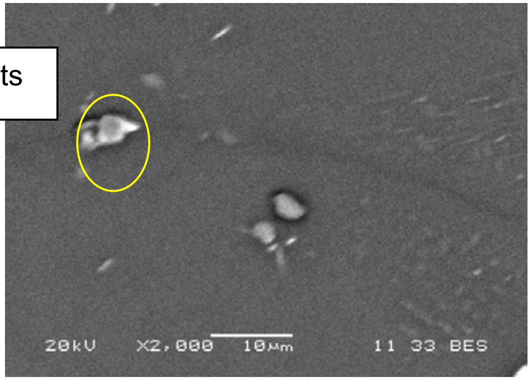

Fig. 4.47: A204R. TiB_2 particles (light grey) found in the interior of a α-Al grain appear linked to Al_2Cu (white).

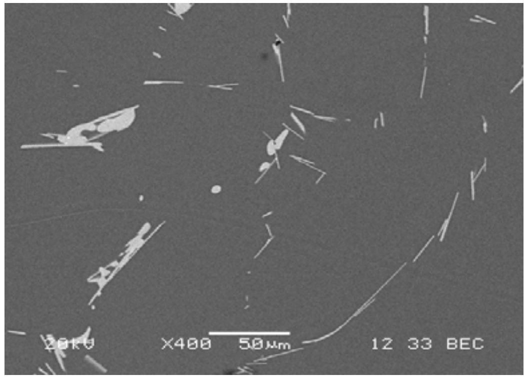

Fig. 4.48: A204RT6. Al_7Cu_2Fe needles can be seen. Low amount of Al_2Cu phases.

4.3.2.3 TEM and AES analysis

The TEM analysis of the reinforced A204R alloy shows some common features concerning the Al-Si based alloy. Figure 4.49 shows a single TiB_2 particulate. The orientation of the different facets was determined and the elemental EDS mapping was also carried out to study the interaction of the TiB_2 particulates with the Al-Cu matrix. Finally the AES analysis was used to obtain additional information.

The figures 4.49 and 4.50 present a hexagonal TiB_2 particle surrounded by the A204R matrix and its diffraction pattern. In this case the edges are not as sharp as in the A356R material (see fig. 4.25). This may point out that some kind of diffusion of some atoms from the particulate into the Al-Cu matrix may have taken place. Anyway the sharpness of the edges is enough to consider that the isolated TiB_2 grain is surely an ex situ particle. The orientations of the main facets of the TiB_2 particle have been identified with the help of the diffraction pattern shown in figure 4.50. The analysis of the TEM image provides the following main features:

1) *The TiB_2 particulate presents sharp edges and therefore it will probably be an ex situ particle. Nevertheless the particle in figure 4.25 corresponding to the A356R alloy presented even sharper edges. It is possible that some chemical interactions may have taken place.*

2) *The density of dislocations around the particulate is small in spite of the CTE mismatch between the particulate and the Al-Cu matrix (8.1 and 25.3 10^{-6} C^{o-1} respectively).*

3) *The grain size of the particles around the TiB_2 particulate is small.*

The TEM analysis was completed with an EDS mapping of the main elements (Al, Cu, Fe,Ti, Si and B). The results are shown in figures 4.51-4.56. Two large TiB_2 particles can be seen that are surrounded by Cu and Al. TiB_2 particles act as nucleation sites for Al_2Cu precipitates.

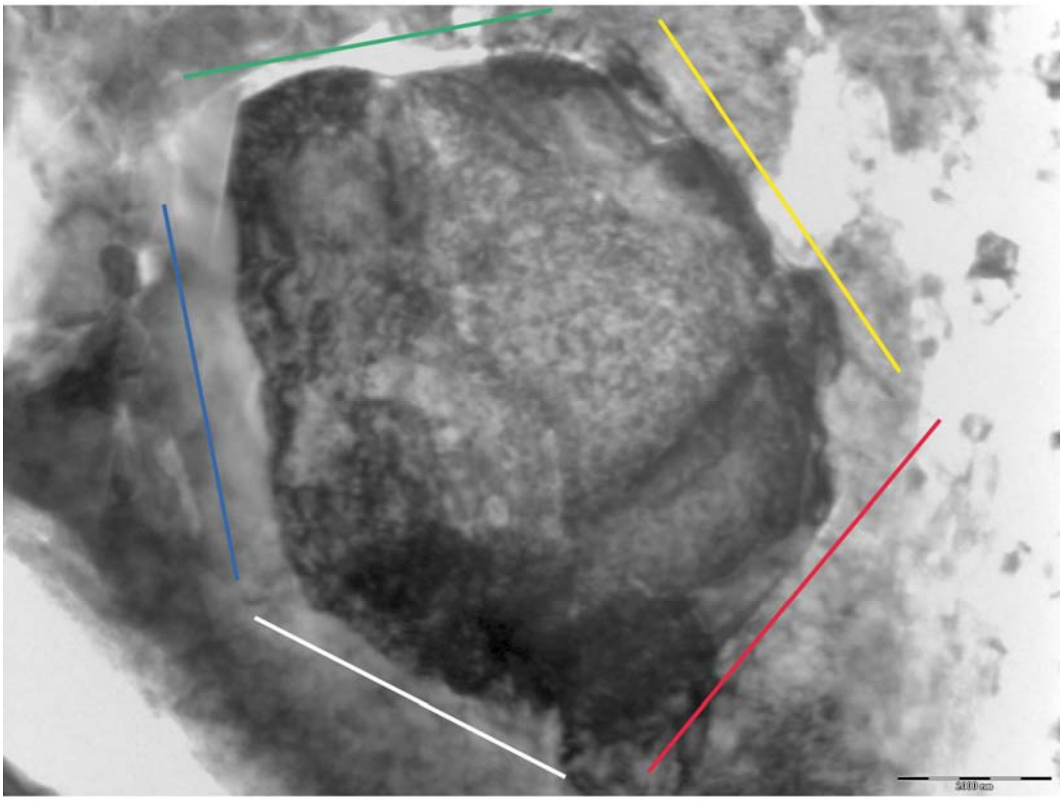

Fig. 4.49: TEM image of an isolated TiB_2 particle within the A204R sample.

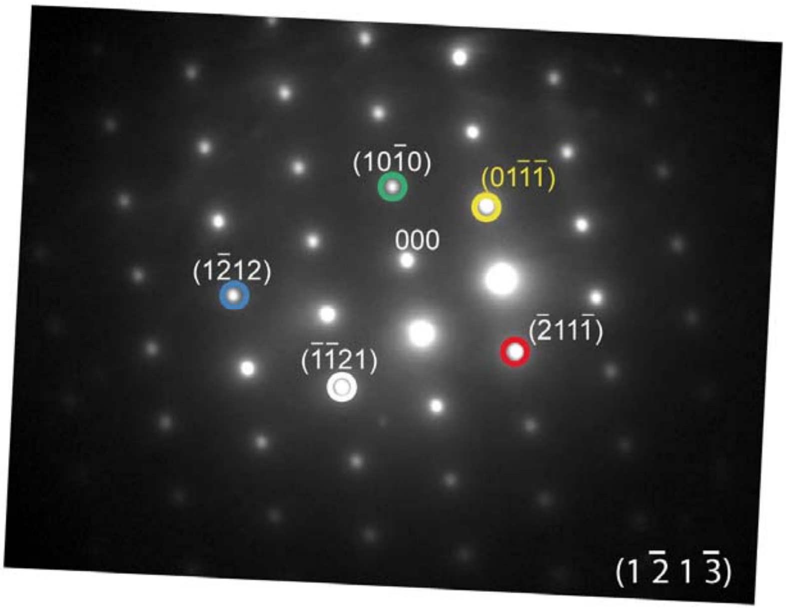

Fig. 4.50: Diffraction pattern of the TiB_2 particulate within the A204R alloy.

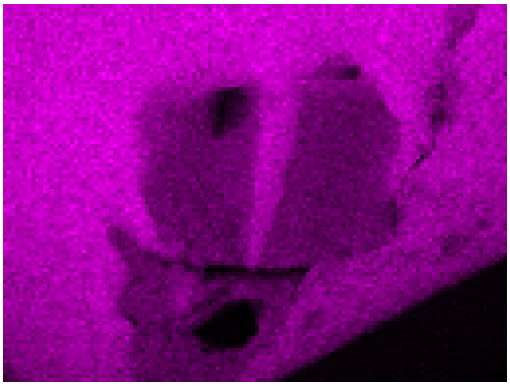

Fig. 4.51: EDS mapping of Al. The two large rounded black areas represent two TiB_2 particles surrounded by Al and Cu.

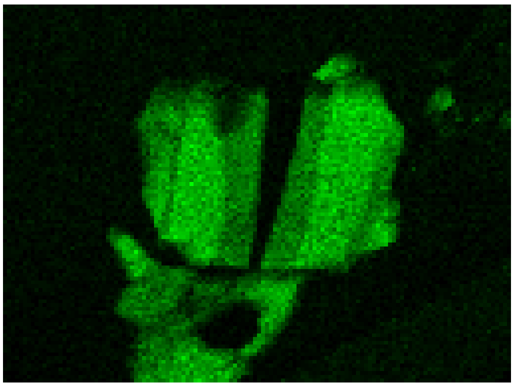

Fig. 4.52: EDS mapping of Cu. Cu appears together with Al (Al_2Cu) linked to TiB_2 particles.

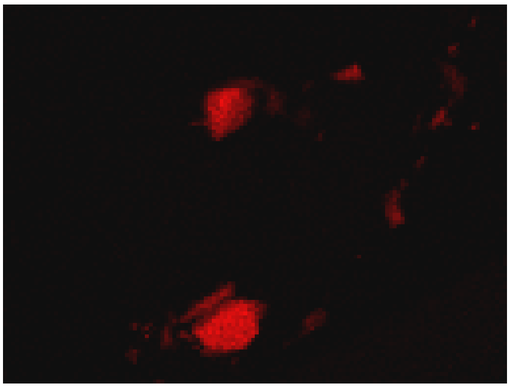

Fig. 4.53: EDS mapping of Ti. Two TiB_2 particles can be clearly identified.

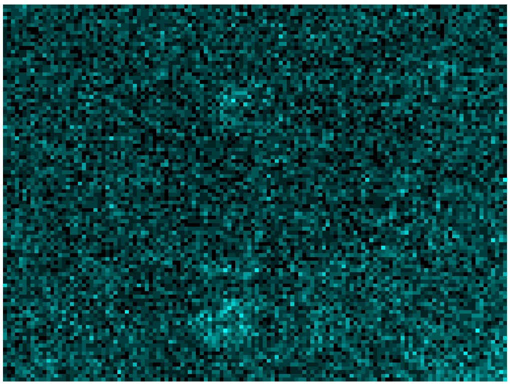

Fig. 4.54: EDS mapping of the Boron. It is associated with Ti forming TiB_2 particles that are surrounded by areas rich in Al and Cu.

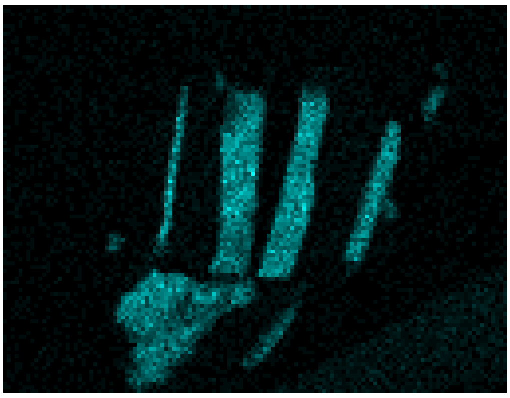

Fig. 4.55: EDS mapping of Fe. The iron appears linked to Al and Cu forming intermetallics that also grow on TiB_2 particles.

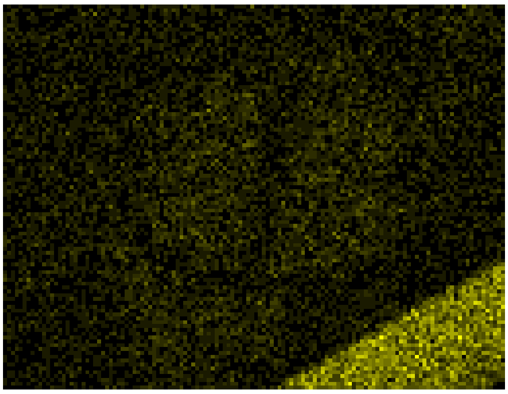

Fig. 4.56: EDS mapping of Si.

Finally the AES analysis was carried out to complete the microstructural analysis. The figures 4.57- 4.59 show one image and two line profiles. Figure 4.57 shows different TiB_2 particles (dark areas) that are identified by the characteristic Ti and B peaks in the line profiles. The 4.58 profile shows that some Al-Cu intermetallic phases are formed in the interface of the TiB_2 particles. It is difficult to define the composition of these intermetallics as they may also contain some Fe, Mg or Si. Nevertheless and according to other data obtained in previous analysis (SEM) of these materials it may be deduced that most of them are Al_2Cu precipitates.

Likewise the A356R alloy the B and Ti appear also distributed all over the sample. This may point out that some diffusion of these elements into the Al-Cu matrix may have taken place. In order to obtain more information, a non linear least squares fitting (NLLSF) software was applied to the 4.57 image. The results showed that there were two different aluminium species related to two different chemical environments. These aluminium species have been marked as Al_1 and Al_2. The analysis of the resulting profile indicates that Al_1 corresponds to α-aluminium and Al_2 corresponds to an intermetallic that is formed by Al-Cu (therefore it is probable to be Al_2Cu) that segregates on the interface of the TiB_2 particles. These results are in agreement with the observations of the X-ray diffraction where Al_2Cu crystals were observed in the A204R material as well as the results obtained with optical microscopy and the image analysis of SEM specimens.

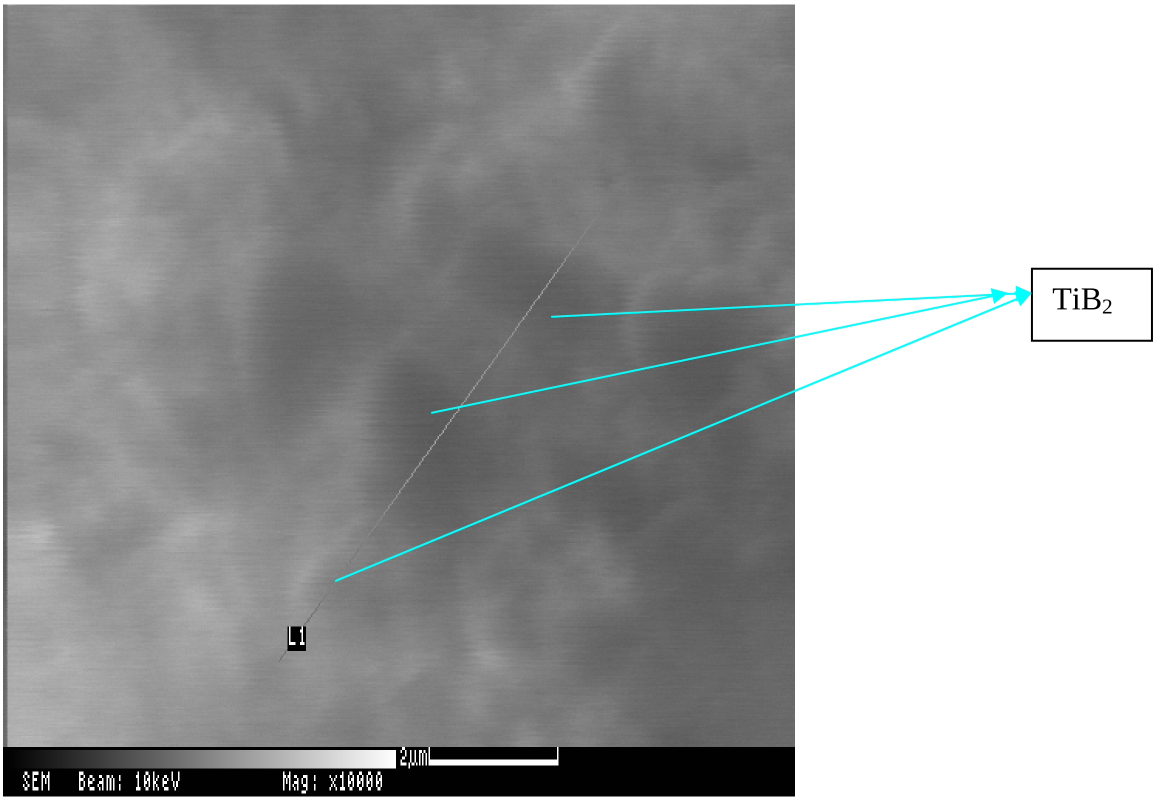

Fig. 4.57: AES image of the A204R alloy. Clear regions contain Al and Cu and dark areas are TiB_2 and intermetallics.

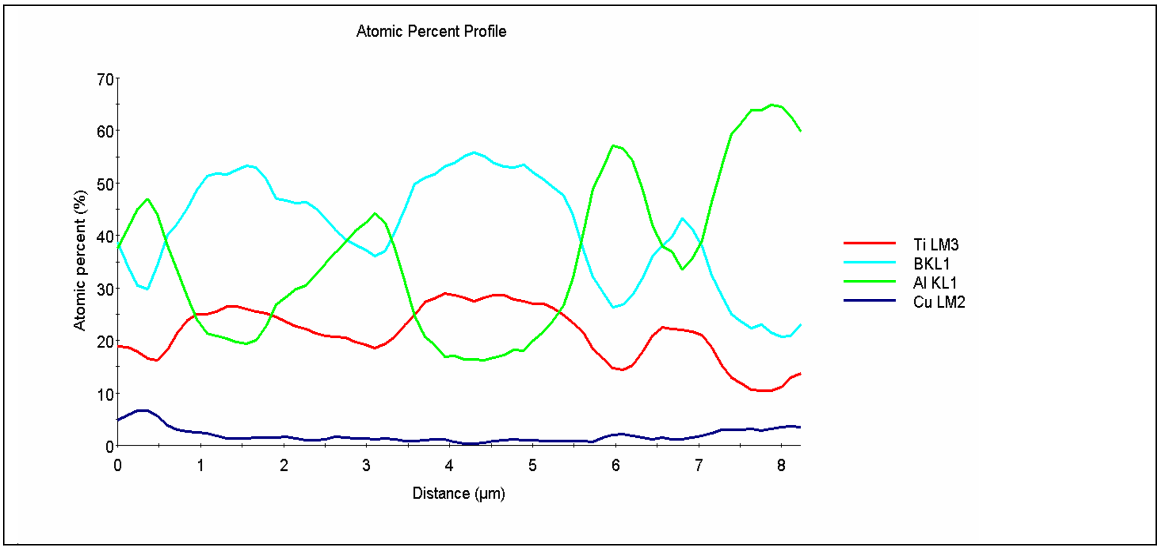

Fig. 4.58: Line profile analysis of the Fig. 4.57 image showing the presence of Al, Ti, B and Cu.

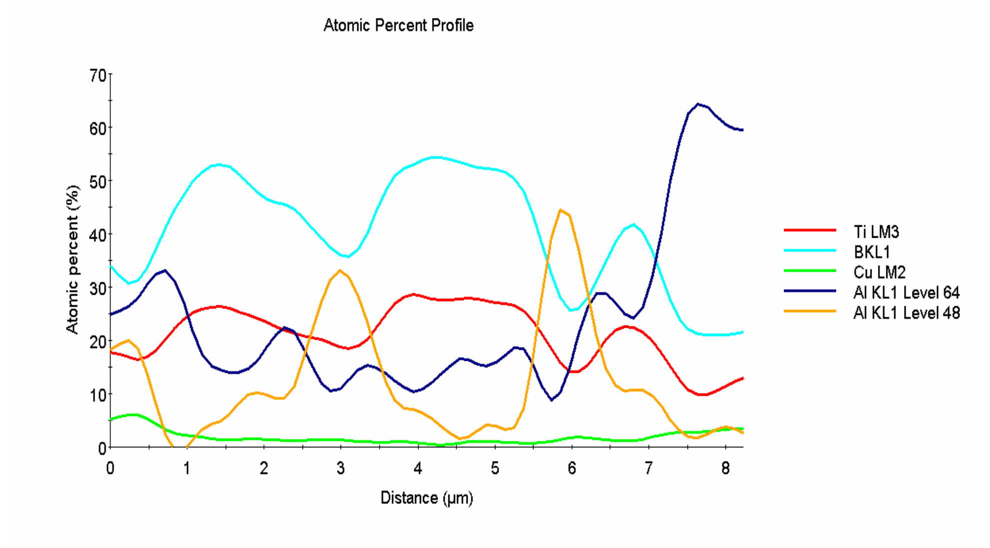

Fig. 4.59: Line profile obtained by applying the NLLSF software. Two different aluminium species can be appreciated. The Al linked to Cu appears to be segregated on the interface of the TiB_2 particulate.

4.3.3 Discussion of the results

The comparison of the reinforced A356R and A204R alloys with the corresponding unreinforced counterparts makes clear that the presence of TiB_2 particles has a large influence in the final microstructure of both materials. These differences are furthermore not limited to the grain refining phenomena that were previously known to take place when small amounts of TiB_2 particles were incorporated as part of Al-Ti-B grain refiners. It has been seen that TiB_2 particles play an important role in the precipitation events of the different phases that are formed during solidification. Furthermore they have a beneficial influence on the decrease of porosity and solidification shrinkage related defects.

In the case of the A356R alloy, the first evident effect of the presence of the TiB_2 particles is the reduction in the grain size of the material when compared to the unreinforced samples. (from around 2000 down to 315-500 μm). Grain boundaries act as a barrier to dislocation movements and therefore contribute to improve mechanical properties. Both TEM and SEM images confirm that TiB_2 particles act as nucleation sites for aluminium grains even though silicon seems to interfere with this mechanism. OM and SEM images show that Silicon particles precipitate around the TiB_2 particles and the former have a more rounded shape in the reinforced alloy when compared to the unreinforced samples (see figure 4.60). The present work confirms the results of previous works on the poisoning effect of Si on the action of the TiB_2 particles. On the opposite, the results of this work show that there are some beneficial effects in the addition of the particles in the Al-Cu alloys (grain size decrease from 315-200 down to 200-125 μm).

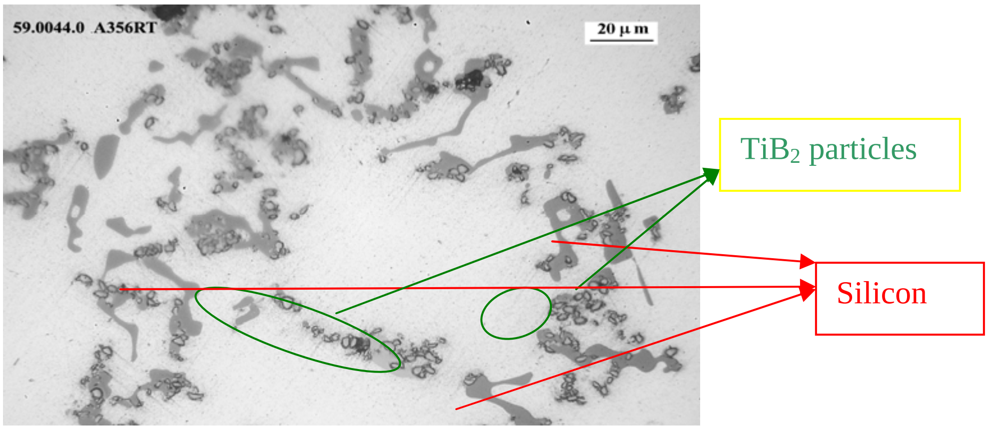

Fig. 4.60: TiB_2 particles (round clear particulates) can be seen surrounded by Si (grey phases).

TiB_2 particles play a role in the modification of the Si particles. The more globular shape of the latter in the reinforced material should entail higher mechanical properties as the silicon may act as a reinforcing agent due to a better transmission of the loads from the matrix. Furthermore the AES analysis and the line profile study confirm that Si segregates onto TiB_2 particles. This Si/TiB_2 interaction provides an explanation to the fact that the final average aluminium grain in the A356R material is larger than 200 μm that is accepted to be the value below which the grain size is low enough as to provide an improvement in the mechanical properties. Silicon poisons TiB_2 particles.

On the other hand the OM and SEM analysis show a decrease in the porosity of the microstructure of the reinforced alloys (Figures 4.11, 4.12 and 4.15) Another aspect that was foreseen to appear that could enhance the mechanical resistance of the reinforced material was an increase in the dislocation density due to the large CTE mismatch between TiB_2 particles and the aluminium matrix. It was to be expected that this mismatch led to an increase of the dislocation density as a way to accommodate the internal stresses created during the solidification. This mechanism is known to work as a barrier to the movement of dislocations in other particulate reinforced MMCs. Nevertheless this effect has not been appreciated in the materials studied in this work.

The TEM analysis has not shown any evident increase in the dislocation density. It is proposed that the reason that explains this fact is that there is another mechanism that is acting to accommodate these stresses. The TEM analysis shows that the regions in the vicinity of TiB_2 particles are formed by low sized grains that appear to be growing on the surface of other grains that have solidified on the TiB_2 facets. These small sized grains have the capacity of rotating freely to accommodate the stresses generated during solidification process due to the CTE mismatch between TiB_2 and the aluminium matrix.

The microstructure of the A204 alloy is also affected by the action of the TiB_2 particles. This kind of effects is comparable to that of the Al-Si based alloys but they are larger and more clearly appreciated. It has been seen that both porosity and grain size get decreased. These effects are furthermore more evident than in the Al-Si based materials (from 2.55 down to 0.71 and from 315-200 down to 125-200 respectively, see points 5.2.2.1 and 5.2.2.2). These effects should have a direct positive influence on the mechanical properties of the alloy. It is known that one of the negative features of Al-Cu alloys is their low castability mainly due to their large solidification interval. The consequence can be seen in the shape of a large density of microshrinkages and hot tear related defects (see figure 4.35). The TiB_2 particles reduce these defects. Porosity levels are lower and no microshrinkages were appreciated in the reinforced alloy.

Furthermore the TiB_2 particles play a role in the selection and amount of precipitations that are formed. This effect has been observed most clearly through the TEM (figure 4.49) and SEM analysis (figures 4.42, 4.43 and 4.47). The Al_2Cu phase precipitates on the surface of the TiB_2 particles. The mapping of the elements in the samples has demonstrated that Al_2Cu and also some Al-Cu-Fe precipitates appear associated with the TiB_2 particles. This effect is very important for the mechanical properties as it is known that the control of the size and distribution of this phase (Al_2Cu) has a direct effect on the mechanical properties as they impinge dislocations, avoiding their movement and increasing the strength of the material.

On the other hand the microstructural analysis of the thermally treated samples has revealed some indications of the effect of TiB_2 particles in the process. The conclusions obtained from the solidification study point out that the solidification interval and temperatures are lower when TiB_2 particles are present. Some TiB_2 particles act as nucleation sites and the rest are pushed by the growing grains and agglomerate in the grain boundaries. The microstructures of the thermally treated A356R and A204R are apparently similar to those of the unreinforced matrices and the only feature that is noticeable is the disappearance of the Al_2Cu phase in the thermally treated reinforced Al-Cu material. (See fig. 4.48). This can be related to an overaging of the alloy as the same ageing time to that of the unreinforced alloy has been selected even though the solidification curves of the reinforced material were shorter. Ageing times should be studied as it is possible that shorter cycles are needed to avoid the overaging of the alloy. Furthermore further studies could be also required to select the maximum temperature of the treatment in order to avoid possible defects related to the burning of the alloy. The temperature of 530 ± 5 ºC recommended for this alloy in the literature [43, 66] is very near the melting temperature of the alloy. In the case of the reinforced alloy the melting temperature is even lower and therefore one of the conclusions of this work is that the parameters of the thermal treatment should be adjusted to these features in the case of working with the reinforced alloy.

4.4 CONCLUSIONS

The solidification pattern of metallic materials is an important factor as it directly affects the microstructure and final features of the alloys. Solidification of both the unreinforced A204 and A356 alloys and the reinforced composites A204R and A356R has been studied through the use of a thermocouple inserted in the middle of a plaster cup in which the different alloys have been cast in conditions similar to the actual castings. Furthermore the analysis of the microstructure has also been carried out. The technologies of OM, SEM, TEM and AES with a mapping of the elements present in the different samples have led to some conclusions on the effect of the TiB_2 particles on the alloys structure and features.

The analysis of the T-t curves and the corresponding derivative curves dT/dt-t have confirmed the interaction of the TiB_2 particles in the solidification events. The main conclusions of the analysis of the solidification curves are following presented:

1) TiB_2 particles make solidification times (curves) shorter as they take part in the nucleation stage of aluminium grains and the precipitation of intermetallic

phases. Solidification events begin earlier and at higher T. This effect is related to the lower undercooling required due to the presence of the particles.

2) The influence of the particles is more clearly seen in the A204R material. The interaction of the TiB_2 particles is stronger with Al-Cu alloys than with Al-Si alloys. This effect is in agreement with the phenomena observed in the use of TiB_2 grain refiners in the aluminium industry where it has been observed that the presence of silicon hinders the action of the grain refiners based on the al-Ti-B system.

3) The influence of the particles should have a positive influence on the mechanical properties of the reinforced alloys since it affects microstructural aspects such as the grain size, reduction of hot tearing related defects and differences in the precipitation of intermetallic phases.

The analysis of the microstructure has led to another set of additional conclusions that certify the effect of the TiB_2 particles on the features of the aluminium alloys studied in the present work. It has been demonstrated that the presence of the TiB_2 particles (6 wt. %) has a direct effect on microstructure features of both A356 and A204 alloys. These effects should have a corresponding effect on the mechanical and thermal properties of the reinforced materials. Following the main conclusions related to microstructural features are presented:

4) The grain sizes of both A356 and A204 alloys get decreased due to the effect of the TiB_2 particles. This decrease is more evident in the Al-Cu alloy where values lower than 200 μm have been obtained. Silicon tends to interact with the grain refining effect of the TiB_2 particles. In the same way the presence of the particles leads to a decrease of defects like porosity and microshrinkages.

5) TiB_2 particles play a role in the selection and precipitation of the phases. This is particularly important with Si in the Al-Si alloy and Al_2Cu phases in the Al-Cu material.

6) Silicon segregates on the surface of TiB_2 particles. This phenomenon affects the shape of silicon platelets that become more globular, less acicular.

7) The presence of the TiB_2 particles leads to the precipitation of small copious Al_2Cu precipitates in the A204R alloy that are linked to the TiB_2.

8) The TiB_2 particles interfere in the T6 thermal treatments on the A356R and A204R alloys. The microstructures of thermally treated reinforced and unreinforced alloys present differences associated with the different precipitation and shape of silicon and other phases. T6 thermal treatments are devised to strengthen the alloys through the solid solutioning of the alloying elements into the aluminium matrix and the subsequent precipitation of fine particulates that hinder the movement of the dislocations. The presence of the TiB_2 particles changes the solidification and precipitation patterns and new thermal treatment parameters should be applied in order to take advantage of the solutioning and ageing effects.

9) The TEM analysis shows that the CTE mismatch between the TiB_2 and both matrices does not lead to a distinct increase in the dislocation densities in the vicinity of the particles. This may be due to the low content of particles and that the CTE mismatch is not as large as in other MMC materials (Al/SiC 20-30%) where this phenomenon has been recorded. The stresses created during solidification get accommodated through other mechanisms such as the rotation of the small grains.

CHAPTER 5: MECHANICAL PROPERTIES.

CHAPTER 5: MECHANICAL PROPERTIES.

5.1 INTRODUCTION. STRENGTHENING MECHANISMS

Introduction

Pure aluminium is a soft material with low mechanical properties and it cannot be used in structural applications unless it is alloyed with other chemical elements. Depending on the nature, amount and combination of these alloying elements, different aluminium alloy families or series are produced that present a wide range of interesting properties.

Alloying is one of the most common methods used to strengthen aluminium and other metals but there is quite a large additional range of other possibilities that are also employed with the same objective, (thermal treatments, dispersion of small sized particles, use of grain refiners, rapid solidification, addition of ceramic reinforcements and cold working). The strengthening approach of all these methods is common though. They are all based on reducing the mobility of dislocations and increasing the stress levels needed to move dislocations through an appreciable distance within the material.

Dislocations are lattice imperfections in the crystals and they have a direct influence in the response of the materials to external stresses and therefore in properties like YS, hardness, ductility, toughness and fatigue resistance. There are two main types of dislocations, edge and screw. The presence of these imperfections makes that the external stresses needed to produce atomic movements in a crystal be much lower than those that would be theoretically needed in the perfect crystal.

The different strengthening mechanisms are mainly based on the reduction of the mobility of dislocations. Usually the final strengthening is obtained through the sum of several different mechanisms. Depending on the composition of the alloy and processing parameters the influence of some mechanisms will be diminished or increased.

Following the most relevant mechanisms that may play an important role in the case of aluminium alloys and AMCs are shortly reviewed:

1) Load transfer between matrix and reinforcement: In the case of some MMCs load can be transferred from the matrix to a non plastically deforming reinforcement. It mainly takes place when the reinforcement has a high aspect-ratio and the mechanism involved in the load transference is considered to take place through shear stresses at the reinforcement-matrix interface**.** In MMCs, an aspect ratio of 10:1 is typically considered to be the lower limit for reinforcement constituent dimensions to make it sure that an effective load transfer takes place [34].

2) Orowan strengthening or Dispersion strengthening: When hard small particles are dispersed into the aluminium melt, usually through mechanical methods, the gliding of the dislocations is hindered, they must bow between these impenetrable particles and bypass them. The loops so created are called Orowan loops and the direct consequence of their creation is an increase in the YS of the material. It is considered that the Orowan strengthening mechanisms may play a role in the contribution of structural materials when particles are small and located nearby from each other. Otherwise dislocations cannot overcome them by looping and this mechanism has not any effect. It is considered that dispersion hardening takes place when the particle diameter range is between 0.01 and 0.7 μm. Otherwise the contribution is considered to be negligeable [66-69].

3) Precipitation strengthening or Age hardening: The mobility of the dislocations is hindered by a fine dispersion of precipitates that is created through a thermal treatment operation. The second phase particles are originally in solid solution and the fine precipitate structure is formed in the alloy following an ageing treatment. The size of these precipitates is usually lower than those in dispersion strengthening. Heat treatment parameters must be closely studied and followed in order to take advantage of this strengthening mechanism.

4) Grain and subgrain size decrease: There is a direct relation between the grain and subgrain size and the mechanical properties of the aluminium alloys, the lower the size the higher the YS. This is directly related to the effect of grain boundaries on the movement of the dislocations. Grain boundaries are a barrier to dislocation movement and therefore all the parameters that may decrease the size of the grains will increase the density of grain boundaries and indirectly dislocation movements [66].

There have been many experimental measurements of the variation of the YS with grain size and the Hall-Petch relationship that accounts for this relationship is much known and applied:

$$\sigma_y = \sigma_0 + kd^{-1/2}$$

σ_y is the YS, σ_0 is the intrinsic YS, d is the grain diameter and k is a constant for a given material.

5) CTE mismatch between the matrix and the reinforcements: This mechanism plays an important role in the case of MMCs and materials where elements having different CTEs may coexist together at microscopical level. When the materials are cooled during the processing or solution treatments CTE misfit strains result due to differential thermal contraction at the matrix-reinforcement interfaces. Subsequently a large number of dislocations is usually created to accommodate the CTE misfit. The increase in the density of dislocations leads to a barrier for their movement and therefore an increase in the YS [68, 70].

6) Solute hardening: Alloying elements, such as Mg, Cu or Ti can deter the movement of dislocations by pinning them down. Solute atoms in solid solution within the aluminium lattice increase the energy of the crystal locally. Likewise the energy of dislocations in the surrounding area gets also increased and therefore the work necessary to move them is higher.

Alloying elements must comply with two main requirements so that solute hardening may take place: To present a large solid solubility as well as an atomic misfit with the matrix.

7) Work hardening: The term work hardening refers to the plastic deformation of metals. This phenomenon increases the dislocation density through the rearrangement of the structure of the crystals and surrounding phases. Subsequently areas of entangled dislocations may form that hinder the movement of other dislocations.

5.2 EXPERIMENTAL RESULTS

5.2.1 Mechanical properties at Room T and 200ºC

The tensile tests were carried out following the standard ASTM A-370 with cylindrical threaded specimens. The dimensions of the specimens were Diameter = 6.25 ± 0.12 mm, L_0 = 25 ± 1, L_c > 32 mm, R = >5 and L =80 mm. and the elongation was measured with an extensometer in the tests at room temperature.

Table 5.1 shows the results obtained in the tensile tests of the A356R and A204R materials and their corresponding unreinforced alloys A356 and A204 respectively.

		Experimental data			
TENSILE PROPERTIES AT 20ºC		**A204**	**A204R**	**A356**	**A356R**
UTS (20ºC) (MPa)	As Cast	124	172	132	128
	T6	176	191	184	220
YS (20ºC) (MPa)	As Cast	78	93	82	78
	T6	126	91	130	216
Elongation % (20ºC)	As Cast	3,2	4,7	4,4	2,8
	T6	4	6,5	4	1,5
Young´s Modulus (20ºC) (GPa)	As Cast	75	82	71	76
	T6	79	75	72	79
TENSILE PROPERTIES AT 200ºC		**A204**	**A204R**	**A356**	**A356R**
UTS (200ºC) (MPa)	As Cast	123	149	100	104
	T6	159	166	172	202
YS (200ºC) (MPa)	As Cast	70	98	69	82
	T6	103	99	124	195

Table 5.1: Tensile properties of the unreinforced and reinforced alloys.

All the samples were cast in the same conditions and the average of the valid values of four tensile tests were obtained for each of the data presented. Half of the specimens were thermally treated.

The T6 treatment was followed with the four materials and it consisted in the following thermal cycles:

□ **A356 and A356R alloys**. Solution treatment at 540ºC during 8 hours, quenching in water and artificial ageing at 160ºC for 6 hours.

□ **A204 and A204R alloys**. Solution treatment at 530ºC during 6 hours followed by quenching in water and artificial ageing at 130ºC for 2 hours.

In addition and taking into account that TiB_2 particles take part in grain refining mechanisms, some additional castings were made with refined alloys. 0.2 vol. % Al-Ti5-B1 commercial refining agent was added to both the A204 and A356 alloys following industrial standards for refining purposes. The analysis of the obtained tensile properties should help discern the mechanisms involved in the strengthening of the reinforced alloys. The refined alloys will henceforth referred as A356A and A204A

Table 5.2 presents the obtained values:

	Experimental data		
TENSILE PROPERTIES AT 20ºC		**A204A**	**A356A**
UTS (20ºC) (MPa)	As Cast	148	130
	T6	213	194
YS (20ºC) (MPa)	As Cast	93	73
	T6	132	132
Elongation % (20ºC)	As Cast	5,2	5,6
	T6	7,6	4,2
Young´s Modulus (20ºC) (GPa)	As Cast	78,3	71,2
	T6	81,2	72,4

Table 5.2: Tensile properties of the alloys refined with the addition of 0.2 vol. % of al-Ti5-B1.

5.2.2 Measurement of physical properties

Physical properties of the materials have a direct influence in their eventual mechanical properties. Therefore the measurement of the grain size, density and porosity was carried out in order to draw data to complete the analysis of the mechanical properties obtained.

5.2.2.1 Grain size

The grain size of each of the materials (see table 5.3) was measured from samples obtained from tensile specimens in regions far from the fractured area. All the specimens were previously submitted to chemical etching in order to appreciate the grain size more distinctly and the measurements were made following the procedures established by the Centre Technique des Industries de la Fonderie (CTIF) in France [58].

The Al-Si based alloys were attacked with an iron chloride $FeCl_3$. The Al-Cu based alloys were attacked with the Keller reactive that is more suitable for this alloy. The images obtained with an optical microscope were compared to a series of standard macrographies (augmentation x10) to determine their grain size range (SG). The latter parameter can be directly converted into grain size ranges following the equivalences shown by the mentioned procedure [58]. (See table 5.3).

The obtained results are presented in the following table:

Grain size /Material	A204		A356		A204R		A356R		A204A		A356A	
As cast /T6	As cast	T6	As cast	T6	As cast	T6	As cast	T6	As cast	T6	As cast	T6
Grain size range [57]	SG 2 -3	SG 3-4	SG 7	SG 7	SG 1-2	S-G 3-4	SG 3-4	SG 4	SG 0-1	SG 3-4	SG 6	SG 6-7
ASTM grain size (μm)	200-315	315-500	2000	2000	125-200	315-500	315-500	500	<125	315-500	1250	1250-2000

Table 5.3 Grain sizes of the six different materials in both as cast and T6 conditions.

Plaster casting is a slow cooling process due to the poor heat conductive nature of the plaster moulds. Therefore the grain sizes that are usually obtained in this process are much larger than in gravity casting and other processes using metallic moulds. The measurements carried out (see OM figures 5.2-5.13) show that it is very difficult to obtain a refined condition of the Al-Si alloys. It is generally accepted that to consider that an alloy is refined it should present grain size values lower than <200 μm [8, 17] and these values are only obtained in the case of some of the Al-Cu based materials. In fact it can be seen that lower grain sizes are obtained with the Al-Cu based materials in all the conditions measured (refined alloys, addition of 6% of TiB_2 particles, as cast or thermally treated). The Al-Si based alloys present large grain sizes (315-2000 µm) even though the solidification intervals are shorter for these alloys (see chapter 4, section 4.2.).

On the other hand it can be seen that thermal treatments tend to increase the grain size of all the samples on the whole and the refining effect that is obtained with the addition of TiB_2 particles seems to get annulled by it.

The addition of TiB_2 reduces the grain size of Al-Cu based alloys in the as cast condition from 200-315 µm down to 125-200 µm in the A204R alloy and to less than 125 µm in the refined condition A204A. This effect is annulled by thermal treatments. In the case of the Al-Si alloys the refined conditions (less than 200 µm) are never obtained. The effect of TiB_2 is not so clear even though it can be seen that the reinforced material A356R presents a much lower grain size both in the as cast and in the thermally treated condition with grain size values of 315-500 and 500 µm respectively (in any case higher than those obtained in the case of the A204R alloy).

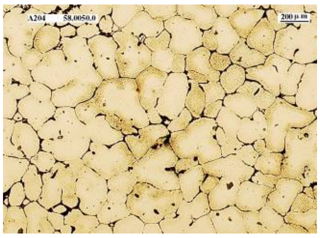

Fig.5.2:A204
Grain size 200-315 µm.

Fig.5.3: A204A
Grain size 0-125 µm.

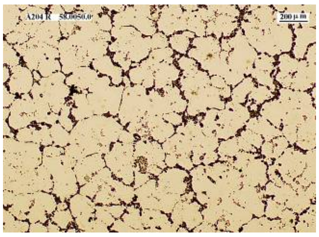

Fig.5.4: A204R
Grain size 125-200 µm.

Fig. 5.5: A204T6
Grain size 315-500 µm.

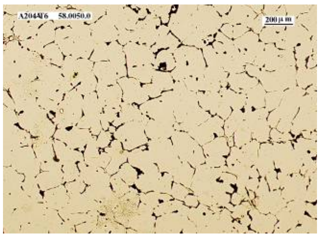

Fig.5.6: A204AT6
Grain size 315-500 µm.

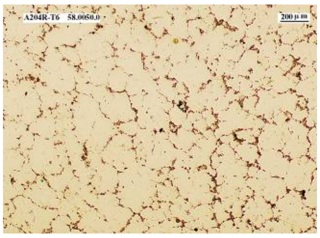

Fig.5.7: A204RT6
Grain size 315-500 µm.

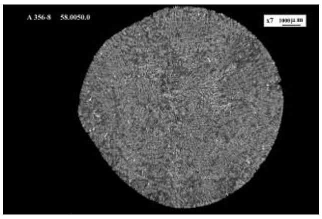

Fig. 5.8: A356
Grain size >2000 µm.

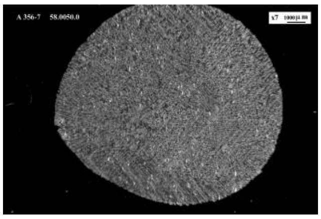

Fig.5.9:A356A
Grain size 1250 µm.

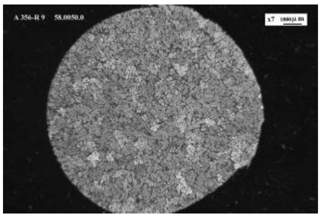

Fig.5.10: A356R
Grain size 315-500 µm.

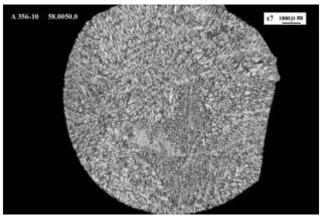

Fig. 5.11: A356T6
Grain size >2000 µm.

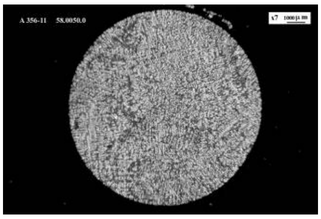

Fig. 5.12: A356AT6
Grain size 1250-2000 µm.

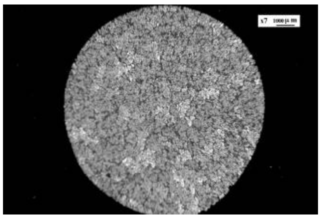

Fig.5.13: A356RT6
Grain size 500 µm.

5.2.2.2 Porosity level and density

The density of the samples was measured through two methods. In the first one, referred to as “geometrical method”, cubic samples were machined and their volume and weight was measured to provide the density values.

On the other hand and in order to confirm the results of the geometrical analysis, the method based on the determination of the density in air compared to its displacement in water or “Archimedes´ principle” was also applied. The same cubic samples are submerged in water and the resultant weight is compared to the weight in air. Another measurement is made after saturating the superficial pores of the samples in water so that the bulk density and porosity of the samples is also known.

The samples were subsequently submitted to the Densal® process, a Hot Isostatic Pressing (HIP) variant, in order to eliminate the internal porosity of the samples. The application of a high temperature, high pressure environment into an autoclave provides the means to remove the internal porosity through diffusion related and plastic yielding effects. In this way and after comparing the results obtained in the “hipped” and “non hipped” conditions the porosity level of the original, non hipped, castings could be measured.

Tables 5.4 and 5.5 present the results obtained by the two methods:

Measurements of the dry bulk density before Hipping. “Geometrical method”.

Reference	Weight (g)	Length (mm)	Width (mm)	Height (mm)	Volume (cm^3)	Density (g/cm^3)
A204-1	54.2	99.88	19.92	10.18	20.3	2.67
A204R -1	55.8	99.98	19.92	10.02	19.9	2.80
A356 -1	51.3	99.78	20.00	10.09	20.1	2.55
A356R-2	53.1	99.86	20.00	10.16	20.3	2.62

Table 5.4: Density of the non hipped samples.

The results of the densities obtained are comparable to data obtained in the literature 2.80 g/cm^3 for an Al-Cu5MgTi alloy [41] and 2.69 g/cm^3 for the Al-Si7Mg0.3 alloy [71] The small variations being accounted for small variations in the composition ranges used. The addition of TiB_2 particles with a density of around 4.5 g/cm^3 [21] increases slightly the density of both alloys, from 2.67 g/cm^3 to 2.80 g/cm^3 in the Al-Cu based alloy and from 2.55 g/cm^3 to 2.62 g/cm^3 in the Al-Si case.

Measurements of the dry bulk density after Hipping "Geometrical method" and calculation of porosity.

Reference	Weight (g)	Length (mm)	Width (mm)	Height (mm)	Volume (cm^3)	Density (g/cm^3)
A204HIP-1	54.2	98.94	19.86	10.06	19.8	2.74
A204RHIP -1	55.8	99.62	19.84	10.00	19.8	2.82
A356HIP -1	51.3	99.25	19.82	10.04	19.7	2.60
A356RHIP -2	53.1	99.64	19.88	10.04	19.9	2.67

Table 5.5: Density of the hipped samples.

The porosity of the originally cast samples has been calculated by considering that the porosity of the hipped samples is negligeable, i.e. ≈ 0%. In that case the porosity of the four casting alloys is as follows:

Reference	A204	A204R	A356	A356R
Porosity (%)	2.55	0.71	2.31	1.87

Table 5.6: Porosity of the cast materials.

It can be seen that the presence of the TiB_2 particles has a direct positive effect on the porosity levels of both alloys. The resulting reinforced materials present very low percentages of internal porosity, 0.71% in the case of the A204R and 1.87% in the A356R. It is also worth noting that even the unreinforced samples presented low porosity content. The results show that the feeding and filling system designed for the lost wax process had been well designed and the castings were correctly produced.

The influence of TiB_2 is much more marked in the case of the Al-Cu based material as the porosity decreases from 2.55 down to 0.71, i.e. 1.84%. In the case of the Al-Si based alloy the diminution is only of 0.44%.

<u>Measurements of the density of hipped and non hipped samples “water displacement or Archimidean density”</u>

	D (Dry mass) (gr.)	S (Suspended mass) (gr.)	M (Saturated mass) (gr.)	V= exterior volume = M-S	**B = bulk density = D/V**	**Porosity %**
A356	18.44	11.38	18.46	7.08	**2.60**	
						2.26
A356-HIP	6.62	4.15	6.64	2.49	**2.66**	
A356R	16.24	10.19	16.26	6.07	**268**	
						1.84
A356RHIP	8.91	5.65	8.91	3.26	**2.73**	
A204	16.66	10.56	16.68	6.12	**2.72**	
						2.16
A204-HIP	3.86	2.48	3.87	1.39	**2.78**	
A204R	16.96	11.01	16.96	5.95	**2.85**	
						0.35
A204RHIP	8.01	5.22	8.02	2.80	**2.86**	

Table 5.7: Density of the cast materials measured following the water displacement method.

The results obtained are in agreement with those previously obtained with the geometrical method and it is confirmed that TiB_2 has an important effect in the decrease of the porosity of the samples. This effect is clearly higher in the A204R alloy.

5.2.3 Fracture analysis

The fracture analysis of specimens drawn from samples in each of the conditions studied in the work was carried out with a SEM. The objective of studying the fracture surfaces of the tensile specimens was to look for possible differences in the fracture mode of the reinforced and unreinforced alloys.

There are two main fracture modes in aluminium alloys; brittle and ductile fractures. The former presents a rapid crack propagation and without appreciable gross plastic deformation. They show a bright and granular appearance and are of the flat-face type. Ductile fractures are characterized by tearing of material accompanied by appreciable plastic deformation. They usually present a grey and fibrous aspect and may be either flat-face or shear face fractures.

5.2.3.1 Fracture analysis of the A356 and A356R tensile specimens

The unreinforced alloy presents a typically brittle fracture both in the as cast and thermally treated conditions with the presence of cleavage facets associated with Si particles (See figures 5.14 and 5.15) and also influenced by the higher presence of microshrinakges. On the other hand the reinforced material presents dimpled fracture surfaces typical of ductile fractures together with brittle regions and the fracture can be considered to be hybrid (see figures 5.16 and 5.17).

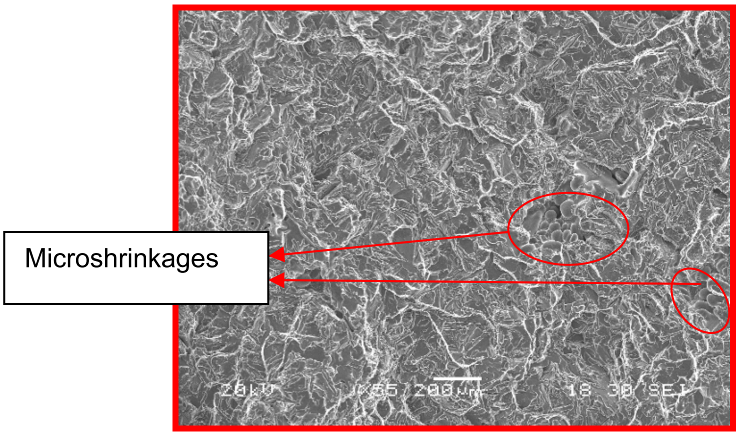

Fig. 5.14: A356 alloy, as cast.

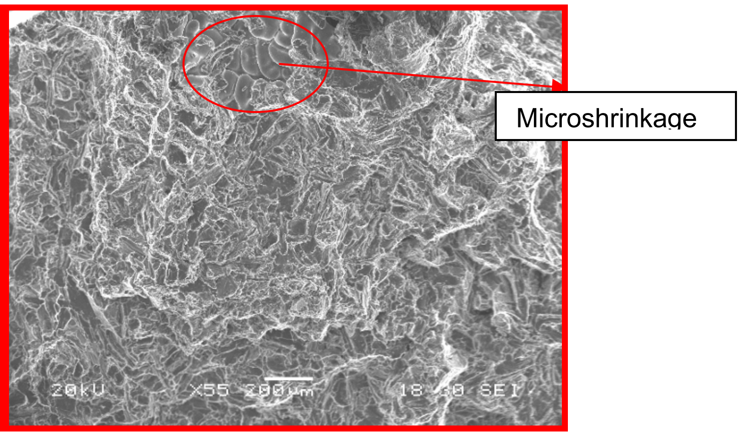

Fig.5.15: A356 alloy, thermally treated T6.

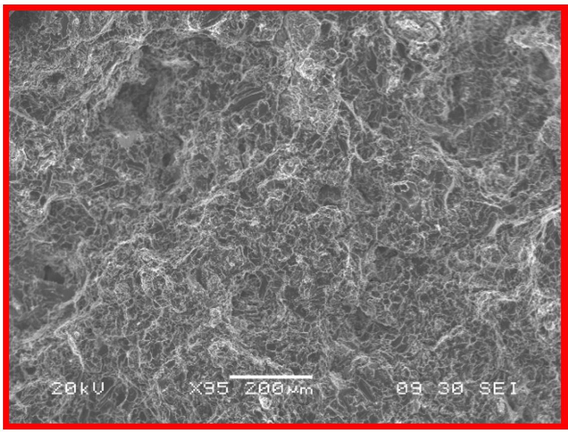

Fig.5.16: A356R as cast.

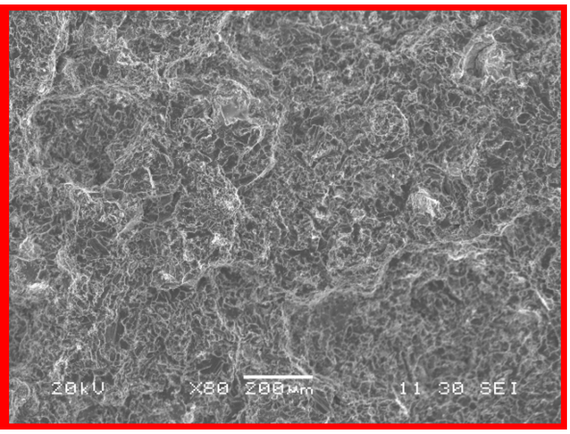

Fig.5.17: A356RT6 thermally treated.

The fracture surfaces of the A356R materials present both ductile and brittle features. The fracture is hybrid and the grain size gets decreased. The number of defects is also lower. The figures 5.18 and 5.19 show a detail of the brittle region of the A356R alloy in both as cast and T6 conditions. Small TiB_2 particles can be seen associated with Si.

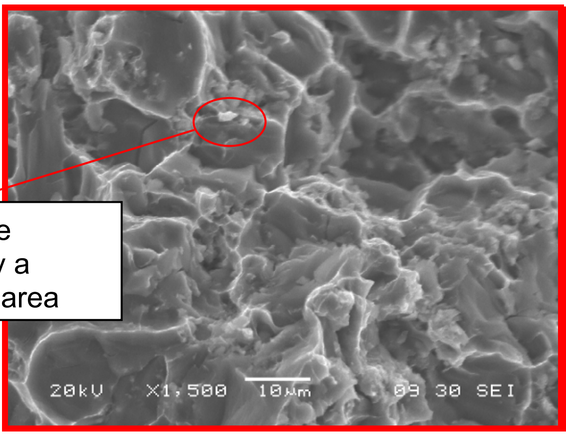

TiB_2 particle engulfed by a silicon-rich area

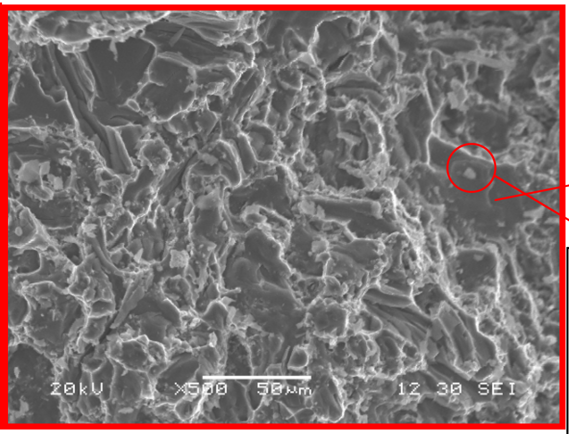

Si phase

TiB_2 particle associated to a silicon phase

Fig. 5.18: Brittle area of A356R material. Fig. 5.19: Brittle area within A356RT6.

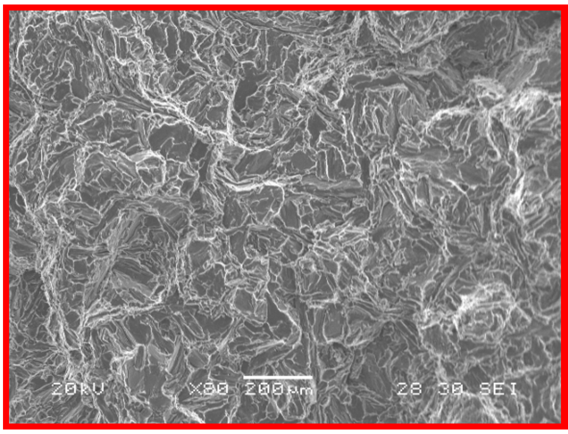

Fig.5.20: A356A refined with 0.2% of Al-5Ti-1B.

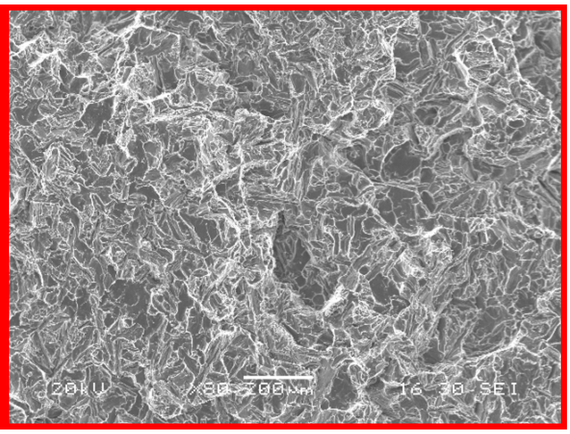

Fig. 5.21: A356AT6 thermally treated.

The addition of the grain refiner master alloy Al-5Ti-1B does not produce any significant change in the fracture mode of the alloy regarding the unreinforced material A356 and fracture is mainly brittle even though a lower presence of microshrinkages in the sample is appreciated.

5.2.3.2 Fracture analysis of the A204 and A204R tensile specimens

TiB_2 particles lead to the reduction of the grain size (more visible in the as cast condition) and the change of fracture mode. The reinforced materials present a ductile fracture clearly identifiable by the dimples associated with this type of fractures (see figures 5.26 and 5.27). The few brittle phases that are present are homogeneously distributed. The disgragation of copper in cleavage zones can be observed. On the other hand abundant cleavage facets can be clearly appreciated in the unreinforced samples in both the as cast and thermally treated conditions.

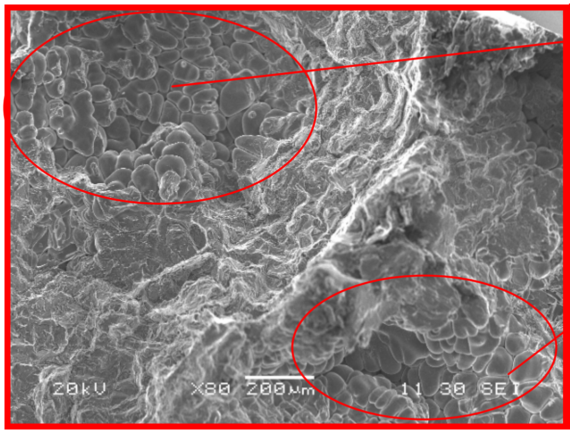

Fig. 5.22: A204 sample as cast, showing large microshrinkage areas.

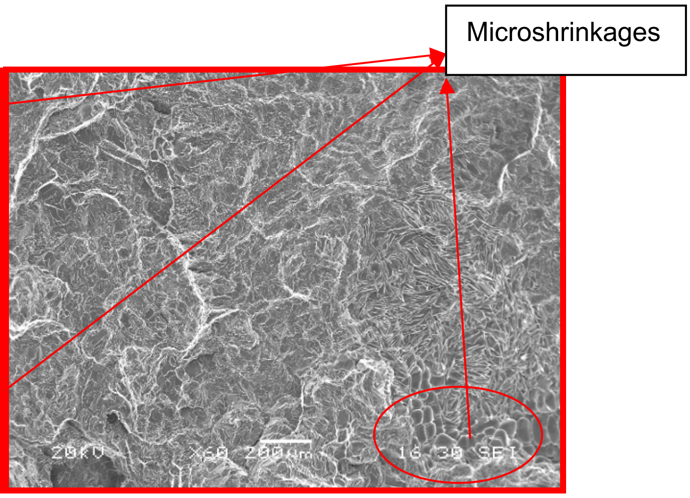

Fig. 5.23: A204T6 sample, thermally treated.

Both samples in figures 5.22 and 5.23 present a brittle fracture. Furthermore the presence of large microshrinkages can be clearly seen in the two conditions (signaled in red). It is known that the castability of this alloy is low and furthermore the plaster casting process is a very low cooling rate technology so microshrinkages and other solidification related defects are difficult to avoid.

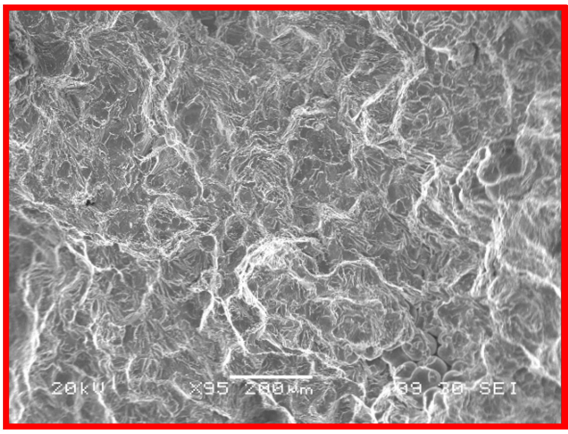

Fig. 5.24: A204A as cast and refined.

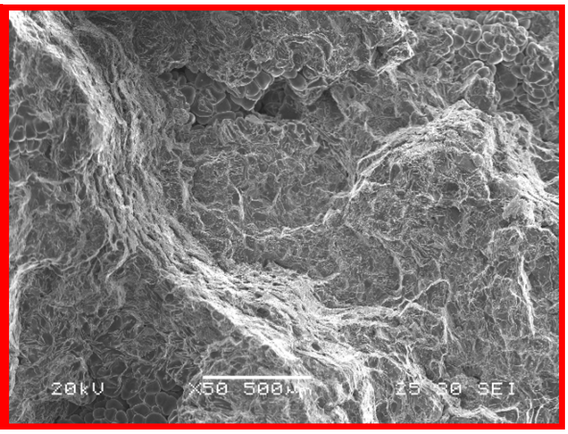

Fig. 5.25: A204AT6 thermally treated and refined.

The figures 5.24 and 5.25 show the fracture surface of the A204A samples to which 0.2 vol. % of the Al-5Ti-1B was added. It can be seen that the presence of microshrinkages is lower than in the non refined case but higher than in the reinforced materials. The grain size is also lower and the fractures are clearly brittle in both states, as cast and T6.

Dimples, ductile fracture surface area

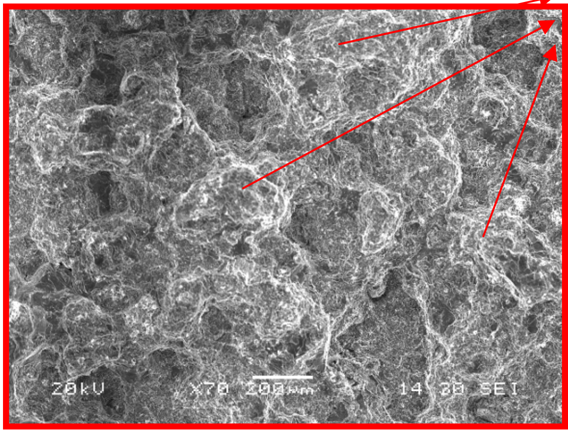

Fig. 5.26: A204R, as cast.

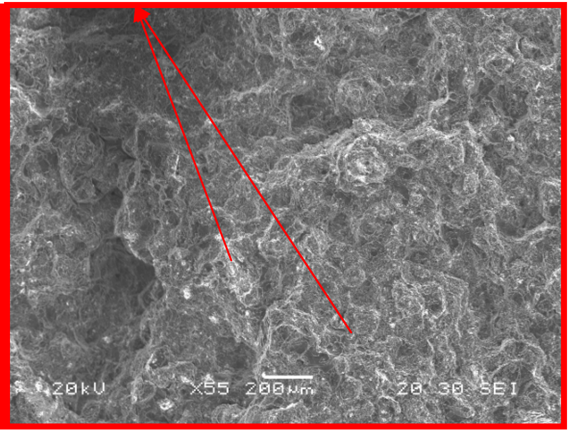

Fig. 5.27: A204RT6, thermally treated T6.

The fracture of the reinforced alloy is shown in fig. 5.26 and 5.27. The surface areas of both the thermally treated and as cast materials present a distinct ductile nature. There are some brittle phases in them but they are well distributed. These phases have been identified to be formed by Al-Ti-Cu combinations. The presence of pure Al_2Cu phases can also be seen in the figures 5.28 and 5.29 obtained from the previous samples A204R and A204RT6.

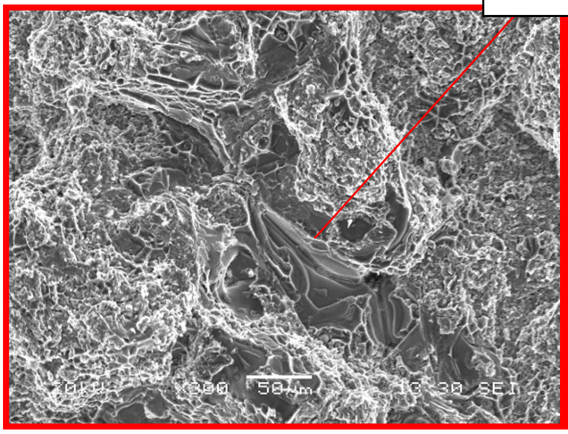

Fig. 5.28: Brittle phase in the A204R.

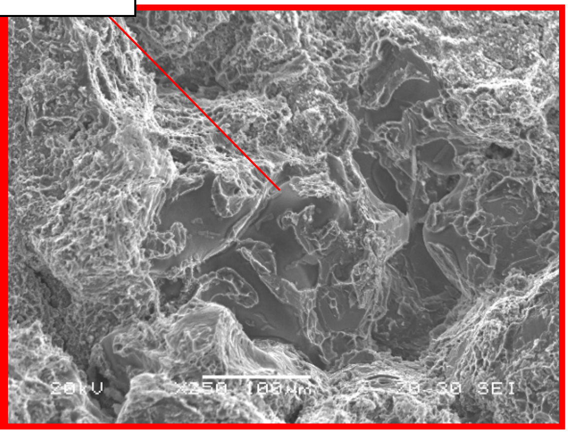

Fig. 5.29: Brittle region in the A204RT6.

5.2.4 Analysis of the experimental results

The tensile properties of the TiB_2 reinforced materials were measured at room temperature and high temperature (200ºC). Tests with the corresponding unreinforced alloys were also carried out for comparison purposes. Internal porosity and grain sizes were also measured in order to get a better understanding of the results obtained. Finally the analysis of the fracture of the different specimens of as cast and thermally treated materials was carried out to complete the study. It has been seen that the presence of TiB_2 in contents of around 6 wt. % has a direct influence in the results obtained in the tensile tests of both alloys even though this is more distinct in the case of the Al-Cu based alloy. The results confirm that there are clear interactions between the TiB_2 particles and different phases of the alloys, mainly silicon. This is in agreement with the conclusions drawn in the previous chapter (Chapter 4 on solidification and microstructure). Furthermore it has been observed that the behaviour of the reinforced alloys regarding the thermal treatment used for the samples is different from that of the unreinforced alloys.

The preliminary comparison between the behaviour of the two alloy systems shows both similarities and differences. TiB_2 particles provide a ductile nature to the fracture of both alloys but this effect is larger in the A204R samples. This is logical taking into account that there is not any cleavage of Si particles in the Al-Cu alloy and the effect of the reinforcement is not interefered by it. This fact has a beneficial effect on the UTS and YS (see table 5.1), the presence of the TiB_2 particles is beneficial for the mechanical properties at both temperatures even though this trend is not uniform. On the other hand the influence of TiB_2 particles on the ductility of the reinforced alloys is different in the two alloys. The ductility of the A204 alloy gets increased in the as cast and T6 conditions in 47% and 63% respectively and on the contrary the ductility of the A356 alloy decreases 36% and 63% respectively.

The fracture type shown by the two reinforced materials is more ductile than the corresponding alloys. Both unreinforced materials show brittle fracture surfaces and the A356R reinforced material present a hybrid fracture and the A204R based one is clearly ductile.

In the case of the reinforced alloys, the brittle phases are more homogeneously distributed, there are almost no microshrinkages or porosity related defects and furthermore the TiB_2 particles are small and the interface with the matrix is clean. Moreover there is not any TiB_2 particle fracture identified probably due to the small size of the particles. The fracture initiation is therefore mainly due to microvoid coalescence and growth as can be deduced from the much dimpled surface of the reinforced materials, the microvoids are created in the grain boundaries where the TiB_2 particles cluster together to reduce the interfacial energy. These areas are sites where strain discontinuities may be created and cluster cracking may take place. When the strain gets increased the microvoids grow, coalesce and form the dimpled fracture surface.

5.2.4.1 Al-Si based materials (A356 and A356R)

The presence of TiB_2 particles in the A356R alloy affects the mechanical properties of the alloy but these effects are not always positive. At room T, the ductility of the as cast reinforced samples gets decreased in 8-9% in both as cast and thermally treated states. This behaviour is common to other particulate reinforced MMCs as the hard particulates tend to act as local strain concentrators and crack initiation begin in the interface with the matrix by mechanisms related to void formation and agglomeration. Nevertheless the microstructural analysis has revealed that the presence of TiB_2 particles provides some positive aspects. One of the main aspects which control the mechanical properties of hypoeutectic Al-Si alloys is the size and shape of the Si eutectic. In this case it has been observed that there is an interaction between the TiB_2 particulates and silicon and the latter presents a more rounded aspect when the former are present. The UTS and YS values present a significative improvement when thermally treated (>20% and >60% improvement respectively) and only ductility remains lower. This improvement takes place in both the A356 and A356R materials but it is more important in the latter. It can be concluded that the presence of TiB_2 particles improves the answer of the alloy to the thermal treatment. The aim of the T6 thermal treatment is to bring the magnesium atoms in solid solution with aluminium and to allow the subsequent precipitation of small Mg_2Si precipitates that reinforce the material through the dispersion strengthening mechanism. Furthermore the thermal treatment makes the silicon phase more rounded. Not any direct interaction has been appreciated between the Mg_2Si phase and the TiB_2 particles and the main reason that explains the better answer to the thermal treatment in the A356R alloy is that the silicon phase gets more rouned in the presence of TiB_2 particles and the lower porosity that it presents in comparison to the A356 alloy.

The positive features of the reinforced materials are more clearly seen at high temperatures as foreseen. Aluminium alloys that are strengthened by precipitation hardening mechanisms tend to lose mechanical properties at high temperatures due to the possibility of coarsening of these precipitates when subjected to high temperatures through diffusion mechanisms. The presence of the thermodinamicaly stable particles can counteract this effect as they are stable at those temperatures and this can explain the good results obtained. 48% increase in the UTS values and 57% increase in the YS.

Unfortunately the obtained data cannot be directly compared to similarly reinforced materials because the only references existing in literature refer to samples produced by other production processes like High pressure Diecasting or gravity casting. Nevertheless the trend is similar to that observed by other researchers working with sand casting. Sprenger et al. [29] point out that an Al-Si7Mg0.3 alloy reinforced with 8% of TiB_2 produced an increase of 15% of Young´s modulus, 20% of the UTS and 30% in the YS but a great reduction in the elongation to fracture.

The analysis of the data and fracture micrographs leads to the conclusion that the improvements obtained by the addition of the TiB_2 in the A356 alloy are mainly related to the reduction of defects and decrease of the grain size. The latter phenomenon is not so important though as the reinforced materials cannot be considered to be in a grain refined condition. Their grain size is around 500 μm and even though this value is much smaller than the unreinforced material (more than 2000 μm) its contribution to the improvement of mechanical properties should not be high. It is known that Si plays a negative role in the effect of Al-Ti-B type refiners. The results obtained in this work show that silicon segregates on the TiB_2 facets hindering its grain refining effect of the latter.

The porosity of the samples gets decreased in the reinforced materials as foreseen. A decrease of around 20% has been measured for the A356R alloy. Furthermore a change in the fracture mode can be clearly appreciated when the TiB_2 particles are present. The unreinforced materials present a brittle fracture but this become hybrid (brittle-ductile) in the case of the reinforced materials. It must be taken into account that in the present study the A356 alloy was neither modified nor refined in order to better identify the effect of the TiB_2 particles. The A356A references, to which Al-Ti5-1B grain refiners have been added, also present a brittle nature in the fracture mainly due to the presence of the silicon phases associated with cleavage phenomena. The presence of TiB_2 has a modifying effect on the Si particles as they get more rounded and therefore less prone to brittle fracture. The A356 alloy presents an excellent castability and the level of porosity and microshrinkages that can be appreciated in the fracture surfaces are very small but even so the addition of 6 wt. % TiB_2 particles further reduces these defects.

5.2.4.2 Al-Cu based materials (A204 and A204R)

The analysis of the results obtained with the Al-Cu based materials shows that there are differences between these alloys and the Al-Si based ones. The observed effect of the TiB_2 particles is usually larger in the A204R alloy due to the absence of poisoning events and the copious precipitation of Al_2Cu phases. On the one hand it is clearly shown that the elongation values obtained in the tensile tests get increased (40% in the as cast condition and 60% in the thermally treated specimens) in opposition to Al-Si based materials. This is attributed to the refining action and the reduction in defects provided by the TiB_2 particles that are not inhibited by the presence of Si atoms in the case of the A204R alloy. The analysis of the fracture shows that the material becomes ductile when 6% of TB_2 particles are present. The A204R reinforced material present a refined state in the as cast condition (i.e. <200 μm). Values of 150-500 μm are obtained in the thermally treated condition. Thermal treatment decreases the refining effect of the reinforcements in some degree. On the other hand the effect of the TiB_2 particles on the porosity of the samples is also larger than that shown by the Al-Si alloys. The porosity decreases from 2.55% down to 0.71%. The microshrinkages are also much less abundant in the case of the reinforced materials. The positive effect of the particles on decreasing the defects in the castings is clearly seen in these alloys known to be very difficult to cast mainly due to the large solidification intervals they present and the resulting hot tearing tendency.

The analysis of the fractures is also a clear indication of the large effect of the TiB_2 particles on the behaviour of the material. The unreinforced alloy A204 shows more microshrinkages due to its large solidification interval and hot tearing tendency. The addition of Al-Ti5-B1 in 0.2 vol. % in the A204A alloy added for grain refining purposes improves the situation but even so the level of microshrinkages is higher than in the reinforced alloys. The fracture is brittle in the unreinforced alloys and become very ductile when 6 wt. % of TiB_2 is present. The fractures present some typical Al-Cu-Fe brittle phases of these Al-Cu5MgTi alloys but they are scarcer and homogeneously distributed within the ductile aluminium matrix.

Nevertheless the improvement of properties that should entail all the previous data are only appreciated in the as cast condition but not so clearly seen in the thermally treated condition. The as cast material presents a clear improvement of both YS and UTS and Young´s Modulus at both room temperature and 200ºC. (Improvements in the range of 20-35% for the YS and UTS and around 8% for the modulus at room temperature) but even though the U.T.S values get improved (5-10%) in the thermally treated condition a decrease can be appreciated in the Young´s Modulus at room temperature (-5%) and YS (-30% at room temperature and -45% at 200ºC). The analysis of the data (grain size, internal defects, fracture, etc.) does not provide a clear clue to explain this effect and it has been worked out that the thermal treatment itself must be the main reason to explain this fact. It is known that the thermal treatment applied to the Al-Cu5MgTi alloy to get the homogeneous precipitation of small Al_2Cu precipitates is a very delicate operation. Temperatures of 530ºC are needed to get that phase in solution that are very near to the start of the melting of the alloy and burning can easily take place if the operation is not perfectly controlled. Burning is the local remelting of the castings and it can substantially affect the mechanical properties negatively. Nevertheless no traces of burning have been appreciated in the A204RT6 samples. Furthermore the ageing step is also delicate as these alloys present a tendency to get overaged when too high temperatures or too long times are used. Some additional castings and thermal treatments were carried out to check these points but the results were again similar. Not any evidence of burning of the material was appreciated but it is possible that the samples are overaged when treated with these conditions. In the solidification and microstructural study of these alloys it was clearly seen that the presence of the TiB_2 particles leads to an enhanced nucleation and growth of the precipitates on their surface. Furthermore there was a shortening of the solidification curves, the precipitation of the different phases took place earlier than in the A204 material and therefore the possibility of overaging the alloy is clear. The reinforced material presents a larger amount of large Al_2Cu precipitates that are less effective in terms of precipitation strengthening. Nevertheless it was decided not to optimize the thermal treatment of the reinforced material as it would then be difficult to compare the results with the unreinforced materials that were submitted to the traditional T6 treatment. This aspect should be further studied if the reinforced materials are to be industrially used.

5.2.5 Analysis of the strengthening mechanisms involved. Modelling of the mechanical properties

One of the most appealing features of MMCs is the possibility of tailoring the mechanical and thermal properties to the requirements of specific applications. Variations in the volume fraction, shape, size, orientation or nature of the reinforcements directly affect their properties and therefore the analysis and modelling of the different factors involved has attracted the attention of a large number of researchers in the last 50 years. In this section the actual contribution of the main potential strengthening mechanisms described in the section 5.1.1 will be analysed for the two alloy systems studied in the present work.

There are two main approaches to model the mechanical behaviour of particle reinforced MMCs. The continuum approach is based on assuming that the material can be described by global parameters and the rule of mixtures and other approaches based on it have been extensively used. It has been applied with success for the Young´smodulus and CTE calculation but the micro-mechanics approach is preferred to calculate the YS. This approach takes into account the deformation mechanisms at an atomic level and its validity for simple systems has been confirmed in many works [1, 66, 69, 72-76].

Modelling of the Young´sModulus

Modelling based on the Eshelby´s Tensor

Another model that has shown its validity for the calculation of the elastic properties of MMCs reinforced with particulates is based on the Eshelby´s tensor application [69]. This model formulates the problem by assuming that the reinforcements are inhomogeneities to which the Eshelby Tensor can be applied to reduce the problem to that of an equivalent homogeneous inclusion. Eshelby´s tensor provides the relation of the effect of the inelastic strain in the equivalent homogeneous inclusion to that of the constrained strain and it depends on the shape of the inclusion.

The Department of Materials Science and Metallurgy of the University of Cambridge through its “Materials Algorithms Project” [78] has produced and made them available several programs for the modeling and analysis of properties of MMCs based on this approach and developed by Clyne et al. [69]. Introducing inputs of the MMC constituents this program provides values on several features of the MMCs taking into account the size, elastic properties, volume fraction and aspect ratio of the main constituents. Following, the results provided by this program with regards to the Young´s modulus for the two A204R and A356R systems are presented together with the input data used to run the program:

Input data:

Young´s Modulus A204 GPa	74.6 (Measured in this work) as cast
Young´s Modulus A356 (GPa)	70.6 (Measured in this work) as cast
Poisson ratio A204	0.33 Estimated
Poisson ratio A356	0.33 Estimated
Young´s Modulus TiB_2 (GPa)	544 [24](R81)
Poisson ratio TiB_2	0.17 [24]
TiB_2 aspect ratio	3
Maximum TiB_2 volume fraction A204R %	0.038
Maximum TiB_2 volume fraction A356R %	0.037

Table 5.8: Data used to run the program to calculate Young´s moduli.

And the results provided by the program have been as follows:

Axial Young´s Modulus of A204R = **82.37 GPa**

Axial Young´s Modulus of A356R = **78.15 GPa**

These values are actually very near the experimental values 881.5 GPa and 76.1 GPa for the A204R and A356R alloys respectively) with deviations lower than 2.6%. Therefore this confirms the validity of the Eshelby´s Tensor approach for the calculation of the elastic modulus of these particulate reinforced composites.

It may be also worthwhile signalling that the same program provides additional output for the two materials without any further inputs needed. Transverse Young´sModulus, axial-transverse shear modulus, transverse-transverse shear modulus, axial-transverse Poisson ratio, transverse-axial Poisson ratio, transverse-transverse Poisson ratio as well as the Eshelby S-tensor values.

Property/material	A204R	A356R
Transverse Young´s Modulus (GPa)	78.84	74.67
Axial-transverse shear modulus (GPa)	29.85	28,27
Transverse-transverse shear modulus (GPa)	29.53	27.96
Axial-transverse Poisson ratio	0.33	0.33
Transverse-axial Poisson ratio	0.31	0.31
Transverse-transverse Poisson ratio	0.33	0.34

Table 5.9: Additional results provided by the program.

Modelling of the Yield Proof Stress 0.2%

The yield of the materials takes place when the applied stress is able to produce a bulk movement of dislocations. There exist different mechanisms that counteract the effect of the stress by hindering the movement of dislocations. In the case of the reinforced materials A356R and A204R the final yield stress is the result of the strength of the alloy together with the solute and precipitation hardening obtained during the thermal treatment and the strengthening provided by the reinforcing particles.

In order to simplify the calculations it will be assumed that all the factors are additive even though it is known that there may be some interrelations among them and the addition is not totally linear [76]. Furthermore the presence of the particles influences the precipitation mechanisms and there are interactions with alloying elements and phases and a decrease in the % of porosity.

If all the strengthening mechanisms considered in section 5.1.1 were taken into account the YS of the two reinforced materials could be expressed as follows:

$$\sigma_{A356R} = \sigma_{A356} + \sigma_{LOAD\ TRANSFER} + \sigma_{OROWAN} + \sigma_{GRAIN} + \sigma_{CTE} + \sigma_{WORK\ HARD}$$

$$\sigma_{A204R} = \sigma_{A204} + \sigma_{LOAD\ TRANSFER} + \sigma_{OROWAN} + \sigma_{GRAIN} + \sigma_{CTE} + \sigma_{WORK\ HARD}$$

The terms σ_{A356} and σ_{A204} refer to the YS of the unreinforced materials and have been directly measured. The calculatios have been carried out with data from as cast samples to eliminate possible interactions in the thermally treated materials. The strengthening provided by solutes impinging the dislocations are considered to be all incorporated into them.

Regarding the contribution provided by the presence of the reinforcements it can be assumed that all the load transfer, dispersion or Orowan hardening and work hardening contributions are negligeable due to the shape size and volume fraction of the TiB_2 particles. Load transfer phenomena are negligeable in particle reinforced composites and are only usually considered with high aspect ratio reinforcements (>10). Dispersion hardening is directly related to the particle size and interparticle spacing and these are both too large in the A204R and A356R materials (it is generally accepted that dispersion hardening takes place with particles of less than 1 micron) and work hardening contribution is important when the materials are plastically deformed at temperatures well below their melting temperature. This effect is difficult to calculate but it has been shown that in other composites with much larger volume fractions of up to 25% it does not really show a large contribution [66, 72-76] and as it is directly related to the volume fraction of reinforcements it will be neglected in the present study. Therefore it is possible to deduce that the grain size reduction effect and the generation of dislocations in the solidification process due to the CTE mismatch between the matrices and the particles are actually the two strengthening mechanisms that may be playing a significant role in the strengthening of the two alloys A204R and A356R.

The YS of the reinforced materials could thus be expressed as follows:

$$\sigma_{A356R} = \sigma_{A356} + \sigma_{GRAIN} + \sigma_{CTE}$$
$$\sigma_{A204R} = \sigma_{A204} + \sigma_{GRAIN} + \sigma_{CTE}$$

The contribution to the yield stress due to the grain refining effect is provided by the Hall Petch equation:

$$\sigma_{GRAIN} = K_y D^{-1/2}$$

K_y is typically 0.1 $MNm^{-3/2}$ for alloys with a low degree of refining [72] as the A204R and A356R. If we consider an average grain size of 150µm A204R and 400µm for the A356R material (see section 5.2.2.1), the contribution of this factor to the YS of the A204R and A356R materials would be of 7.3 and 5 MPa respectively.

The contribution to the YS due to the generation of dislocations created during solidification due to the CTE mismatch between the matrices and the reinforcements has been calculated as follows [68] :

$\sigma_{CTE} = \alpha G b\, \rho^{1/2}$ where α is a constant, that is 1.25 for aluminium, G is the shear modulus and b is the Burgers vector (0.25-0.29 nm for Aluminium).

ρ is the dislocation density that can be calculated as:

$$\rho = \frac{12 \times 2^{1/2} \times \Delta\alpha \times \Delta T \times f}{b \times d \times (1-f)}$$

Δα is the difference in the CTEs, ΔT is the temperature interval, f is the volume fraction for particles, b is the Burgers vector and d is the grain size.

For the A204R alloy we will consider b to be 0.27nm, Δα is $1.6\ 10^{-5}\ ^{\circ}C^{-1}$ and d = 150 µm, ΔT = 615ºC and f =0.037 (experimental values), the dislocation density ρ would therefore be **1.6×10^{7} cm^{-2}.**

The σ_{CTE} value for the A204R system obtained through the $\sigma_{CTE} = \alpha G b\ \rho^{1/2}$ expression (where G is 28.27 GPa (see table 5.9), α is 1.25, b has been taken as 0.27nm and ρ has been calculated to be 1.6×10^{7} cm^{-2}), would be only **3.8 KPa**. Due to the low volume fraction content of the TiB_2 particles which is directly related to the low density of dislocations created the effect of the CTE mismatch on the mechanical properties is therefore negligeable.

For the A356R alloy we will consider b to be 0.27nm, Δα is $1.5\ 10^{-5}\ ^{\circ}C^{-1}$ and d= 400 microns, ΔT =580ºC and f = 0.038 the dislocation density ρ would therefore be **0.54×10^{7} cm^{-2}.**

The σ_{CTE} value for the A356R system obtained through the $\sigma_{CTE} = \alpha G b\ \rho^{1/2}$ expression (where G is 29.85 GPa (see table 5.9), α is 1.25, b has been taken as 0.27nm and ρ has been calculated to be 0.54×10^{7} cm^{-2}), would be only **2.3 KPa**. Due to the low volume fraction content of the TiB_2 particles this effect is also negligeable.

Therefore substituting these values in the $\sigma_{Reinforced} = \sigma_{Unreinforced} + \sigma_{GRAIN} + \sigma_{CTE}$ equation we obtain the following theoretical values for both systems:

$\sigma_{A356R} = 82 + 5 = 87$ MPa $\qquad$ $\sigma_{A204R} = 78 + 7.3 = 85.3$ MPa

The experimental variation between the YS of the reinforced and unreinforced alloys in the as cast condition is of + 15.3 MPa in the A204R system and - 4 MPa in the A356R system. The theoretical approach detailed above provides an explanation for the increase of the YS of the A204R based material. Furthermore, a larger influence of the TiB_2 particles on the A204 based alloy should be foreseen as the grain refining effect is the main strengthening effect that has been considered and is larger with the A204R alloy. Nevertheless the experimental decrease of the YS value in the A356R material cannot be explained theoretically. It must be concluded that it is related to defects produced during the processing or in the raw material and in fact it is true that the amount of residual contamination coming from the salts used in the preparation of the alloy is larger in the A356R alloy. The K content is 0.17% in the A356R alloy and only 0.11% in the A204R alloy.

5.3 CONCLUSIONS

The mechanical properties of two Al-Si and Al-Cu aluminium alloys reinforced with 6 wt. % of TiB_2 particles with a distribution of sizes comprising from 0.5 to 5 μm have been measured and compared with the corresponding unreinforced alloys. The influence of the refining agent Al-5Ti-1B has been also analysed and porosity levels and grain sizes of all the obtained materials have been measured to help make it clear which are the main strengthening mechanisms involved.

The main conclusions of the analysis of the mechanical properties of these materials are as follows:

1) The presence of 6 wt. % of TiB_2 particles in the Al-Si and Al-Cu alloys has a positive effect on the properties of the materials even though the ductility decreases in the case of the A356 based material and the as cast A356R alloy does not present any improvement at room temperatures.

2) The porosity and microshrinkages are clearly lower due to the presence of TiB_2 particles. This effect is more distinct in the Al-Cu based alloy. This is linked to the poisoning effect of the silicon that segregates on the TiB_2 facets and hinder the grain refining effect of the latter on the A356R alloy.

3) The TiB_2 particles increase the ductility of the Al-Cu based alloy. The Al-Si material behaves otherwise and the material becomes less ductile. The TiB_2 particulates have both positive (reduction of defects, reduction of grain size, decrease on the precipitation of brittle phases, modification of silicon precipitates) and negative effects (presence of hard particles tha can get fractured and act as stress concentrators and lead to the creation of voids in the interfaces and contamination of the salts used to produce the reinforcements) on ductility. The balance of the positive and negative effects is favourable in the A204R case but it is otherwise in the ductility of the A356R alloy. The main aspect that explains this situation is the different chemical composition of the two alloys and the strong interaction of the Si present in the A356R alloy with the TiB_2 particles.

4) The presence of the TiB_2 particles makes the fracture of the materials more ductile. This is also more evident in the A204R alloy and it is linked to the change in the precipitaion mechanisms. TiB_2 particles act as nucleation sites for the precipitation of silicon and Al_2Cu phases and decrease the amount of solute available for the precipitation of more brittle precipitates. This effect is larger in the A204R alloy where furthermore there is not any cleavage phenomena related to silicon particles.

5) The main strengthening mechanisms involved are related to the grain refining effect of the TiB_2 particles and decrease of porosity and microshrinkages. The increase in the dislocation density due to the CTE mismatches between the aluminium alloys and the TiB_2 particles has not been appreciated. The stresses produced during solidification are relieved through other mechanisms such as the rotation of the small precipitates forming around TiB_2 particles.

6) The high percentage of silicon in the Al-Si alloy hinders the grain refining power of the reinforcing phases. Silicon segregates on the surface of the TiB_2 particles and hinders the precipitation of aluminium grains.

7) The grain refining capability of both Al-5Ti-1B grain refiner and the TiB_2 particles incorporated as reinforcements gets impaired by the very low cooling rates of the plaster casting process and refined states (<200 μm) are only obtained with the as cast A204R alloy.

The improvement of mechanical properties takes place in both room temperature and high temperatures. This may have industrial applications at temperatures where dispersion strengthened alloys lose their properties due to the coarsening of the precipitates.

CHAPTER 6: THERMAL PROPERTIES.

CHAPTER 6: THERMAL PROPERTIES.

6.1 INTRODUCTION. THERMAL PROPERTIES OF MMCS

Introduction

The chapter 6 is focused on the influence of the TiB_2 particles on the CTE and Thermal Conductivity of the A204R and A356R reinforced materials. It is known that the thermal properties of MMCs are directly related to geometrical parameters of the reinforcements such as the shape, size, spatial distribution and volume fraction. Moreover thermal properties can be tailored to specific requirements. This fact together with the high specific mechanical properties provided by these materials explain that sectors like the electronic industry have invested much efforts in the development and research of MMC materials.

MMCs usually present a lower CTE than their corresponding unreinforced alloys. Their thermal conductivity is high even though it is usually lower than that of the unreinfoced alloys. There is a large body of literature supporting these observations [30, 69, 79-85].

The thermal conductivity of metals is high due mainly to the free electrons that are present in their structures. The heat flow can be transmitted through them much more easily than in ceramic materials where the main mechanism within the material is through phonons (lattice vibrations). Nevertheless the conductivity of metals is directly affected by the presence of defects or solute atoms that cause electron scattering and subsequently diminish the conductivity capacity of the bulk material.

On the other hand, the addition of ceramic particles usually produces a decrease in the thermal expansion. Ceramic materials usually present a much lower CTE than most of the metals and this property is additive in a large extent. This CTE mismatch paves the way to the generation of localized stresses during the solidification stage or thermal treatments if applied. When the material is subsequently heated part of the energy is spent in the relaxation of these internal stresses generated due to the large difference in the CTEs and therefore the eventual expansion of the material is lower than the corresponding unreinforced metal. In this way aluminium based MMCs with very high ceramic particle contents (up to 70-80%) have been produced for electronical applications where a low CTE was required.

The thermal properties of the reinforced A204R and A356R materials have been measured and compared to those of the corresponding unreinforced materials (see section 6.2). In section 6.3 existing models to calculate the CTE and thermal conductivities of particulate reinforced MMCs are discussed and applied to the materials studied in the present work. The mechanisms involved in the change of thermal properties have been analysed to check whether these materials could be interesting for thermal management applications in the future.

6.2 EXPERIMENTAL RESULTS

Specimens of the four materials A204, A204R, A356 and A356R were obtained from samples cast through the plaster casting process in the same conditions used for the production of tensile test specimens and samples for the microstructural analysis. As cast samples (without any thermal treatment) were machined and sent to be hipped before the thermal measurements. It is known that porosity affects in a large extent the thermal conductivity and therefore all the samples were submitted to a hipping process in order to eliminate the internal porosity.

6.2.1 CTE

Samples of 10 x 10 x 10 mm^3 were prepared and the CTE was measured in the range of temperatures from 25ºC up to 300ºC. The following table shows the average values obtained with the four materials.

Materials	**CTE (10^{-6} C^{-1}) 25°C→300°C**
A204	25,3
A204R	23,9 (-5.5%)
A356	22,9
A356R	22,4 (-2.1%)

Table 6.1: Experimental values of the CTEs of the four materials.

The table shows that the addition of the TiB_2 particles produces a decrease in the CTE of both alloys even though this decrease is not large. The reduction is more pronounced, 5.5%, in the case of the A204R based material and lower, only 2.1%, in the case of the A356R based alloy.

6.2.2 Thermal conductivity

The thermal conductivity was measured using the flash method equipment. This method is based on the measurement of the diffusivity of the samples. The surface of a small disc of the material is subjected to a very quick irradiation of a laser beam during some miliseconds. The resulting temperature rise of the rear part of the sample is measured and thermal diffusivity values are obtained taking into account the time that is needed for the rear surface to reach 50% of its maximum temperature [86].

Subsequently thermal conductivity values are directly obtained through the following expression that links both properties:

$$k = \alpha \, \delta \, C_p$$

k is the thermal conductivity, α is the thermal diffusivity, δ is the density of the material and C_p is the specific heat.

The table 6.2 shows the thermal diffusivity (*α)* values obtained with the four materials and the thermal conductivity values (*k*) obtained through the application of the expression above.

Material (hipped)	α (cm^2/s)	δ (g/cm^3)	Cp (J/K.mol)	*k* (W/gK)
A204	0.55	2.74	0.87	131.11
A204R	0.64	2.82	0.85	153.41 (+17%)
A356	0.75	2.60	0.88	171.60
A356R	0.79	2.67	0.87	183.51 (+7%)

Table 6.2: Experimental values of diffusivity and calculation of the thermal conductivity.

The table shows that the TiB_2 particles have the effect of increasing the thermal conductivity of the alloys and this effect is larger in the case of the A204 alloy (17% and 7% for the A204R and A356R alloys respectively).

6.2.3 Analysis of the experimental results

The presence of the TiB_2 particles has a direct effect on the thermal properties of the two reinforced materials studied. The behaviour of these materials follows the same trend of most of the MMCs with regards to the CTE value that gets decreased but exhibits a different behaviour with regards to the thermal conductivity. In this case and contrary to data found in the literature for other aluminium based composites the thermal conductivity gets increased in 7% and 17% for the A356R and A204R materials respectively.

Even though TiB_2 is one of the few ceramic materials having a thermal conductive nature with values of the λ around 100 $W.m^{-1} K^{-1}$, these lay far from the aluminium alloy values, 152 and 140 *W/mºK* for the AlSi7Mg0.3 and Al-Cu5MgTi alloys respectively. [11, 21, 78] and a decrease of the thermal conductivity values of the reinforced materials was expected but the results of the measurements showed the opposite behaviour.

The presence of the TiB_2 particles leads to a 5.54% reduction of the CTE in the case of the Al-Cu based material and of 2.09% in the case of the Al-Si based alloy. CTE is an additive property and this decrease was foreseen. The behaviour of both alloys is therefore similar even though it seems that the effect is more appreciable in the Al-Cu based alloy. The microstructural analysis of the reinforced samples shows that even though in both materials a large amount of the TiB_2 particles tend to agglomerate together and lay at the grain boundaries clustering themselves with different intermetallic phases, TiB_2 particles present further interactions with the A204 matrix. They appear in the interior of the grains and the size of the grains is low in the A204R alloy (<200 µm). The silicon prevents the obtention of so low grain sizes to their interaction with TiB_2 particles in the A356R alloy. The lower grain sizes obtained through the addition of TiB_2 particles in the case of the A204R alloy provide an explanation to the larger decrease in the CTE. Furthermore the CTE difference of the particles and the matrix is larger for the A204R alloy (the CTEs of the A204 and A356 alloys are 25,3 and 22,9 $10^{-6} C^{-1}$ and the TiB_2 presents a CTE of 7.4-8.1 $10^{-6} C^{-1}$) [4, 21] and therefore it is logical that the CTE decrease in the A204R be larger as this property is largely additive.

On the opposite, the thermal conductivity values present an increase of 17% and 7% for the A204R and A356R alloys respectively. In principle these results may seem surprising as the conductivity of the TiB_2 particles is lower than that of the aluminium alloys and even though the amount of particles in the final materials A204R and A356R is small the results do not follow the pattern of other particulate reinforced materials where the addition of ceramic particles such as SiC or Al_2O_3 lead to a decrease in the thermal conductivity values [80, 82]. Tthis increase in the thermal conductivity is an interesting feature for a potential industrial application of the studied reinforced alloys for thermal management applications where light and structural materials are needed that present a large heat dissipation capacity and low CTEs.

The TiB_2 particles help to reduce the presence of defects within the alloys and change the precipitation pattern of the phases during solidification. All the samples were hipped to eliminate the porosity decrease factor but it is possible that some residual porosity remains and this be lower in the reinforced alloys. On the other hand, the amount of solutes that are in solid solution I the reinforced alloys is lower and there exist a 6 wt. % of particles that have some conductive nature. It has been shown in previous chapters that TiB_2 interact in the precipitation of both Si and Al_2Cu phases and that the composition of the reinforced alloys is different from the one of the unreinforced alloys , not only due to the presence of the TiB_2 particles but also because different phases precipitate. In the case of the reinforced alloys the α-aluminium grains become smaller and depleted of alloying elements like Fe, Cu and Si that precipitate due to the presence of the TiB_2 particles that have the role of nucleating agents. The direct effect is that there is less solute in solid solution within the aluminium. It is known that the purer the aluminium grains the higher the thermal conductivity. The reinforced alloys are formed by purer aluminium grains surrounded by conductive TiB_2 particulates and intermetallic phases and that can explain the increase in the final thermal conductivity values.

On the othe hand it is known that porosity has a large effect on the thermal conductivity and therefore the A204R and A356R samples whose thermal conductivities were to be measured were submitted to a hipping process in order to eliminate this factor. TiB_2 particles have an indirect effect in the thermal conductivity as they tend to decrease the amount of porosity and microshrinkages of the alloys. From an industrial point of view this aspect may be interesting as it is not always possible or economically suitable to hip all the components.

6.3 MODELLING OF THERMAL PROPERTIES

6.3.1 Introduction

The possibility of modelling the thermal properties of MMCs has always been a subject that has attracted the attention of researchers due to the practical consequences of these calculations. Thermal stability is a critical issue for many applications where the components must work at different temperature ranges. Heat dissipation is also a feature that may be essential for several applications where the accumulated heat must be eliminated if the component is to continue working at its maximum capability. Furthermore, MMCs present a good combination of high strength and thermal conductivities that may not be obtained through alloying that usually result in a excessive decrease of the thermal conductivity of metals. Moreover MMCs are tailorable materials, i.e. their composition may be selected according to the desired properties in a rather extensive range.

Many different models have been created to foresee the thermal expansion and conductivity of MMCs. The rule of mixtures is the simplest one but it does neither take into account of many essential features of the reinforcements (shape, size, spatial distribution) nor the thermally induced residual stresses within the material and the results can only be used as a rough preliminary approximation.

The models proposed by Turner, Kerner and Schapery to calculate the CTE have been extensively used in the case of MMCs due to the ease of calculations to be made and good accuracy provided by them [69, 84-85, 87]. The latter is very suitable for the long fibers reinforced composites but its validity is limited for particulate reinforced MMCs and furthermore it only provides upper and lower bounds of the CTE. Turner´s model is based on the assumption that only uniform hydrostatic stresses exist in the phases and furthermore it does not consider the influence of the shape of the reinforcements so Kerner´s model usually provides better results for particulate reinforced materials. It accounts for both the shear and isostatic stresses that are developed in the material. It provides very accurate results for spherical inhomogeneities randomly orientated. There are further models available but they are either based on the latter or are designed for specific temperature ranges or volume fractions. An additional model used by different researcher groups is based on Eshelby´s Tensor. It can account for the effect of different fiber shapes and volume fractions and it is based on understanding the stresses which arise within the composite material with temperature changes [60, 84]. Due to the CTE difference between the matrix and the reinforcements misfit strains are produced during solidification which, if elastically accommodated, give rise to a set of internal stresses. According to Clyne and Withers [69], these stresses will have associated strains and their net effect on the length of the composite in any given direction can be calculated or estimated. In their model, this net length change arising from the internal stresses is simply added to the natural thermal expansion of the matrix to give the overall length change and hence the composite expansivity [69].

In this study both Kerner´s model and that based on Eshelby´s tensor have been used to model the CTE of the A204R and A356R materials and the resultant values have been compared to those obtained experimentally.

On the other hand, thermal conductivity of heterogeneous metals has also been modelled by many different approaches. The main difficulties arise from the fact that, in order to reach a complete solution, a deep knowledge of the shape, size, spatial distribution, understanding of interfacial effects, conductivity of each particle and interaction between particles would be required and some of these parameters are difficult to model. Simplifying approaches have been therefore used by different researchers. Maxwell made one of the first trials in 1873 by applying Laplace´s equation to calculate the thermal conductivity of a composite with spherical inhomogeneities. Further theories have appeared later that are variants of this basic approach. In this study both Maxwell´s modelling (suitable for spherical inhomogeneities) and the model based on the Eshelby´s Tensor as developed by Clyne and Withers will be applied [69]. The latter approach is based on the same concepts explained for the calculation of the expansion of particulate reinforced materials.

6.3.2 Modelling of the CTE

Kerner´s model

This model assumes that the reinforcements are spherical and wetted by a uniform layer of the matrix. The model proposes that the CTE of the composite is that of a volume element composed of a spherical reinforcement particle surrounded by a shell of a matrix. It is also assumed that the reinforcements are randomly oriented. Taking into account the volume fraction of each constituent the expression of the CTE of the composite results as follows [79]:

$$\alpha_c = \alpha_m V_m + \alpha_p V_p - (\alpha_m - \alpha_p)\,\frac{1/k_m - 1/k_p}{V_m/k_p + V_m/k_m + 3G_m/4}$$

Where α is the CTE, k represents the bulk modulus ($K = E/3(3-E/G)$), V is the volume fraction and G is the shear modulus. The m, p and c subindexes represent the matrix, particulate and composite respectively.

the theoretical values obtained for the two materials are as follows:

$$\alpha_{A204R} = \alpha_{Al\text{-}Cu} V_{Al\text{-}Cu} + \alpha_{TiB2} V_{TiB2} - (\alpha_{Al\text{-}Cu} - \alpha_{TiB2})\,\frac{1/k_{Al\text{-}Cu} - 1/k_{TiB2}}{V_{Al\text{-}Cu}/k_{TiB2} + V_{Al\text{-}Cu}/k_{Al\text{-}Cu} + 3G_{Al\text{-}Cu}/4}$$

$= 24{,}60 \times 10^{-6} = \alpha_{A204R}$

$$\alpha_{A356R} = \alpha_{Al\text{-}Si} V_{Al\text{-}Si} + \alpha_{TiB2} V_{TiB2} - (\alpha_{Al\text{-}Si} - \alpha_{TiB2})\,\frac{1/k_{Al\text{-}Si} - 1/k_{TiB2}}{V_{Al\text{-}Si}/k_{TiB2} + V_{Al\text{-}Si}/k_{Al\text{-}Si} + 3G_{Al\text{-}Si}/4}$$

$= 22{,}35 \times 10^{-6} = \alpha_{A356R}$

The values obtained with Kerner´s model are very close to the experimental values and therefore the validity of this model for the calculation of the CTE of spherical and low aspect ratio particulates has been confirmed. Deviations of only +3.1% and -0,40% for the Al-Cu based and Al-Si based materials have been obtained.

The following values have been used for the calculation of the CTEs corresponding to the A204R and A356R materials:

Properties	Data
A204 Young´s Modulus (GPa)	74.6 as cast
A356 Young´s Modulus (GPa)	70.6 as cast
A204 Shear Modulus (GPa)	28.74 (estimated)
A356 Shear Modulus (GPa)	27.2 (estimated)
A204 Bullk Modulus (GPa)	61.49 (estimated)
A356 Bulk Modulus (GPa)	58.19 (estimated)
TiB_2 Young´s Modulus (GPa)	544 [24]
TiB_2 Bulk Modulus (GPa)	240 ± 57 [11,7]
A204 thermal expansion (microstrain/K)	25.26
A356 thermal expansion (microstrain /K)	22.91
TiB_2 thermal expansion (microstrain/K)	8.1 [24]
A204 volume fraction	0.962
A356 volume fraction	0.963
TiB_2 volume fraction in A204R	0.038
TiB_2 volume fraction in A356R	0.037

Table 6.3: Input data used for the calculation of the CTEs following Kerner´s model.

Model based on Eshelby´s tensor

This model formulates the problem by assuming that the reinforcements are inhomogeneities to which the Eshelby´s Tensor can be applied to reduce the problem to that of an equivalent homogeneous inclusion. Eshelby´s tensor provides the relation of the effect of the inelastic strain in the equivalent homogeneous inclusion to that of the constrained strain and it depends on the shape of the inclusion.

Following the approach taken by Clyne and Withers [69] the following expression can be obtained for the coefficient of thermal expansion of a metal matrix composite:

$$\alpha_c = \alpha_m - V_p \{C_m - C_p\}[S - V_p (S-1)] - C_m\}^{-1} C_p(\alpha_p - \alpha_m)$$

Where α is the CTE, V_p is the reinforcement volume fraction, S is the Eshelby´s Tensor and C_m and Cp are the matrix and particulates elastic tensor components.

The calculation of the CTE can be carried out through the use of a software developed by Clyne T.W. et al. in the University of Cambridge and based on the approach explained in the above paragraphs [87].

The program requires some input on the matrix and reinforcements of the composite material and calculates the expansivity of the particulate reinforced composites. The input data that is needed to run the program are detailed in the following table:

Properties	Data
A204 Young´s Modulus (GPa)	74.6 as cast
A356 Young´s Modulus (GPa)	70.6 as cast
A204 Poisson ratio	0.33 estimated
A356 Poisson ratio	0.33 estimated
TiB_2 Young´s modulus (GPa)	544 [24]
TiB_2 Poisson ratio	0.17 [24]
A204 thermal expansion (microstrain/K)	25.26
A356 thermal expansion (microstrain /K)	22.91
TiB_2 thermal expansion (microstrain/K)	8.1 [24]
TiB_2 aspect ratio	3
Reinforcement volume fraction A204R	0.038
Reinforcement volume fraction A356R	0.037
Number of reinforcement volume fraction	6

Table 6.4: Input data used to run the program [87] for the calculation of the CTEs.

Following the results obtained through this software are shown:

Material	A204R	A356R
CTE 10^{-6} ºC	23.45	21.36

Table 6.5: Output data, CTE values of the reinforced alloys obtained with the program.

The results provided by this method are in accordance with the experimental values. The CTEs of the composite materials are lower than their unreinforced counterparts as foreseen and the divergence between the experimental CTEs of the reinforced values and those calculated with Eshelby´s Tensor approach are only 5.46% and 4.79%. The non homogeneous distribution of the particles within the reinforced materials and clustering effects, may be accounted for this divergence but nevertheless Eshelby´s method may be a good tool to predict the CTE and tailor the composite composition to the specific requirements of the components.

Model/material	Experimental CTE value	Kerner CTE and deviation%	Eshelby CTE and deviation %
A204R	23.86 x$10^{-6\ /^{\circ}C}$	24.60 x$10^{-6\ /^{\circ}C}$ (+3.1%)	23.45 x$10^{-6\ /^{\circ}C}$ (-1.72%)
A356R	22.44 x$10^{-6\ /^{\circ}C}$	22.35 x$10^{-6\ /^{\circ}C}$ (-0.40%)	21.36 x$10^{-6\ /^{\circ}C}$ (-4.81%)
A204	25.26 x$10^{-6\ /^{\circ}C}$		
A356	22.91 x$10^{-6\ /^{\circ}C}$		

Table 6.6: CTE values obtained experimentally and through modeling.

The CTEs of the reinforced materials have been measured experimentally and it has been seen that they present a slight decrease (<10%) when compared to unreinforced alloys. Both models are in agreement with the experimentally measured decrease in the CTE and not many differences can be appreciated between them. The method based on Eshelby´s tensor provides a decrease that is slightly higher than the reality and the method based on Kerner´s is dependent on the alloy but both are near the actual values and can be used as a first approximation.

6.3.3 Modelling of Thermal Conductivity

Maxwell´s model

Maxwell calculated the thermal conductivity of a composite with a spherical inhomogeneous phase solving the Laplace´s equation in 1873 [69, 85]. In this equation the spheres are supposed to be sufficiently separated as to avoid any interaction among them. The final formulation of this model is as follows:

$$k_c = k_m \left(\frac{k_p + 2\,k_m + 2\,V_p\,(k_p - k_m)}{k_p + 2\,k_m - V_p\,(k_p - k_m)} \right)$$

Where k_m, k_p and k_c are the thermal conductivities of the matrix, particulates and composite respectively and V_p is the volume fraction of particulates.

The following values have been used for the calculation of the parameters corresponding to the A204R and A356R materials:

$k_{Al\text{-}Si}$ = 171.60 W/m.K [88]
$k_{Al\text{-}Cu}$ = 131.11 W/mK [88]
k_{TiB2} = 96 W/mK [21]
V_{TiB2} = 0.038 and 0.037 for the A204R and A·%&R alloys respectively.

The theoretical values eventually obtained with the Maxwell´s model approach for the two reinforced materials are as follows:

$$k_{A204R} = k_{Al\text{-}Cu} \left(\frac{k_{TiB2} + 2\,k_{Al\text{-}Cu} + 2\,V_{TiB2}\,(k_{TiB2} - k_{Al\text{-}Cu})}{k_{TiB2} + 2\,k_{Al\text{-}Cu} - V_{TiB2}\,(k_{TiB2} - k_{Al\text{-}Cu})} \right) = \boxed{\mathbf{129.69\ W/m.K}}$$

$$k_{A356R} = k_{Al\text{-}Si} \left(\frac{k_{TiB2} + 2\,k_{Al\text{-}Si} + 2\,V_{TiB2}\,(k_{TiB2} - k_{Al\text{-}Si})}{k_{TiB2} + 2\,k_{Al\text{-}Si} - V_{TiB2}\,(k_{TiB2} - k_{Al\text{-}Si})} \right) = \boxed{\mathbf{168.25\ W/m.K}}$$

According to the Maxwell´s model the decrease in the thermal conductivity of the reinforced materials with regards to their unreinforced counterparts should be very low mainly due to the low percentage of particles present in the material. This point is interesting from a potential use in industry as the reinforcement is able to produce an improvement in mechanical properties and ductility together with a reduction of the CTE and keeping high values of thermal conductivity.

Model based on Eshelby´s tensor

The model based on the Eshelby´s Tensor has been applied to the modeling of the conductivity following the same approach used for the calculation of the CTE.

Following the approach taken by Clyne and Withers [69] the following expression can be obtained for the thermal condctivity of a MMC:

$$\boxed{\mathbf{k_c = [k_m^{-1} + v_p\{(k_m - k_p)[S - v_p(S-1)] - k_m\}^{-1}\,(k_p - k_m)k_m^{-1}]^{-1}}}$$

Where k is the thermal conductivity, V_p is the reinforcement volume fraction and S is the Eshelby´s Tensor.

The calculation of the thermal conductivity can be carried out through the use of the suitable software developed by Clyne T.W. et al. in the University of Cambridge and based on the approach explained in section 6.3.1 [89].

The program requires some input on the matrix and reinforcements of the composite material and calculates the thermal conductivity of the particulate reinforced composites. The input data that is needed to run the program are the thermal conductivity of the unreinforced matrices, the thermal conductivity of the reinforcements in both axial and transverse directions, reinforcement aspect ratio, the maximum reinforcement volume fraction and the number of reinforcement volume fractions that are wished to be considered.

The input data provided for each of the two materials is following detailed:

Properties	Data
Thermal conductivity of the A204 alloy	131.11 $W.m^{-1} K^{-1}$
Thermal conductivity of the A356 alloy	171.60 $W.m^{-1} K^{-1}$
Thermal conductivity of the TiB_2 particulates	96 $W.m^{-1} K^{-1}$ [7,24]
Reinforcement aspect ratio	3
Maximum reinforcement volume fraction in the A204R material	3.8%
Maximum reinforcement volume fraction in the A356R material	3.7%

Table 6.7 Data used for the calculation of the thermal conductivity according to the model based on the Eshelby´s tensor.

Following the results obtained through this software are shown:

Material	A356R	A204R
Thermal conductivity W/mK	169.15	129.47

Table 6.8 Results obtained after the application of the software based on Eshelby´s model.

The results obtained with the Eshelby´s Tensor approach show that the presence of the TiB_2 particles in the low amounts used in this work has almost no effect on the thermal conductivity of both alloys and the decrease in the final values is only of 1.43 % and 1.25% for the Al-Si and Al-Cu based alloys respectively.

Table 6.9 shows the data obtained with the two models and compares them with the experimental data.

Model/material	Experimental Thermal conductivity (W/gK)	Maxwell model for Thermal Conductivity and deviation%	Eshelby´s tensor model for Thermal Conductivity and deviation %
A204R	153.41	129.69 (-15.5%)	129.17 (-15.8%
A356R	183.51	168.25 (-8.3%)	169.15 (-7.8%)
A204	131.11		
A356	171.60		

Table 6.9: CTE values obtained experimentally and through modeling.

The results obtained through the two different models show that they cannot account for the influence of the TiB_2 particles on the thermal conductivity. The amount of reinforcement being so low, it was to foreseen that the thermal conductivity would change only slightly and it was to be expected that in fact the conductivity were lower than the corresponding alloys following the behaviour of other particulate reinforced MMCs (when reinforced with SiC, Al_2O_3, B_4C) [82]. Usually unreinforced metals have higher conductivity because electrons have a much larger mean free path for phonons. The presence of solute atoms, particles or defects may cause electron scattering and subsequently a reduction of the thermal conductivity values but this phenomenon does not take place in the two reinforced materials studied and the thermal conductivity gets increased 7% and 17% for A356R and A204R respectively. The different models available do not take into account several factors that affect the thermal conductivity of the materials studied in this work such as the role of the TiB_2 particles in the amount, shape and nature of the precipitates that are formed during the solidification of the alloys and the change of the solute concentration in the alloy. Therefore the obtained results with the models are not valid for the calculation of these reinforced materials.

6.4 CONCLUSIONS

The following conclusions have been drawn from the measurement and analysis of the CTE and thermal conductivity of the reinforced materials A204R and A356R:

1) The presence of the TiB_2 particles has a direct influence on the thermal properties of the materials and particularly on the thermal conductivity. A content of 6 wt. % of particles produces an increase of 7% and 17% in the conductivity for the A356R and A204R alloys respectively.

2) The thermal conductivity of both the A204R and A356R alloys is larger than that of the unreinforced counterparts. This fact is in opposition with values obtained with other commercial composites reinforced with SiC or Al_2O_3. This phenomenon is explained by the fact that TiB_2 particulates decrease the amount of solutes available that can take part in the solid solution state within aluminium crystals. The presence of the TiB_2 particulates promotes the precipitation of Silicon and Al_2Cu and Al-Cu-Fe phases in the A356R and A204R phases respectively. Furthermore TiB_2 are thermally conductive ceramics, i.e. they present a larger conductivity than most of the ceramic materials.

3) The influence of the TiB_2 particles is more clearly seen in the Al-Cu based alloys. On the one hand the CTE difference between the particles and the matrix is higher (25.3 $x10^{-6}$ C^{-1} and 8.1 $x10^{-6}$ C^{-1} respectively) than in the A356 alloy (22.9 $x10^{-6}$ C^{-1} and 8.1 $x10^{-6}$ C^{-1}). On the other hand the ceramic particles play an important role in the precipitation of the Al_2Cu and Al-Cu-Fe phase resulting in a material with a different composition from that of the unreinforced alloy. Less Cu is present within the aluminium grains and more Al_2Cu is present together with the TiB_2 particles.

4) The application of modelling tools for the calculation of the thermal properties of the materials studied along this work has proved to be a suitable approach for CTE calculation. Fairly good approximations have been obtained with the Eshelby´s Tensor approach that takes into account the shape of the reinforcements. The studied models do not fit to the actual thermal conductivity as they do not take into account the indirect influence of the TiB_2 particles on the solidification pattern and precipitation of phases.

CHAPTER 7: CONCLUSIONS.

7.1 CONCLUSIONS

7.1.1 Introduction

The present work has been focused on studying the influence of TiB_2 particles on the solidification pattern, microstructure features, tensile and thermal properties of two casting alloys, Al-Si7Mg0.3 and Al-Cu5MgTi. Samples of reinforced materials have been cast through the plaster casting process in the same process conditions used for the corresponding unreinforced alloys used as a reference. It has been demonstrated that the TiB_2 particles have a direct influence on several important features of the alloys such as the microstructure and selection of the precipitating phases during solidification, mechanical properties, decrease of the amount of defects and change of thermal properties. TiB_2 particles can be used to taylor the properties of casting alloys and be valuable for the aluminium casting industry when specific thermal and mechanical properties are required.

Following the main conclusions on the effect of TiB_2 particles are summarized:

7.1.2 Influence of TiB_2 particles on microstructure

1) TiB_2 particles make solidification times (curves) shorter as they take part in the nucleation stage of aluminium grains and the precipitation of intermetallic phases. Solidification events begin earlier and at higher T. This phenomenon is related to the lower undercooling required to begin the precipitation events due to the presence of the particles.

2) The grain sizes of both A356 and A204 alloys get decreased due to the effect of the TiB_2 particles. This decrease is more evident in the A204 alloy where values lower than 200 μm have been obtained. Silicon tends to interfere with the grain refining effect of the TiB_2 particles. In the same way the presence of the particles leads to a decrease of defects like porosity and microshrinkages.

3) TiB_2 particles play a role in the selection and precipitation of the different phases. Moreover, they interact with Si in the A356R alloy and Al_2Cu precipitates in the A204R material.

4) Silicon segregates on the surface of TiB_2 particles. This phenomenon affects the shape of silicon platelets that become more globular, less acicular. Furthermore the grain size refining effect of the TiB_2 particles is hindered as α-aluminium cannot grow directly on the TiB_2 particles.

5) The presence of the TiB_2 particles leads to the precipitation of small copious Al_2Cu precipitates linked to hem in the A204R alloy. This effect has a direct influence on the mechanical and thermal properties of the reinforced material.

6) The TiB_2 particles interfere in the T6 thermal treatments of the A356 and A204 alloys. T6 thermal treatments are devised to strengthen the alloys through the solid solution of the alloying elements into the aluminium matrix and subsequent precipitation of fine particulates that hinder the movement of the dislocations. The presence of the TiB_2 particles changes the solidification and precipitation patterns and new thermal treatment parameters should be applied in order to take advantage of the solutioning and ageing effects.

7) The TEM analysis show that the CTE mismatch between the TiB_2 and both matrices A204 and A356 does not lead to a distinct increase in the dislocations density in the vicinity of the particles. The low content of particles (6 wt. %) and the fact that the CTE difference is not as large as in other aluminium composite systems (lAl/SiC or Al/Al_2O_3) partially explain this behaviour. Furthermore TiB_2 particles play the role of rgain refiners. The stresses created during solidification get accommodated through other mechanisms such as the rotation of the small grains that are created around the particulates.

7.1.3 Influence of TiB_2 particles on the mechanical properties

8) The presence of 6 wt. % of TiB_2 particles in the A356R and A204R alloys has a positive effect on the properties of the materials even though the ductility decreases in the case of the A356 based material and the as cast A356R alloy does not present any improvement at room temperatures. TiB_2 particles influence the selection of the precipitates and subsequently the mechanical properties.

9) The porosity and microshrinkages are clearly lower due to the presence of TiB_2 particles. This effect is more distinct in the A204 based alloy where no poisoning phenomena have been observed. In the A356R alloy there exists a poisoning effect of the silicon that segregates on the TiB_2 facets and hinder the grain refining effect of the latter on the A356R alloy.

10) The TiB_2 particles increase the ductility of the A204 alloy. The A356 material behaves otherwise and the material becomes less ductile. The TiB_2 particulates have both positive (reduction of defects, reduction of grain size, precipitation of ductile phases and decrease on the precipitation of brittle phases, modification of the shape of silicon precipitates) and negative effects (presence of hard particles, contamination of the salts used to produce the reinforcements, creation of agglomerations at the grai boundaries, interaction with silicon) on ductility. The balance of the positive and negative effects is favourable in the A204R case but it is otherwise in the A356R state. There are several aspects that explain this situation such as the segregation of the Si present in the A356R alloy on the TiB_2 particles. They hinder the grain refining power of the latter and lead to higher porosity levels and a higher amount of brittle phases.

11) The presence of the TiB_2 particles makes the fracture of the materials more ductile. This is also more evident in the A204R alloy. TiB_2 particles act as nucleation sites for the precipitation of silicon and Al_2Cu phases and decrease the amount of solute available for the precipitation of more brittle precipitates. The amount of microshrinkages decreases and furthermore silicon particles become more round shaped.

12) The main strengthening mechanisms involved are related to the grain refining effect of the TiB_2 particles and to the decrease of porosity and microshrinkages.The increase in the dislocation density due to the CTE mismatches between the aluminium alloys and the TiB_2 particles has not been appreciated due to th low particle content (6 wt. %). The stresses produced during solidification are relieved through other mechanisms such as the rotation of the small precipitates forming around TiB_2 particles.

13) The grain refining capability of both Al-5Ti-1B grain refiner and the TiB_2 particles incorporated as reinforcements get impaired by the very low cooling rates of the plaster casting process in which the mould is composed of a material with very low heat dissipation capacity. Refined states (<200 μm) are only obtained with the as cast A204R alloy.

14) The improvement of mechanical properties takes place in both room temperature and high temperatures. This may have industrial applications at temperatures where dispersion strengthened alloys lose their properties due to the coarsening of the precipitates. TiB_2 particulates do not melt or dissolve and even though the unreinforced alloys do not seem to lose properties in the range of temperatures studied (up to 200ºC) in a large degree, it is deemed that a more pronounced difference should be seen at higher temperatures (up to 250-300ºC).

7.1.4 Influence of TiB_2 particles on the thermal properties

15) The presence of the TiB_2 particles has a direct influence on the thermal properties of the materials and particularly on the thermal conductivity. A 6 wt. % content produces an increase of 7% and 17% in the thermal conductivity of the A356R and A204R alloys respectively.

16) The thermal conductivity of both the A204R and A356R alloys is larger than that of the unreinforced counterparts. This fact is in opposition with values obtained with other commercial composites reinforced with SiC or Al_2O_3. This phenomenon is explained by the fact that TiB_2 particulates decrease the amount of solutes available that can take part in the solid solution state within aluminium crystals through precipitation mechanisms on the surfce of the

particles. Furthermore TiB_2 are thermally conductive ceramics, i.e. they present a larger conductivity than most of the ceramic materials.

17) The influence of the TiB_2 particles is more clearly seen in the A204 based alloy in both the CTE and thermal conductivity values. On the one hand the CTE difference between the particles and the matrix is higher ($25.3 \times 10^{-6} C^{-1}$ and $8.1 \times 10^{-6} C^{-1}$ respectively) than in the A356 alloy ($22.9 \times 10^{-6} C^{-1}$ and $8.1 \times 10^{-6} C^{-1}$). On the other hand the ceramic particles play an important role in the precipitation of the Al_2Cu phase and Al-Cu-Fe precipitates. More Al_2Cu phases precipitate in the presence of TiB_2 particles resulting in a material with a different composition from that of the unreinforced alloy. Aluminium grains are purer than in the unreinforced alloy.

18) The application of modelling tools for the calculation of the thermal properties of the materials studied along this work has proved to be a suitable approach for CTE calculation. Fairly good approximations have been obtained with the Eshelby´s Tensor approach that takes into account the shape of the reinforcements. Otherwise the studied models do not fit to the actual thermal conductivity as they do not take into account the indirect influence of the TiB_2 particles on the solidification pattern and the selection of precipitates.

7.2 FUTURE DIRECTIONS

It has been shown that the addition of TiB_2 particles to aluminium casting alloys has a direct effect on some important features such as microstructure, thermal properties and mechanical properties. Contents higher than those traditionally used for grain refining purposes (only around 0.2 vol. %) provide additional advantages that may compensate the higher cost of the material. Furthermore properties may be tailored and adjusted to the specific requirements of the industry based on the TiB_2 content within the alloy.

In order to advance in the use TiB_2 reinforced aluminium alloys for industrial applications some additional works that might be useful are following pointed out:

* **Optimisation of the production of the reinforced material.** Absence of the rests of salts that have been detected along the present work, agglomeration of TiB_2 particles in the grain boundaries, increase in the content and optimization of the distribution of the TiB_2 particles and a more homogeneous size and shape distribution of the particles would all provide further improvements in the final properties of the materials.

* **Study and optimisation of thermal treatments**. It has been demonstrated that the TiB_2 interfere in the solidification of the material and therefore traditionally used thermal treatment parameters should be further studied so that they fit to the features of the reinforced materials.

* **Study of the behaviour of the reinforced materials with other production processes.** The present study has been based on the plaster casting technology that is characterized by slow cooling rates due to the nature of the moulds which are made of plaster. Processes that use metallic moulds have shorter solidification intervals and therefore the materials will behave differently.

* **Use of other additives like silicon modifiers, fluxes or grain refiners**. The castings in the study have been made in the absence of any other additives usually used in the casting industry. TiB_2 particles may interfere in the action of such additives like strontium or sodium modifiers or Al-B and Al-Ti-B grain refiners or other alloying elements and vice versa.

REFERENCES

[1] Backërud L., Chai G. and Tamminen J. “Solidification characteristics of Aluminium alloys”.Alloy 204.2 (AlCu4.6MgTi). pp. 55-61. Volume 2: Foundry alloys. AFS/Skanluminium 1990.

[2] “Titanium diboride” http://www.azom.com/details.asp/Article ID=492.

[3] Abi-Nader F.N., Borhan M.A., Shenouda S., Attallah M.M. and Haitham A. “High performance ceramics”.http://biotsavart.tripod.com/327.htm.

[4] Munro R.G. “Material properties of Titanium Diboride”. Journal of research of the national institute of standards and technology. Vol. 105, number 5, Sept.-Oct. 2000.

[5] Vajeeston P. and Asokamani R. “The electronic structure and ground state properties of Ti_2B, TiB and TiB_2.

[6] “Titanium diboride powder. Commercial leaflet from GE Advanced ceramics”. (http: //www.advceramics.com/acc/products/titanium_diboride_powder/).

[7] “NIST Property data summaries, Titanium Diboride TiB_2”. http://www.ceramics,nist.gov/srd/summary/csdtib2.htm.

[8] Iqbal N. “Solidification: Real-Time investigation of grain nucleation and growth during liquid to solid phase transformation of aluminium alloys”. Delft University Press.2005.

[9] Loong C.A. and Hetahcock C.J. “Grain refining of aluminium foundry alloys” pp. 21-33.

[10] Karantzalis A.E. and Kennedy A.R. “Nucleation behaviour of TiB_2 particles in pure Al and effect of elemental additions”. Materials Science and technology. November 1998. Vol. 14. pp 1092-1096.

[11] Peña X. et al. “Propiedades mecánicas de las piezas obtenidas por moldeo magnético”. Fundidores Febrero 2006.

[12] Greer A.L. "Grain refinement of alloys by inoculation of melts". Phil. Trans. R. Soc. Lond. A (2003) 361, 479-495.

[13] Whitehead A.J., Danilak S.A. and Granger D.A. "The development of a Commercial Al-3%-Ti-0.15%C Grain Refining Master alloy". The 126th TMS annual meeting & exhibition.February 9-13th, 1997, Orlando, Florida, USA.

[14] Quested T. E. "Understanding the mechanisms of grain refinement by inoculation" Mater. Sci. Tech., 20, 1357. (2004).

[15] Kim W.T. and Cantor B. "An adsorption model of the heterogeneous nucleation of solidification". Acta metallurgica et materialia 42 (9): pp. 3115-3127 Sept. 1994.

[16] Greer A.L., Bunn A.M., Tronche A., Evans P.V. and Bristow D.J. "Modelling of inoculation of metallic melts: application to grain refinement of aluminium by Al-Ti-B". Acta Mater. 48, pp. 2823-2835. 2000.

[17] Schumacher P., Greer A.L., Worth J., Evans P.V., Kearns M.A., Fisher P. and Green A.H. "New studies of nucleation mechanisms in aluminium alloys: implications for grain refinement practice". Materials Science and Technology May 1998 Vol. 14. pp 394-404.

[18] TiBAl™ "World leading titanium boron grain refiners". http://www.metallurgaluminium.com/tibalmain.html.

[19] Hardman A. and Hayes F.H. "Al-Ti-B Grain refining alloys from Al, B_2O_3 and TiO_2. Materials Science Forum, Vols. 217-222, pp. 247-252, 1996.

[20] Fjellsedt, J. Division of casting metals. Department of production engineering. The Royal institute of technology (KTH). SAE-100 44 Stockholm. Sweden. June 2001. "On the crystallisation processing of Al-Base alloys". Doctoral thesis.ISSN-1104-7127.TRITA-MG 2001:01. Printed in Stockholm by US-AB.

REFERENCES

[21] Wang, Brydson, Jha & Ellis. "Microstructural analysis of Al alloys dispersed with TiB_2 particulate for MMC applications". Journal of microscopy. Volume 196 Issue 2 page 137-November 1999.

[22] Arjuna Rao A., Murty B.S. and Chakraborty M. "Role of zirconium and impurities in grain refinement of aluminium with Al-Ti-B". Materials Science and Technology. September 1997. Vol. 13 pp. 769-777.

[23] Zhang Q., Wu G., Jiang L. and Chen G. "Thermal expansion and dimensional stability of Al-Si matrix composite reinforced with high content SiC". Material chemistry and physics 82 (2003). Pp- 780-785.

[24] Bryant R.W. "Metal matrix composites: New developments, applications and markets". Business Communications Company Inc. (BCC).Norwark Connecticut. Dec. 1988.

[25] Evans A., San Marchi C. and Mortensen A. "Metal matrix composites in industry. An introduction and a survey. 2003 by Kluwer Academic Publishers. 423 pages.

[26] Surappa M.K. "Aluminium matrix composites: Challenges and opportunities". Sadhana Vol. 28, Parts 1 & 2, February/April 2003, pp. 319-334 © Printed in India.

[27] Sito T. "The automotive application of discontinuously reinforced TiB-Ti composites". 2004 May JOM.

[28] Miracle D. B. "Aeronautical applications of Metal-Matrix composites". pp. 1043-1049. ASM Handbook Volume 21: Composites. 2001.

[29] Miserez A., Muller R. Rossoll A. et al. 2004. "Particle reinforced metals of high ceramic content" MAT SCI ENG A-STRUCT 387-89: pp. 822-831.

[30] Sonuparlak B., Lehigh M.D. and Robbins M.A. "Silicon carbide reinforced aluminium for performance electronic packages". PCC advanced forming technology. Metal matrix composites business unit. http: //www.pcc-aft.com/library/SilCarbideReinforced.html.

[31] Davies P., Kellie J-L-F. and Woods J.V. 1992 UK patent 2257985A, ASM , Paris.

[32] Kuruvilla A.K., Prasad K.S., Bhanuprasad V.V. and Mahajan Y.R. “Microstructure-property correlation in Al/TiB2Composites” Scripta Materalia, 1990, 24. pp. 873-878.

[33] Tee K.L., Lu L., and Lai M.O. “In situ stir cast Al-TiB_2 composite: processing and mechanical properties”. Material Science and Technology. February 2001. Vol. 17 pp 201-206.

[34] Aikin, Jr. R.M. ”The mechanical properties of in situ composites”. JOM. 49 (8) (1997), pp. 35-39.

[35] Forster M.F., Hamilton R.W., Dashwood R.J. “Processing of TiB_2 containing Aluminium alloy 2618”. Lee.http://www.mt.ic.ac.uk/groups/mpg/p_ TiB_2/proj_tib2.html.

[36] Tjong S.C. and Ma Z.Y. “Microstructural and mechanical characteristics of in situ metal matrix composites”. Materials Science and Engineering, Nos. 3-4, 15 August 2000.

[37] Tongxiang F., Guang Y. and Di Z. “Thermodynamic effect of alloying addition on in situ reinforced TiB_2/Al composites”. Metallurgical and materials transactions, Jan. 2005; 36A, 1: academic research library.

[38] Hardman A., “Personal e-mail communication”. London Scandinavian. October 2003.

[39] Hardman A. “Personal e-mail communication”. London Scandinavian. February 2005.

[40] “Properties of typical alloys for investment casting”. Investment casting. pp.362-265.

[41] “Quelques caractéristiques physiques de matériaux”. http ://www.ivaldi.fr/pages_anglaises/donneestech2us.html.

[42] “The Atlas of microstructures of aluminium casting alloys”. Ed. Edimet.

[43] “Traitements thermiques des principaux alliages d´aluminium de fonderie“, Revue de l´áluminium Juin 1972. p. 542.

[44] Brophy H., Marder J.M. and Grensing F.C. “Aluminium alloys containing beryllium and investment casting of such alloys”. nº of patent: US5642773, July 1997.

[45] Castable aluminium-beryllium alloys. Starmet Corporation (Concord, MA), www.business.com.

[46] William F. Jobbins Inc. Aluminium- magnesium casting alloy.Nº of patent: GB685873, January 1953.

[47] Hollrigl G., Wahrisch K,, Wuest J. and Winkler R. “AlMgSi casting alloy”. nº of patent: US2002155022, October 2002.

[48] “Aluminium-zinc-magnesium alloys”. www.key-to-metals.com.

[49] “Cast Metal Matrix Composites, Technical Update”. Hitchiner Manufacturing Co, Inc.

[50] Pillai U.T.S., Duszczyk J. and Katgerman L. “Casting characteristics of high silicon added F3S.20S Duralcan Composites”. Int. J. Cast Metals Res., 2000, 13, 59-65.

[51] Rohatgi P. “Foundry Processing of Metal Matrix Composites”, Modern Casting, April 1998.

[52] Cook A. “Investment casting of metal matrix composites”. , Nº of patent: US5297609, 1994.

[53] Kennerknecht S. Cercast Group, "MCC Studies via the Investment Casting Process". The Materials Information Society, Montreal, Quebec, Canada, Sep. 17-29, 1990, pp. 87-100.

[54] Rohatgi P.K., Asthana R. and Yarandi F. “Formation of solidification microstructures in cast metal matrix composites”. Book. Solidification of metal matrix composites. TMS.pp. 51-75.

[55] Binney M.N. et al. “Grain refinement of secondary aluminium-silicon casting alloys”. Light metals 2003. Edited by P.Crepeau TMS (The Minerals, Metals & Materials Society), 2003. pp.

[56] “Specification for the aluminium alloy AlSi7Mg”. Commercial information. A/S Temponik . Denmark.

[57] ”Atlas de micrographie quantitative des A-S7G”. CTIF. Centre technique des industries de la fonderie. Editions techniques des industries de la fonderie.1976.

[58] Taghiabadi R., Mahmoudi M., Emamy Ghomy M. and Campbell J. ”Effect of casting techniques on tensile properties of cast aluminium alloy (Al-Si-Mg) and TiB_2 containing metal matrix composite”. Materials Science and Technology, April 2003 Vol.19.

[59] Mackay R.I. and Gruzleski J.E. “Quantification of magnesium in 356 alloy via thermal analysis”. Int. J. Cast Metals Res., 1998, 10, 225-265.

[60] Ghomy M.E. and Campbell J. “The flowability of particulate TiB_2 containing metal matrix composite”. Cast Metals, 8, (1) (1994), pp. 13-20.

[61] Grandier Vazeille P. and Morice J. “Mise au point d´eprouvettes technologiques pour l´aptitude au moulage des alliages d´aluminium”. Revue de l´aluminium.Fevrier 1971. pp.177-187.

[62] “Aluminium alloys-Effects of alloying elements”. http://www.key-to-metals.com/Article 55.htm.

[63] Sahoo, M, “An investigation of the influence of convection inducted by buoyancy and marangoni forces on the hot tearing of light metal alloys used in aerospace applications”. NASA Marshall Space Flight Center through Auburn University Solidification and Design Casting consortium. 2002.

[64] Menard G. and Richard M. Centre technique des industries de la fonderie. “Atlas microfractographique des alliages d´aluminium moules”. CTIF. Al-Cu5MgTi. pp. 102-3,108-111, 120-1, 124-5, 178-180.

[65] Youssef Y. M., Richard W Hamilton, Peter D. Lee and Richard J. Dashwood. “Effect of TiB_2 particles on the solidification behaviour of aluminium-TiB_2 alloys”. http://www.mt.ic.ac.uk/groups/mpg/p_effect_tib2/Effect_tib2.html.

[66] LeMay I. “Strengthening mechanisms and strength-structure relations”. Chapter 6 of the book Principles of Mechanical Metallurgy. pp. 155-211.

[67] ASM Committee on analysis of ductile and brittle fractures “Ductile and Brittle fractures”. pp. 61-94.

[68] Han J. “Processing, microstructure evolution and properties of nanoscale aluminium alloys”. PhD. University of Cincinnati July 2005. pp. 38-44.

[69] Clyne T.W. and Withers P.J. “An introduction to metal matrix composites”. Cambridge University Press, 1993, ISBN 0-521-41808-9.

[70] Arpón R., Molina J.M., Saravanan R.A., García Cordobilla C.,Louis E. and Narciso j. “Thermal expansion behaviour of aluminium/SiC composites with bimodal particle distributions. Acta Materalia 51 (2003) 3145-3156.

[71] “Typical property comparison for MMC and traditional engineering alloys”. http://www.ofalloncasting.com/MMCtable.html.

[72] Miller W.S. and Humphreys F.J. “Strengthening mechanisms in metal matrix composites”.Fundamental relatuionships between microstructure & mechanical properties of metal matrix composites. Edited by P.K.law and M.N. Gunger. The Minerals, metals and materials society, 1990.

[73] Mummery, P. and Derby, B. “Micromechanisms of fracture in particle reinforced metal matrix composites”. Book. Fundamental relationships between microstructures and mechanical properties of metal matrix composites. 1990. pp. 161-172.

[74] Böh H.J. “Continuum models for the thermomechanical behaviour of discontinuously reinforced materials”. Advanced engineering materials 2004, 6 No. 8.pp.626-633.

[75] Chawla N. and Shen Y-L. “Mechanical behaviour of particle reinforced metal matrix composites”. Advanced engineering materials 2001, 3, No. 6. pp. 357-370.

[76] Humphreys F.J., Basu A. and Djazeb, M.R. “The microstructure and strength of particulate metal-matrix composites”. Metal matrix composites. Processing, microstructure and properties. 12th Riso International Symposium on materials science. 1991. pp.51-66.

[77] Hong S.J., Kim H.M., Huh D., Suryanarayana C. and Chun B.S. “Effect of clustering on the mechanical properties of SiC particulate-reinforced aluminium alloy 2024 metal matrix composites”.

[78] González-Rivera, C., Baez J., Chávez R., Alvarez O. and Juárez-Islas J. “Effect of SiC_p content on cooling curve characteristics and solidification kinetics of Al-Si/SiC_p cast composites”. International Journal of cast metals research, 16 (6): 531-536;2003.

[79] Rajendra U. Vaidya, K. and Charla K. “Thermal expansion in particle reinforced metal-matrix composite”. Developments in Ceramic and Metal-Matrix Composites. The Minerals, Metals & Materials Society 1991. pp.253-272.

[80] Korb G. and Neubauer E. ”Thermophysical properties of Metal Matrix Composites“. MMC-Assess Thematic Network. Vol. 7.http:(//mmc-assess.tuwien.ac.at/).

[81] Taya M. and Arsenault R.J., “Metal matrix composites. Thermomechanical behaviour”. Chapter 5. Pergamon Press.

[82] Taylor R.E. and Bogaard R.H. “Thermophysical properties of dispersion-strengthened alloys”. Mechanical properties of metallic composites. Edited by Shojiro Ochiai. pp. 59-74.

[83] Elomari S., Skibo S., Sundarrajan M.D. and Richards, H. “Thermal expansion behaviour of particulate metal-matrix composites”. Composites Science and Technology 58 (1998) pp. 369-376.

[84] Lemieux S., Elomari S., Nemes S., Skibo S. “Thermal expansion of isotropic Duralcan metal-matrix composites”. Journal of Materials Science 33 (1988) pp. 4381-4387.

[85] Khare G., Chandra N. and Silvain J.F. “Application of Eshelby´s tensor and rotation matrix for the evaluation of thermal transport properties of composites”.

[86] Overfelt R.A., Taylor R.E., Bakhtiyarov S.I. and Wang D. “Thermophysical properties of 201 aluminium, ductile iron and Sebiloy II”. AFS Transactions 02-146.

[87] Clyne T.W. “Materials Algorithms project Program Library”. http://www.msm.cam.ac.uk/map/composites/programs/eshcon-e.html.

[88] 100) http: //www.knovel.com/knovel2.

RESUME

Le travail a été dédié á l´étude de l´influence de particules de di borure de titane (TiB_2) sur la solidification, la microstructure et les propriétés thermiques et mécaniques de deux alliages d´aluminium renforcés, Al-Si7Mg0.3 et Al-Cu5MgTi. Les matériaux ont été obtenus par un procédé de fonderie à la cire perdue en coulant les alliages dans les mêmes conditions que les alliages non renforcés correspondants.

On a constaté que les particules de TiB_2 ont une influence directe sur les caractéristiques des alliages telles que la microstructure, la sélection des phases qui précipitent pendant la solidification, les propriétés mécaniques, le coefficient d´expansion et de conductivité thermique. On a ainsi montré que les particules de TiB_2 peuvent être utilisées pour ajuster les caractéristiques des alliages et obtenir des propriétés spécifiques pour des applications dans les secteurs du transport et de l'électronique.

MOTS-CLES

Di borure de titane, Composite, Fonderie à la cire perdue, Moules en plâtre, Microstructure, Propriétés mécaniques, Propriétés thermiques, Particules.

ABSTRACT

The work has been focused on the study of the influence of Titanium diboride (TiB_2) particles on the solidification, microstructure and mechanical and thermal properties of two aluminium reinforced alloys, Al-Si7Mg0.3 et Al-Cu5MgTi. Samples have been obtained through the lost wax process known as plaster casting and compared with unreinforced samples obtained at the same conditions. It has been observed that the TiB_2 particles have a direct influence on several features of the alloys such as the microstructure and selection of precipitating phases as well as in the improvement of the soundness and mechanical properties. The coefficient of thermal expansion (CTE) and thermal conductivities are also affected. TiB_2 particles can be used to tailor the properties of the alloys and to match the specifications of transport and electronic applications.

KEYWORDS

Titanium diboride, Composites, Lost wax, Plaster moulds, Microstructure, Mechanical properties, Thermal properties, Particles.